MEMBRANE OXIDATION GOVERNED DIRECT PLASMA MEMBRANE TRANSLOCATION OF CELL-PENETRATING PEPTIDES IN LIVE CELLS: MECHANISMS AND IMPLICATIONS

A Dissertation

by

TING-YI WANG

Submitted to the Office of Graduate and Professional Studies of
Texas A&M University
in partial fulfillment of the requirements for the degree of

DOCTOR OF PHILOSOPHY

Chair of Committee,	Jean-Philippe Pellois
Committee Members,	Hays S. Rye
	Vladislav M. Panin
	Karen L. Wooley
Head of Department,	Gregory D. Reinhart

August 2016

Major Subject: Biochemistry

ABSTRACT

Cell-penetrating peptides (CPPs) enter cells primarily through escaping from endosomal compartments or directly translocating across the plasma membrane. Due to their capability of permeating into the cytosolic space of the cell, CPPs are utilized for the delivery of cell-impermeable molecules. However, the fundamental mechanisms and parameters managing the penetration of CPPs and their cargos through the lipid bilayer have not been fully determined. This hampers their usage as a tool to study biological processes as well as for future therapeutic applications. In this work, I report the first observation that the cell penetration of linear polyarginine CPPs is dependent on the cellular oxidation state. Peptide delivery efficiency and the entry mechanism were evaluated in live human cells using fluorescence microscopy and flow cytometry. Additionally, lipophilic fluorescent probes were employed to detect the cell membrane oxidation level. Lastly, the mechanism of peptides penetrating the oxidized membrane was studied using live cells and *in vitro* partitioning assays.

The presence of antioxidants and a hypoxic environment reduced the cell penetration of polyarginine CPPs. In contrast, oxidants promoted cytosolic entry with an efficiency proportional to the level of reactive oxygen species (ROS) generated within membranes. Moreover, a monoclonal antibody that recognizes oxidized lipids inhibited peptide penetration while extracellularly supplemented pure anionic oxidized lipids enhanced peptide transport into cells. The results support a model in which positively-charged peptides bind negatively-charged lipids present on the cell surface as a result of

oxidative damage and cross the membrane via formation of inverted micelles. This may explain the variability in the cell delivery efficiency of a CPP in different experiments. These new findings therefore also provide opportunities for the design of future cell-permeable compounds and for optimization of delivery protocols.

DEDICATION

This work is dedicated to my grandmother, parents, sister, and to my dear wife from thousands of miles away for their infinite love and support.

ACKNOWLEDGEMENTS

I would like to thank my advisor Dr. Jean-Philippe Pellois from the bottom of my heart for his endless patience guiding and training me to be a qualified researcher. I also thank Dr. Hays Rye, Dr. Vladislav Panin, and Dr. Karen Wooley for serving as my committee members and for the valuable suggestions to my research. In addition, I would like to thank all the former and current members of the Pellois laboratory, in particular, Alfredo Erazo-Oliveras, Nandhini Muthukrishnan, and Kristina Najjar, who contributed my growth during my PhD study. I am also grateful to my colleagues for their insights and the department faculty and staff who were always there willing to help. Finally, I would like to thank my parents, sister, and wife for their support and encouragement without which this work would not have been possible.

NOMENCLATURE

BMP	bis(monoacylglycero)phosphate
BODIPY	boron-dipyrromethene
CBD	chitin binding domain
CHCA	α-cyano-4-hydroxycinnamic acid
CHO	Chinese hamster ovary
CPP	cell-penetrating peptide
cumene-OOH	cumene hydroperoxide
CytD	cytochalasin D
DC	dendritic cell
DEAC	7-diethylaminocoumarin
dH_2O	distilled water
DIEA	*N*,*N*-Diisopropylethylamine
DMEM	Dulbecco's Modified Eagle's Medium
DMF	dimethylformamide
DMSO	dimethyl sulfoxide
DOPC	1,2-dioleoyl-*sn*-glycero-3-phosphocholine
DOPE	1,2-dioleoyl-*sn*-glycero-3-phosphoethanolamine
DOPS	1,2-dioleoyl-*sn*-glycero-3-phospho-L-serine
DPPP	diphenyl 1-pyrenylphosphine
EGF	epidermal growth factor

EGFP	enhanced green fluorescent protein
EIPA	5-(*N*-ethyl-*N*-isopropyl)amirolide
EMCCD	electron-multiplying charge-coupled device
FBS	fetal bovine serum
FPLC	fast protein liquid chromatography
GAGs	glycosaminoglycans
GFP	green fluorescent protein
GPMVs	giant plasma membrane vesicles
GPx	glutathione peroxidase
$H^{\bullet}$	hydrogen atom with an unpaired electron
H_2O_2	hydrogen peroxide
H9	nona-histidine
HA	hemagglutinin
HBTU	2-(1H-Benzotriazole-1-yl)-1,1,3,3-tetramethyluronium
HDF	human dermal fibroblast
HEPES	4-(2-hydroxyethyl)-1-piperazineethanesulfonic acid
HIV-1	human immunodeficiency virus type 1
HPLC	high performance liquid chromatography
HPMA	*N*-(2-hydroxypropyl)methacrylamide
HS	heparan sulfate
HSPGs	heparan sulfate proteoglycans
K9	nona-lysine

K_d	disassociation constant
Klf4	Krüppel-like factor 4
$L^{\bullet}$	lipid radical
LH	unsaturated fatty acid
$LOO^{\bullet}$	lipoperoxyl radical
LOOH	lipid hydroperoxide
LPS	lipopolysaccharides
MALDI-TOF	matrix-assisted laser desorption/ionization time-of-flight
MDA	malondialdehyde
MTT	3-(4,5-dimethylthiazol-2-yl)-2,5-diphenyltetrazolium bromide
MTX	methotrexate
NBD	NF-κB essential modulator binding domain
NS	not significant
O9	nona-ornithine
Oct4	octamer-binding transcription factor 4
OVA	ovalbumin
oxPC	oxidized phosphatidylcholine
PAD	pro-apoptotic domain
PazePC	1-palmitoyl-2-glutaryl-*sn*-glycero-3-phosphocholine
PBS	phosphate buffered saline
PCI	photochemical internalization
PGPC	1-palmitoyl-2-glutaryl-*sn*-glycero-3-phosphocholine

PKI	protein kinase inhibitor
PNA	peptide nucleic acid
P/S	penicillin/streptomycin
PC	phosphatidylcholine
PE	phosphatidylethanolamine
POVPC	1-palmitoyl-2-(5'-oxo-valeroyl)-*sn*-glycero-3-phosphocholine
PoxnoPC	1-palmitoyl-2-(9'-oxo-valeroyl)-*sn*-glycero-3-phosphocholine
PS	phosphatidylserine
PTDs	protein transduction domains
R4	tetra-arginine peptide
R8	octa-arginine peptide
R9	nona-arginine peptide
RBCs	red blood cells
RFP	red fluorescent protein
ROS	reactive oxygen species
Ru(II)	Ruthenium(II)
SDC4	syndecan-4
siRNA	small interfering RNA
SOD	superoxide dismutase
Sox2	sex determining region Y- box 2
SPPS	solid-phase peptide synthesis
TALEN	transcription activator-like effector nucleases

TAT	*trans*-activator of transcription
TFA	trifluoroacetic acid
TIS	triisopropylsilane
TMR	tetramethylrhodamine
TPC	5-(4-carboxyphenyl)-10,15,20-triphenyl-2,3-dihydroxychlorin
tRBCs	trypsinized red blood cells

TABLE OF CONTENTS

Page

LIST OF FIGURES

Page

LIST OF TABLES

Page

1. INTRODUCTION

1.1. Significance of biomolecule delivery

Delivery of exogenous biomolecules into cells is significant for applications in cell biology studies and therapeutic treatments. Two notable examples are delivery of transcription factors to reprogram stem cells and transport of oligonucleotides to repair gene alterations. Both applications along with others, however, have experienced inefficient cell penetration of cargo into the cytoplasm and cell nuclei. This is due to the hydrophobic nature of plasma membrane, which selectively filters the entry of extracellular molecules. Biomolecules are generally hydrophilic and large that cannot penetrate the lipid bilayer without the assistance of membrane transporters[1]. The cell membrane is therefore a hurdle to overcome in order to transport the biomolecules to their cytosolic targets. Electroporation and microinjection are two traditional physical approaches to achieve cytosolic delivery. Yet, their utilization to transport bioactive molecule is limited by their high cytotoxicity, delivery inefficiency, and high labor intensive requirements[2]. In contrast, macromolecules can be distributed intracellularly using a viral vector with high efficiency. However, this biological method has a high risk of insertion of viral DNA into the host genome[2]. Over the past twenty years, cell-penetrating peptides (CPPs) have become promising carriers to deliver various biomolecules into cells[3].

1.2. Cell-penetrating peptides as delivery carriers: focusing on polyarginine peptides

1.2.1. History of cell-penetrating peptides

As early as the 1960's, researchers observed that polylysine facilitates the cellular internalization of covalently conjugated or co-incubated albumin proteins[4, 5]. In 1988, two independent research groups, Loewenstein and Pabo, both detected the activation of microinjected viral polynucleotides in human cells by adding the *trans*-activator of transcription (TAT) protein from human immunodeficiency virus type 1 (HIV-1) to the cell culture medium[6, 7]. These results suggested an unexpected membrane translocation activity of a hydrophilic macromolecule. The effective peptide sequence of TAT protein that is essential for its membrane transport activity was later identified to be RKKRRQRRR (residues 49 to 57)[8-10]. Similarly, the *Drosophila* Antennapedia homeoprotein with a *trans*-activating function was also shown to penetrate cells[11]. Its 16-amino acid sequence, RQIKIWFQNRRMKWKK (residues 43 to 58, also known as Penetratin peptide), was responsible for the cell-penetrating activity[12]. Since then, around 800 different peptide sequences have been reported to be able to transport into cells along with their carried cargo[13]. These peptides are therefore called CPPs or protein transduction domains (PTDs).

1.2.2. Characteristics of cell-penetrating peptides

CPPs are short polypeptides (generally 5 to 30 amino acids) that carry cargo with a wide range of sizes, from small-molecule compounds and short peptides to large

molecules such as proteins, polynucleotides, and nanoparticles, into the cytoplasmic space of live cells without causing cell death. Cargo delivery can be achieved by covalent attachment of a CPP to a cargo of interest or simply by co-incubation. Most CPPs show no cell specificity as the peptides penetrate various cell types including plant, insect, and stem cells, as well as both cancerous and noncancerous cells[14-19].

CPPs can be classified into three groups by their origin: protein-derived, chimeric, and synthetic[20, 21]. Protein-derived CPPs are peptides that originate from native protein sequences. Model peptides in this group are TAT and penetratin. Peptides fused from two or more natural peptide sequences are chimeric CPPs. Two of the best known examples are HA2-TAT, composed of HA2 peptide derived from hemagglutinin (HA) protein of influenza virus and TAT peptide[22, 23], and transportan, a fusion peptide of galanin neuropeptide and mastoparan toxin peptide from wasp venom[24]. The third group consist of synthetic CPPs which are developed from rational design and mutational analysis. GALA, KALA, and polyarginines are among the best known representatives[25, 26].

From the prospective of physicochemical properties in the sequence, CPPs can also be grouped into two categories: cationic and amphipathic. Cationic CPPs contain a cluster of cationic amino acids, such as arginine and lysine. TAT and polyarginine peptide are two prototypical examples. Due to the high *pKa* values of arginine and lysine side chains, these peptides bear high positive charges in the physiological environment (pH 7.4). On the other hand, amphipathic CPPs possess both hydrophobic and hydrophilic stretches in their sequences. The most studied constructs are HA2-TAT, KALA, and GALA. The net charge of these peptides varies and is dependent upon residue

compositions. Unlike cationic CPPs carrying no apparent secondary structures, most amphipathic peptides adopt an α-helical or β-sheet conformation upon binding to the membrane[27]. Recently two anionic peptides, which were considered to be cell-impermeable due to their unfavorable overall negative charge, were reported to be able to traverse cell membrane[28, 29].

An emerging group of peptides displaying the cell-penetrating activities is cyclic peptides[30, 31]. This type of peptide contains at least one ring, synthesized by side chain-to-side chain, terminus-to-terminus or side chain-to-terminus linkage[32]. The stapled peptide is a famous example in this category where the peptide gains cell permeability through "stapling" the side chains of the linear sequence[33]. The stapling method has been shown to increase and stabilize the α-helicity of peptide; however, that does not correlate with its membrane penetrating activity[34, 35]. Yet, multiple studies have demonstrated that the cyclized version of CPPs are even more potent in cell delivery than their linear counterparts[35-37].

1.2.3. "Arginine magic" of cell-penetrating peptides

The significance of arginine residues in the TAT peptide sequence contributing to cell penetrating activity was established by the mutational analyses led by Wender, Rothbard and Futaki[10, 38, 39]. Wender found that nona-arginine peptide (R9), a homogenous arginine analog of TAT peptide, is efficiently internalized into Jurkat cells. This activity declined with decreasing number of arginine residues in the peptide sequence[10]. Similarly, Rothbard showed that other polycationic peptides, nona-lysine (K9), nona-histidine (H9),

and nona-ornithine (O9), failed to translocate into the cells[38]. However, results of these two studies were obtained by flow cytometry analysis which can not differentiate cytosolically penetrated peptides from peptides entrapped in the endocytic pathways or sticking to the cell membranes[40] (the detailed cell entry mechanism of polyarginine CPPs will be discussed in the next section). Futaki, on the other hand, investigated the cell penetrating activities of polyarginine peptides using fluorescence microscopy. The octa-arginine peptide (R8) displayed a cytosolic distribution and nuclear staining after cell delivery, while the shorter peptide, tetra-arginine peptide (R4), showed no activity[39]. Unfortunately, this result was acquired from cells after fixation, which later was demonstrated to be able to stimulate the artificial cell membrane translocation of CPPs[40, 41]. Though results from these pioneering studies were inconclusive, in 2003 polyarginine peptides were shown to have promising cytosolic penetration in live cells detected by fluorescence microscopy[42, 43].

The cell penetrating activity of polyarginine peptides is generally chirality-independent, as both L- and D-arginine polypeptides can internalize into most live cells and tissues[10, 38, 44-46]. On the other hand, the activity is length-dependent such that the longer polyarginine peptides (R10, R11, R12) can achieve higher activities at the same or lower concentrations without increasing cytotoxicity comparing to the shorter peptides (R7, R8 and R9)[47, 48], except that a much longer peptide (with more than 15 arginine residues) loses activity presumably by sticking to the cell membranes[38, 49]. Interestingly, peptides lose cell delivery activity when lysine residues are substituted for arginine, even with lengthy peptides such as K12 or K16[38, 47, 50, 51]. This revealed that the overall cationic

charges alone are not sufficient to provide membrane translocation activity, as the amino group of lysine side chain is also positively charged at physiological pH (pH 7). This phenomenon can be explained by the model that the guanidinium moiety of arginine pairs bidentate hydrogen bonding with the anionic groups, such as phosphate, sulfate, and carboxylate, on the membrane components, while only monodentate hydrogen bonding can be formed by the ammonium of lysine[52-54]. This hypothesis was supported by the observation that the polyarginine peptide has a smaller disassociation constant (K_d) towards anionic membranes than the polylysine peptide[55] and that the cellular uptake of polyarginine was greatly reduced when the guanidino group was methylated[56]. Moreover, grafting the guanidinium moiety or arginine residue-like side chains into the delivery vector have displayed superior cell uptake or penetration activities[10, 38, 43, 57-61].

1.3. Cell entry mechanism of polyarginine peptides

The route and underlying mechanism by which an extracellular CPP enters the cytosolic space of a cell remains a matter of debate in the field. It is, however, widely accepted that the peptide can penetrate the cell by two routes. The first route is endocytosis followed by endosomal escape[62-67]. This is a two-step process involving endocytic uptake of the peptides upon binding to the cell surface and translocation across the membranes of the endocytic compartments. The majority of CPPs, not limited to polyarginine peptides, penetrate the cells and deliver their carried cargo via this pathway. Another route is a single step process in which the peptide transverses the lipid bilayer directly at the plasma membrane of the cell[65, 68-70]. This pathway was only observed in a few CPPs, including

polyarginine peptides. The evidence supporting the molecular mechanisms by which the polyarginine peptide permeates the cell membrane via these two distinct routes will be discussed in greater detail.

1.3.1. Endocytosis and endosomolysis

The current model of the cytosolic entry of CPPs and their cargo through endocytic pathways involves four major stages (Figure 1-1)[62]. First, the peptides bind to the cell surface. Next, the binding promotes the endocytic internalization of the peptides into transport vesicles. Third, the peptides in the vesicles travel along the endocytic pathways. Finally, the CPPs translocate across the membranes of the endocytic compartments and reach the cell cytosol. The molecular details of each step will be discussed, focusing on studies with polyarginine peptides.

Accumulating evidence suggests that, as in the first step, the ability of polyarginine peptides to interact with the mammalian cell plasma membrane is due to binding to the cell-surface glycosaminoglycans (GAGs), specifically from heparan sulfate proteoglycans (HSPGs)[71]. HSPGs are membrane-anchored glycoproteins that contain one or more heparan sulfate (HS) chains that are exposed extracellularly[72]. Due to the abundance and negative charge that is contributed by sulfates and carboxylates (structure shown in Figure 1-1), it is believed that the endocytosis is triggered upon binding and clustering between cationic polyarginine peptides and anionic HSPGs. This model is supported by the results that nona-arginine peptides are unable to internalize into HS-deficient cell lines[63, 73] and that the cellular uptake of the octa-arginine peptide is increased when syndecan-4 (SDC4),

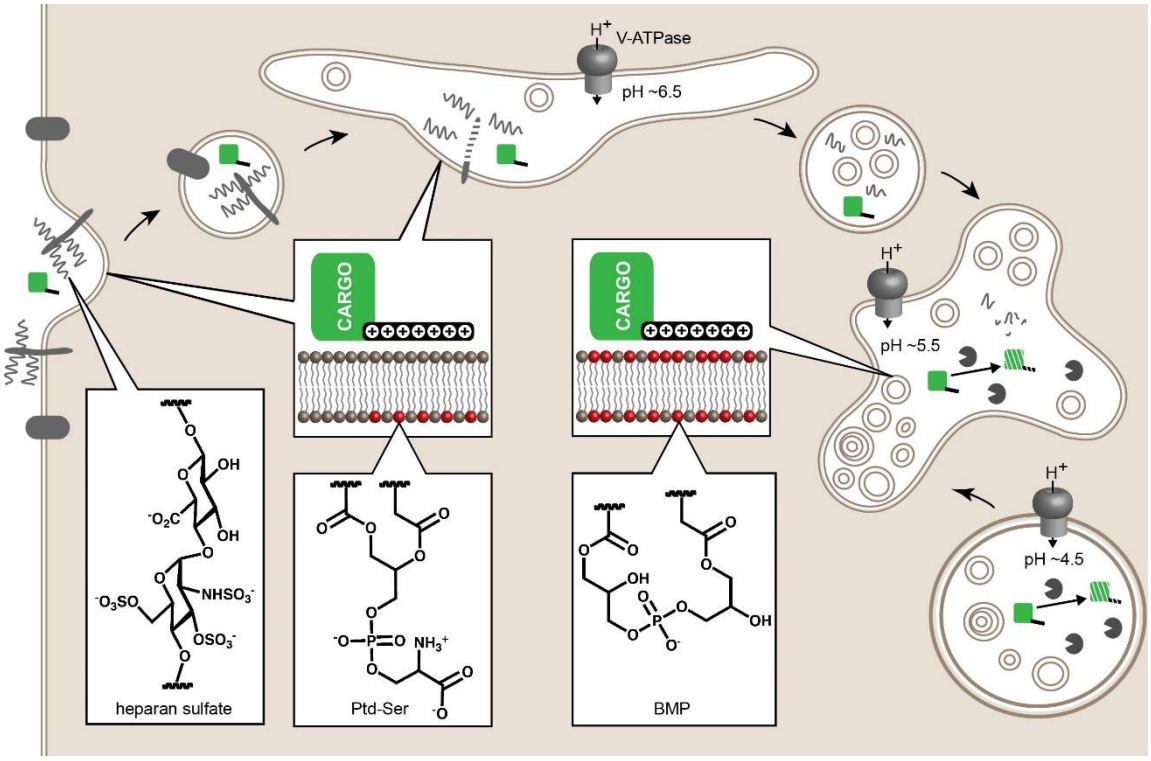

Figure 1-1. Model of the trafficking of a CPP-cargo conjugate through the endocytic pathway. From left to right: A CPP-cargo binds to heparan sulfate proteoglycans (HSPGs) on the cell surface and induces endocytosis. Endocytosis leads to uptake and entrapment of the CPP-cargo inside an endocytic vesicle. The endosomal membrane contains phosphatidylserine (PS) in its outer leaflet. During endosomal maturation, a vacuolar H^+-ATPase acidifies the lumen of endocytic organelles. The CPP-cargo reaches early endosomes (pH~6.5). Concurrently, hydrolases partially degrade HSPGs and release heparan sulfate (HS) fragments. Upon further maturation, the CPP-cargo reaches multivesicular bodies, late endosomes (pH~5.5), and lysosomes (pH~4.5). The membrane of the intraluminal vesicles of late endosomes is enriched with phospholipid bis(monoacylglycero)phosphate (BMP). HS is further degraded to smaller fragments. The CPP-cargo is susceptible to degradation due to the low pH and lysosomal hydrolases. The figure is used with permission[62].

a HSPG protein, was overexpressed[74]. Moreover, in the *in vitro* assays, the peptides show a high affinity to HS or to the analog heparin with a K_d of between 100 and 320 nM[63, 75-78]. Notably, the polyarginine peptides also show strong interactions with anionic lipids[55, 79, 80]. However, considering the relatively low abundance of anionic lipid species (less than 10% of the total lipids)[81-83] and the lipid asymmetry of plasma membrane[84, 85], the high density of GAGs (the molar ratio of total GAGs to total lipids is about 1:15)[86, 87], similar binding affinities of the peptide to GAGs and to negatively charged lipids[55, 63, 75, 76], and no *in cellulo* experimental proof, all these facts make it unlikely that lipids are the primary binding target of the peptides at the plasma membrane of mammalian cell which initiates endocytosis. Yet, lipids were suggested to play an important role in assisting the translocation of the peptide directly across the plasma membrane, which will be introduced in the next section. Interestingly, proteins located at the plasma membrane were recently reported to play roles in the endocytic entry of polyarginine peptides[88, 89].

Unlike some other CPPs which are internalized in endocytic vesicles via caveolae-mediated or clathrin-mediated endocytosis upon binding to the cell plasma membrane, the polyarginine peptides enter cells mainly via macropinocytosis. This notion is supported by the results that the cellular uptake of the peptides was reduced when treating cells with macropinocytosis inhibitor 5-(*N*-ethyl-*N*-isopropyl)amirolide (EIPA)[49, 90]. Furthermore, it has been shown that membrane ruffles and the rearrangement of actin filaments are involved in the process of macropinocytosis[91, 92]. With the presence of the membrane ruffling inducer, epidermal growth factor (EGF), or F-actin depolymerizor, cytochalasin D (CytD), the cellular internalization of the peptide significantly increases or decreases,

respectively[49]. Yet, the cell delivery efficiency of polyarginine peptide was insignificantly affected by macropinocytosis inhibitor EIPA in some cells lines, leaving the endocytosis mechanism a matter of debate[93-95]. However, the cellular uptake of polyarginines is certainly reduced by other endocytic pathway inhibitors [49, 94-96]. Moreover, when arresting all cellular endocytic processes by incubating cells at low temperature (4-22^{o}C) without causing cytotoxicity, the peptide fails to internalize into the cells at the same level[93, 97, 98]. All together, these data suggest that endocytosis, presumably macropinocytosis, is the major endocytic route of cell entry of the peptide.

Live-cell experiments have confirmed that polyarginines trafficking within endocytic vesicles. Under microscopic examination, the endosome-like vesicular structures were observed to fuse with organelles containing the peptide signal[49]. Furthermore, the cells loaded with the endocytic pathway marker, dextran, or expressed with the fluorescently labeled early or late endosomal proteins, Rab-5 or Rab-7, have shown co-localization with the peptide[93, 96]. Inhibition of microtubules by a depolymerizing compound, nocodazole, also affects the internalization of the peptide[49, 93]. When trafficking along the endocytic pathways, the polyarginine peptides and their cargo can escape from the vesicles to reach targets in the cytoplasm or nucleus. The molecular mechanism of the endosomal release of polyarginine peptides, however, is still unresolved. This could result from the inefficient endosomolytic activity of the peptide[99-104], which makes their study difficult.

1.3.2. Direct plasma membrane translocation

Aside from endocytic entry, polyarginines can directly permeate the lipid bilayer in a non-endocytic fashion at the plasma membrane of live cells. Cells treated with endocytic inhibitors or incubated at low temperature, in order to impair cellular endocytosis including macropinocytosis, still were still found to take up polyarginine peptides[42, 45, 94, 105-108]. However, the validity of these results was questioned by specificities of the inhibitors as well as their impacts on cell physiology[109, 110]. Most of the experiments also did not include proper controls to validate the effectiveness of inhibition treatments. Yet, lines of evidences, such as the fast cytosolic entry of polyarginine peptides and formation of multivesicular peptide-membrane complexed structures at the plasma membrane upon peptide delivery, strongly support the direct plasma membrane translocation model[70, 105, 107, 111]. Moreover, the peptide can penetrate proteo-liposomes derived from cell plasma membrane, named giant plasma membrane vesicles (GPMVs) that retain similar lipidic and proteinaceous components of plasma membrane, with the inability of endocytosis[112, 113]. This result confirms that endocytosis is not required for penetration. The direct membrane penetration of the peptide was also observed with liposomes composed of anionic lipids[51].

The mechanism by which the polyarginine peptides penetrate through the plasma membrane is still largely inconclusive. Several models were proposed, including that penetration with the assistance of membrane potential difference across the membrane by Wender and Herce[14, 56]. Brock suggested that the translocation occurred at nucleation zones that were involved in the formation of ceramide-enriched domains[111]. The

nucleation zone model is in agreement with the observation of multivesicular peptide-lipid structure published by Futaki[70].

1.4. Roadblocks of cell delivery using polyarginine CPPs

Despite the promise of the broad utility of polyarginine CPPs to intracellularly deliver bioactive cargo *in cellulo* and *in vivo*[46, 114-130], general rules of cytosolic penetration have not yet clearly been established. In some instances, cytosolic penetration appears to be involved in direct plasma membrane translocation. Alternatively, a two-step process of endocytosis followed by escape from endosomes has also been observed. It is currently plausible that polyarginine CPPs utilize these two distinct routes of cellular entry to varying degrees. Additionally, molecular details that explain how a peptide crosses cellular membranes are also lacking. A wide variety of translocation models have been proposed, most of which highlight the ability of polyarginine CPPs to interact with lipid bilayers[14, 70, 111, 131-133]. These mechanisms, while potentially non-exclusive, remain a matter of debate.

In the absence of understanding the parameters that control cytosolic penetration and the mechanistic insights of a peptide traversing across the lipid bilayer, designing better delivery tools or strategies often replies on a process of trial and error. It is clear that the peptide concentration, number of arginine residues, cell types, and physical-chemical properties of the cargo impact the delivery route [68, 129, 134, 135]. Moreover, the results obtained with polyarginine CPPs are often unpredictable with high variability in

cytosolic penetration (Table 1-1). In particular, minor changes in experimental conditions can impact the results obtained, indicating that unknown variables modulate this process.

Table 1-1. Polyarginine peptides, cargo, and cell line utilized in the selected publications

Peptide	Cell Line	Cargo	Ref.
R3-R9, R15, R20, R25, R30; r4-r9	Jurkat	fluorescein	[38]
R7	Jurkat	Cyclosporin A	[130]
R5-R9	Jurkat	fluorescein	[10]
R4, R8, R12, R16	COS-7	plasmid	[136]
R4, R6, R8, R10, R12, R16	RAW264.7	fluorescein	[39]
R7, R9, R11	COS-7, C2C12, U251-MG, PC12, primary neurons	EGFP, PKI peptide, fluorescein	[135]
R8	HeLa	fluorescein	[137]
R4, R6, R8, R10, R12	CHO-K1, HIG-82, HeLa, A549, Jurkat, pgsD-677, pgsA-745	streptavidin-β-galactosidase, Streptavidin-Alexa Fluor 488	[129]
R7	primary keratinocytes	biotin, HA peptide	[138]
R7, R10; r7, r13	Jurkat	fluorescein	[48]
R8, R16	RAW264.7, HeLa, COS-7	TMR	[139]
R11	SAOS-2, NOS-1, SAS, HSC-3, HSC-4	p53	[140]
r5, r7, r9	Jurkat	fluorescein	[57]
R9	$10T^{1}/_{2}$, HeLa	BODIPY, fluorescein	[43]
R8	CHO	GFP	[41]
R7	COS-7	plasmid	[141]
R9	MC57	fluorescein	[142]
R9	CHO-K1, pgsD-677, pgsA-745	TMR	[63]
R8	NIH/3T3	fluorescein, plasmid	[143]
R4, R8, R16; r8	HeLa	Texas Red, fluorescein, PAD peptide	[49]
r8	Jurkat	fluorescein	[56]
R9	CHO	biotin	[144]

Table 1-1. Continued

Peptide	Cell Line	Cargo	Ref.
R11	A549, HeLa, CHO-K1	TMR, PKI peptide, NBD peptide	145
R11	U251-MG, KR158	p53	101
R6, R7, R9	HeLa	peptide nucleic acid (PNA)	146
R8	K562, KG1a	Alexa Fluor 488, Texas Red	93
R7	MDA-MB-468	5-(4-carboxyphenyl)-10,15,20-triphenyl-2,3-dihydroxychlorin (TPC)	147
R9	dendritic cell (DC)	ovalbumin (OVA), HA peptide	127
R7; r6, r7, r8, r9	HeLa, p53R	PNA	148
R8	HeLa	Alexa Fluor 488, EGFP, PAD peptide	100
R9	HeLa, MC57, CHO, dendritic cell, Jurkat	fluorescein, Smac peptide	94
R8; r8	KG1a	Alexa Fluor 488	45
R9	HeLa	N/A	149
R4, R6, R8	HL-60	Ferrocenecarboxylic acid	125
R8	CHO-K1, pgsD-677, pgsA-745, 293T	Alexa Fluor 488	150
r8	Jurkat	luciferin	151
r4, r8	UCI-101, UCI-107, SCOV-3, OVCA-429, OVCA-433, MCF-7	Taxol, coelenterazine, luciferin	126
R4, R8, R12, R16	HeLa, CHO-K1, pgsA-745	Alexa Fluor 488, PAD peptide	107
R5-R12	C2C12, Wistar, HeLa, MDCKII, BJ-hTERT	fluorescein, TMR	47
R9	HeLa	fluorescein	152
R9	HeLa	Fluorescein, oligonucleotide mixmer	153
R9	A549	GFP, RFP, mCherry	154
R9	CHO-K1, pgsA-745	biotin	106
R9	HEK293	Klf4, c-Myc, Oct4, Sox2	124
r8	HeLa	Ru(II) dipyridophenazine	104
R8	HeLa	Alexa Fluor 488	99
R8	KG1a, KG1, K562, A549	Alexa Fluor 488	105
R11	MEF	Klf4, c-Myc, Oct4, Sox2	122
R4, R6, R8	HL-60	17-desacetylvinblastineTrp	121
R8	K562	fluorescein, Alexa Fluor 555	74

Table 1-1. Continued

Peptide	Cell Line	Cargo	Ref.
R9	HeLa	HPMA polymer, Smac peptide	111
r9	HEK293, H9c2, L2	plasmid	155
R8	iPS cells	Texas Red	120
R7, R9	A549	plasmid	156
r8	NIH/3T3	fluorescein	157
r10	C2C12	fluorescein	36
R9	C6, B16F10, MDA-MB-231, MCF-7	fluorescein	158
R9	CHO	TMR, fluorescein labeled dextran	159
R16	CHO-K1, pgsA-745	plasmid, fluorescein	50
R9	HeLa	TMR	160
R9	HEK293T	NBD	60
R9; r9	HeLa, MC57, Jurkat	fluorescein	161
R9	CHO-K1, pgsA-745	biotin	98
R8	HeLa, A431	Alexa Fluor 488, siRNA, FITC-Dex40, TMR-Dex70	95
R8	HeLa	TMR, fluorescein, dexamethasone	96
R4, R12	HeLa	Alexa Fluor 488, HAtag	70
R3, R5, R7, R9, R11	U251-MG, mouse primary fibroblast, H520, U87MG, LNZ308, K562	TMR, EGFP, p53	162
r9	HeLa, Lovo, A549, MCF7, U2OS, HepG2, K562, NHDF, primary AML cells, PBMC, AML3639, primary colon adenocarcinoma cells,	fluorescein	163
R11	HEK293, HeLa	fluorescein	164
R8; r8; rR7; (rR)2R4; (rR)3R2; (rR)4; r2(rR)3	HeLa	fluorescein	165
R6	Huh7.5	siRNA	166
R8; r8, r12	HeLa, T98G	Alexa Fluor 488, FITC-Dex-70, p53C' peptide, $p27^{Kip1}C$ peptide, PAD peptide	103
R4, R12	CHO-K1, HeLa	Alexa Fluor 568	88
R5, R7, R9, R11	A549	plasmid	118
R9	CHO	TMR	97

Table 1-1. Continued

Peptide	Cell Line	Cargo	Ref.
R9	A549	quantum dots	[167]
R8	HeLa	fluorescein, saporin	[102]
R9	HeLa	fluorescein	[168]
R9	HeLa, HEK293	TALEN	[117]
R8	HeLa	Alexa Fluor 488	[169]
R9	HeLa	fluorescein, siRNA	[89]
R9	CHO-K1, pgsA-745	biotin	[73]
R8	T98G,	PNA	[170]
R8, R15	CHO-K1	siRNA	[171]
R9	PT45, HepG2	Fluorescein, ferrocene, ruthenocene	[172]
R8	HeLa	Lissamine rhodamine B	[173]
R9; r9	TE671	Cre recombinase, biotin	[174]
R9	HeLa	TMR	[175]
R9	Huh-7, HeLa	plasmid	[116]
R9	Jurkat	FITC-siRNA	[176]
R6, R7, R8, R9	HeLa	fluorescein	[177]
R11	T24	fluorescein, p53C peptide, Con peptide	[114]
R9	A549, HEK293	plasmid	[178]
R8	HeLa	fluorescein	[179]
R8; r8	Caco-2	nanoparticle	[180]
R8	HeLa	Alexa Fluor 488, TMR, Cre recombinase	[181]
R9	Huh-7, HeLa	TMR, plasmid	[182]
R9	MA-104, Caco-2	Fluorescein	[183]
R8	MCF-7, MDA-MB-231	methotrexate (MTX), fluorescein	[184]

1.5. Membrane oxidation and its role in membrane translocation activity

The delivery efficiencies of polyarginine CPPs are often sub-optimal such that most of associated cargo remains trapped in the endocytic organelles. One approach to overcome this problem is to enhance endosomal release by light irradiation, also known as photochemical internalization (PCI)[160, 185, 186]. Upon exciting the photosensitizer conjugated to the CPPs, generated reactive oxygen species (ROS) oxidize the adjacent membrane which leads to the efficient translocation of the peptide. With the photosensitizer alone, the inability to permeabilize the lipid bilayer indicates the importance of interactions between the CPPs and oxidized membrane components in the translocation activity[55, 160, 187].

The oxidation of the membrane can be induced by artificial photoradiation, but can also take place under physiological conditions. Lipid peroxidation has been shown to exist under physiological conditions and relates to the development of cardiovascular disease, diabetes, renal dysfunction, neurological disorders, lung injury and cancer[188-190]. Oxidized lipids also play important roles in modulating intracellular signaling and serving as markers for innate and adaptive immune recognition[189]. Cellular antioxidants, such as ascorbic acid and α-tocopherol, and detoxifying enzymes, such as superoxide dismutase (SOD) and glutathione peroxidase (GPx) can prevent the initiation and progression of oxidative damage[191, 192]. It has been shown that oxidized membrane components enhance

the electropermeabilization of the membrane. Cells treated with oxidizing compounds displayed greater electroporation efficiency[193, 194]. Results obtained from i*n vitro* and *in silico* studies suggest that the generation of oxidized phospholipids, as a result of membrane oxidation, altered membrane fluidity and permeability[195-197].

1.6. Goal of this study

Membrane oxidation has been shown to play a role in the efficiency of membrane permeation in electroporation and as a way to translocate across the membrane by photo-induction. It is, however, unclear how innate membrane oxidation levels would correlate to the delivery efficiency of polyarginine CPPs. In order to address this issue, this study first focused on identifying a highly efficient polyarginine CPP and established its cellular entry route. Whether the cellular membrane oxidation level affects peptide penetrating activity will be evaluated in cultured cells, by altering the surrounding cellular oxidative stresses. The cell membrane oxidation level under different culture conditions was quantitatively analyzed with a fluorescent probe. Moreover, the important component of oxidized membrane that involves in the mediation of membrane translocation of the peptide was analyzed *in cellulo* and *in vitro*.

2. MEMBRANE OXIDATION MEDIATES DIRECT PLASMA MEMBRANE TRANSLOCATION OF CELL-PENETRATING PEPTIDES[1]

2.1. Introduction

It is well appreciated that oxidation occurs during typical tissue culture growth conditions and that oxidized lipids and proteins are physiologically relevant components of cellular membranes[198, 199]. In principle, the relative abundance of these species varies depending on the level of oxidative stress attacking cells and on the efficiency of various repair mechanisms. Membrane oxidation has already been shown to affect transport processes such as viral infections, the diffusion of small-molecule drugs across lipid bilayers, or electroporation[194, 200, 201]. Based on these observations, I postulated that membrane oxidation might also modulate the cytosolic penetration of CPPs.

2.2. Results

2.2.1. Identification of efficient CPPs and robust cytosolic penetration assay

To identify a CPP construct that would penetrate cells efficiently, I first synthesized a group of linear polyarginine peptides that contains an increasing number of arginine residues (from 5 to 13) and labeled them with the fluorophore tetramethylrhodamine (TMR) for monitoring the cytosolic penetration by using

[1] Reprinted with permission from "Membrane oxidation enables the cytosolic entry of polyarginine cell-penetrating peptides" by Wang, T.-Y., Sun, Y., Muthukrishnan, N., Erazo-Oliverase, A., Najjar, K., and Pellois, J.-P., 2016. *The Journal of Biological Chemistry*, 291(15): 7902-7914. Copyright 2016 by the American Society for Biochemistry and Molecular Biology.

fluorescence microscopy. Peptides were synthesized with all L or all D amino acids (named as L-CPPs or D-CPPs respectively) (Figure 2-1). The peptides containing seven or fewer arginines showed no apparent cytosolic penetration in human skin fibroblasts (human dermal fibroblast, HDF, and immortalized human skin fibroblast, MCH58). In contrast, the peptide with 9 arginine residues displayed cytosolic penetration in MCH58 cells but not in HDF cells. Finally, peptides with 11 or 13 arginines displayed significant levels of cytosolic penetration in both cell types (Figure 2-2). Penetration was established by observing nucleolar staining by the peptides at high magnification (100X) (Figure 2-3). This staining is common for arginine-rich peptides and, because cytosolic entry presumably precedes nucleolar staining, it indicates that CPPs reach the intracellular cytosolic/nuclear milieu[70, 94, 107, 202, 203]. Importantly, this specific staining was observable at 20X magnification for D-CPPs but not for L-CPPs (Figure 2-3). This is presumably because, unlike the protease-resistant D-CPPs, L-CPPs degrade rapidly inside cells. Consequently, the fluorescence associated with L-CPPs was more diffuse overall and nucleolar staining was not clearly detectable at low magnification. In turn, at low magnification the cytosolic/nucleolar signal could not be convincingly distinguished from unrelated signals (peptides inside endosomes, peptides bound to cell surface, etc.), making quantification of the penetration of L-CPPs problematic and unconvincing. In contrast, quantification of cell penetration was straightforward with D-CPPs as these reagents led to unequivocal nucleolar/cytosolic staining at a magnification compatible with surveying a large number of cells. I therefore focused on this class of reagent for the rest of the study and used a penetration assay that relies on simply counting the number of cells that show

nucleolar staining in a culture after incubation with peptides. In this assay, dead cells are identified by staining with the dye SYTOX Blue. Overall, cells displaying nucleolar staining and excluding SYTOX Blue are considered positive for peptide cytosolic penetration (presented as Penetration (+) (%) in Figures).

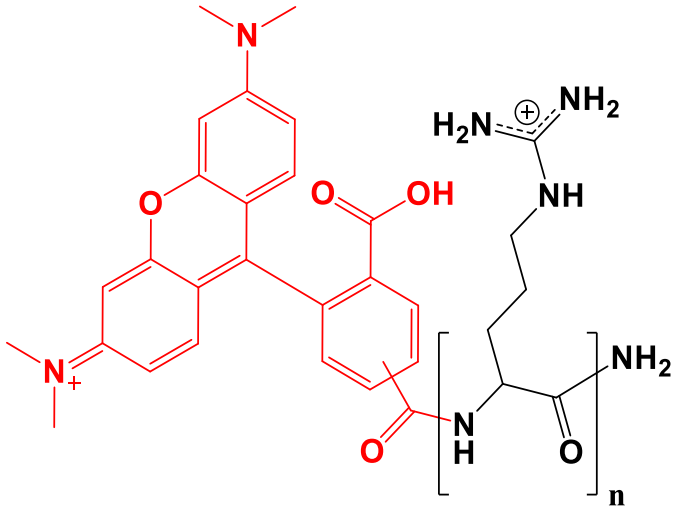

TMR-Rn, n = 5, 7, 9, 11, and 13

Figure 2-1. Structures of TMR-Rn peptides.

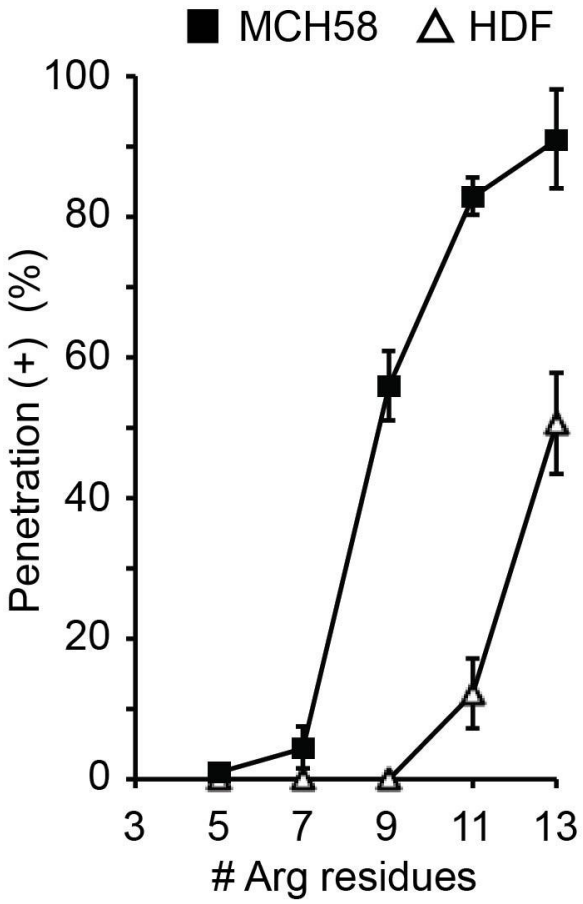

Figure 2-2. Delivery efficiencies of polyarginine peptides in HDF and MCH58 cells. To identify polyarginine CPPs with high cytosolic delivery efficiencies, HDF or MCH58 cells were incubated with each peptides containing five to thirteen arginine residues (TMR-Rn, n = 5-13). The N-terminus of peptide was labeled with a red fluorophore, tetramethylrhodamine (TMR), in order to visualize the localization of the peptide inside the cell after delivery. The cells were incubated with 3 μM peptide for one hour at 37°C. After incubation, unincorporated peptides were removed by washing cells with PBS and heparin solution (1 mg/mL heparin sodium salt in L-15 medium) for three times. The cells were imaged with fluorescence microscope by detecting TMR fluorescence (RFP filter). Penetration (+) (%) was scored as the cells with distinct cytosolic distribution and nucleoli staining of the peptide but without nuclear staining of cell-impermeable dye SYTOX Blue.

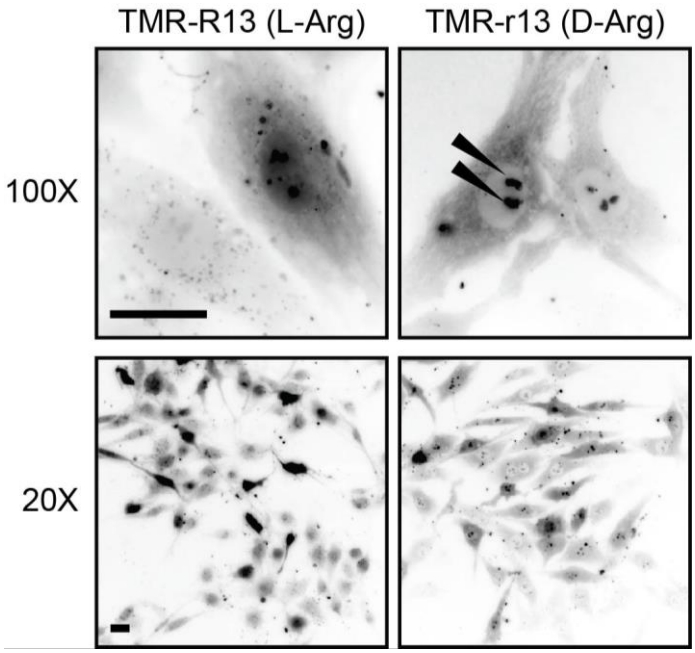

Figure 2-3. Representative images of MCH58 cells incubated with the TMR-R13 or TMR-r13 peptide. TMR-R13 and TMR-r13 were synthesized with L-arginine (L-Arg) and D-arginine (D-Arg), respectively. Nucleolar staining can be seen with TMR-R13 peptide at 100X magnification. However, this staining is less pronounced upon 20X imaging. In contrast, nucleolar staining is visible with the TMR-r13 peptide using both 100X and 20X imaging (highlighted by arrows). The acquired images are inverted monochromes of TMR fluorescence emission (RFP filter). Scale bars, 20 µm.

As the most active compound in the series, TMR-r13, where r is the one letter code for D-Arg, was characterized in greater detail. The dose-dependence of TMR-r13 on penetration showed that the peptide penetrates both MCH58 and HDF cells equally efficiently at 5 μM or above (Figure 2-4). At lower concentrations, MCH58 are, however, more prone to penetration than HDF. Notably, cells examined were resistant to staining with SYTOX Blue and were variable and proliferating up to sixty hours after incubation with the peptide (Figure 2-5 and 2-6). The rate of proliferation of cells treated with TMR-r13 was markedly lower than untreated cells, a phenomenon that I attribute to the prolonged retention of the protease-resistant CPP inside cells (unpublished data). Overall, TMR-r13 nonetheless displays a cytosolic penetration activity that is high, easily quantifiable, and non-toxic at the concentrations tested.

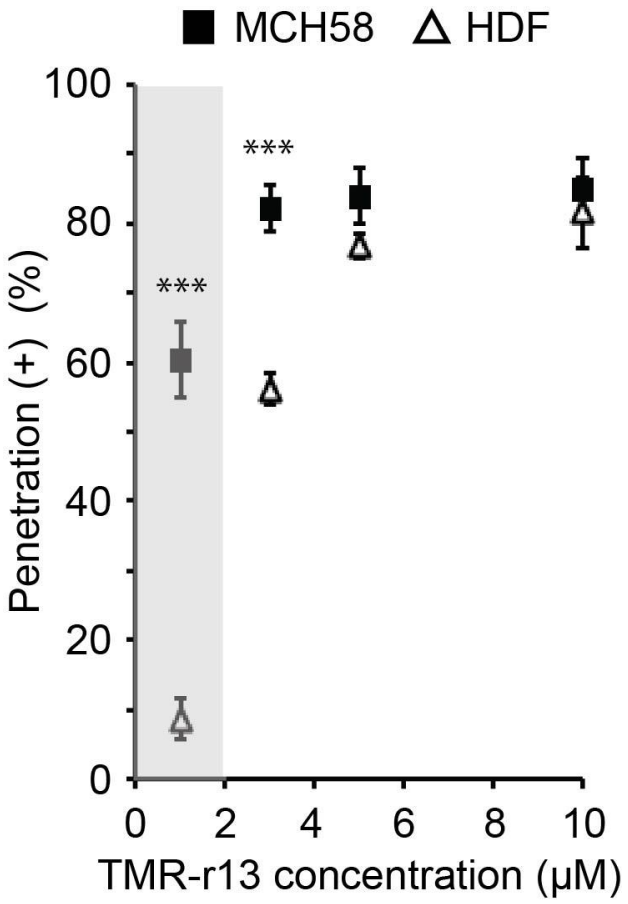

Figure 2-4. Cytosolic penetration efficiency and cytotoxicity of TMR-r13 peptide in MCH58 and HDF cells. Dose-dependence of the cytosolic penetration of TMR-r13. The efficiency of cytosolic penetration was measured in MCH58 and HDF cells as the percentage of cells positive for nucleolar peptide staining and negative for SYTOX Blue staining. The region marked in grey highlights how MCH58 cells are significantly more prone to cellular penetration than HDF cells at 1 μM of TMR-r13 peptide. *** represents $P \leq 0.001$ compared to HDF cells at the same peptide concentration.

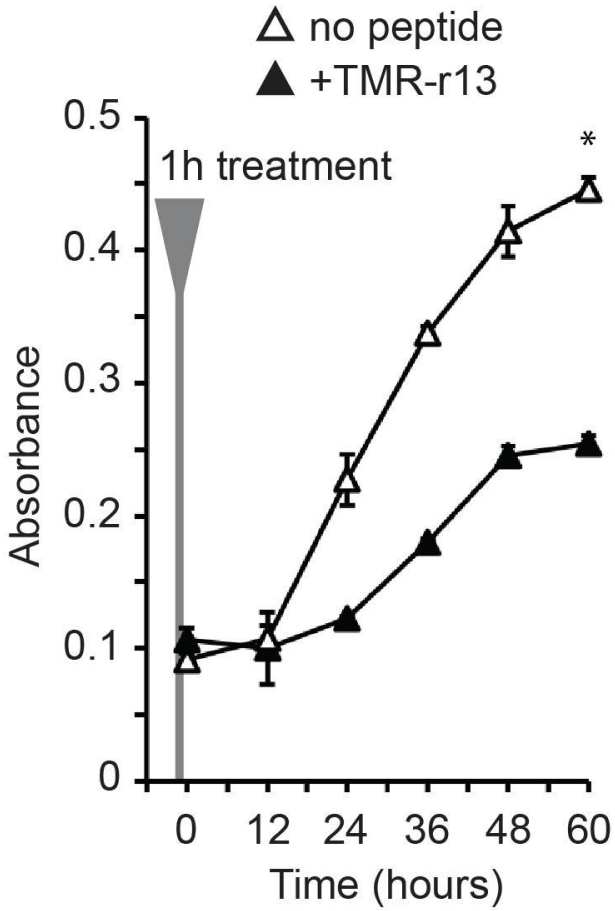

Figure 2-5. The proliferation rate of HDF cells treated with TMR-r13 peptide is reduced when compared to untreated cells. The cell proliferation of HDF cells were measured using the MTT assay. Detailed steps for performing MTT assay can be found in the method section. Briefly, cells were treated with 5 μM TMR-r13 for 1 hour at 37ºC. After removing extracellular peptides, cells were cultured for up to 60 hours. The proliferation rate of cells were examined by measuring the production of formazan as an indicative of the enzymatic activity of a mitochondrial reductase. The measurement was carried out every 12 hours. The production of formazan was quantified by measuring the absorbance at 570 nm. Cells without pre-treating with TMR-r13 peptide serve as a control. * represents $P \leq 0.05$ compared to untreated cells.

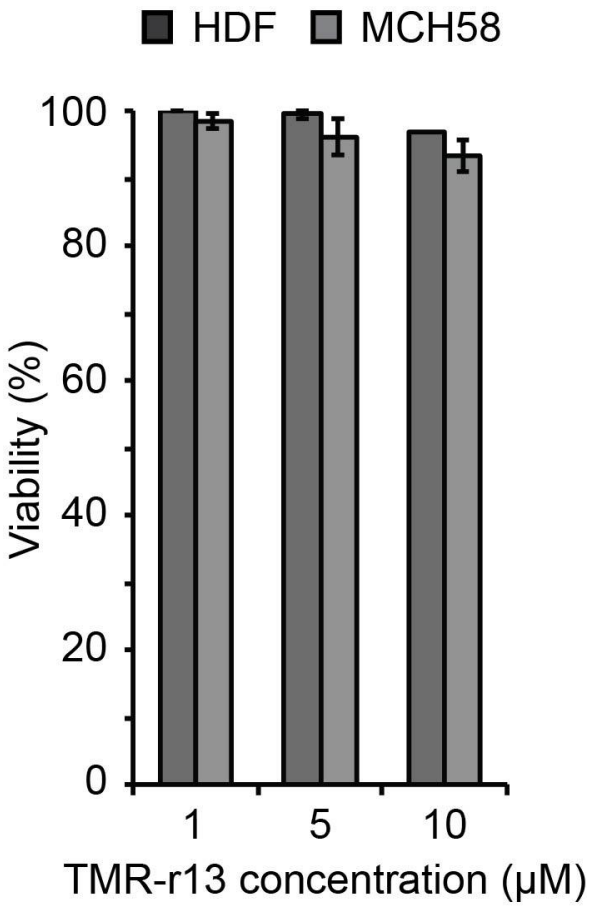

Figure 2-6. Treatment of HDF and MCH58 cells with TMR-r13 peptide did not reduce cell viability. The cell viability of HDF and MCH58 cells after incubating with TMR-r13 was determined by SYTOX Blue exclusion assay. After peptide incubation, cells were incubated with 5 μM SYTOX Blue for 5 min. The signal distribution of SYTOX Blue inside the cells were determined by fluorescence microscope using CFP filter. Cells without staining with SYTOX Blue were considered as viable.

2.2.2. TMR-r13 peptide directly translocates across the plasma membrane

In cells without a strong cytosolic/nucleolar signal, TMR-r13 can be seen trapped inside endosomes (Figure 2-7), indicating that TMR-r13 is capable of endocytosis. This mode of entry is common for arginine-rich CPPs as these compounds are often internalized by macropinocytosis. This then raises the question of whether endocytosis is a required step preceding cytosolic entry or whether it is a process occurring in parallel with an endocytosis-independent penetration mechanism. To address this, I first tested the effect of amiloride and bafilomycin, inhibitors of macropinocytosis and endosomal acidification, respectively, on cellular entry. These inhibitors did not decrease the cytosolic penetration activity of TMR-r13. Similarly, incubation with cells was performed at 4^{o}C, a condition that inhibits energy-dependent endocytic uptake, only led to a minor reduction in cell penetration (Figure 2-8). In addition, cytosolic penetration was achieved in a relatively high percentage of cells within 1 or 3 min of incubation, making a process involving endocytosis and endosomal escape upon slow endocytic maturation unlikely (typical time frame varies from 5 to 30 min) (Figure 2-9)[204]. Furthermore, TMR-r13 did not cause the release of fluorescent material preloaded within endosomes (Figure 2-10 and 2-11). In contrast, the positive control, dfTAT, an endosomolytic reagent, efficiently induced the endosomal escape of endocytosed material (Figure 2-11)[17]. This suggests that the cytosolic penetration of TMR-r13 does not involve leakage from the endocytic pathway. Overall, these data indicate that the peptide does not require endocytosis to gain access to the cytosol. In turn, exclusion of this possibility instead indicates that the peptide enters the cytosolic space by crossing the plasma membrane directly. To test whether the

plasma membrane translocation of the peptide enhanced the permeation of other molecules, TMR-r13 was co-incubated with fluorescent molecules of various sizes, including the small molecule SYTOX Green, fluorescently-labeled peptides (DEAC-k5, 0.9 kDa), and macromolecule enhanced green fluorescent protein (EGFP, 26.8 kDa). While TMR-r13 entered cells in all assays, no other fluorescent materials could be detected within cells, indicating that the TMR-r13 mediated translocation was not accompanied by transient membrane leakage (Figure 2-12).

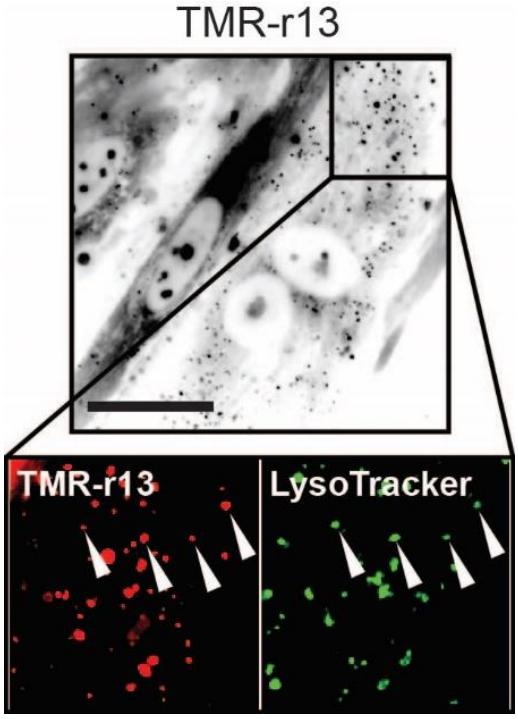

Figure 2-7. TMR-r13 is capable of internalizing into HDF cells through endocytosis. In HDF cells, a cell type less prone to cell penetration, the peptide shows a punctate distribution. The image is the inverted monochrome of fluorescence emission of TMR. The zoomed-in images show co-localization of puncta (highlighted by arrows) containing TMR-r13 (pseudocolored red) and LysoTracker (pseudocolored green), suggesting entrapment of TMR-r13 in acidic endocytic organelles. Scale bar, 20 μm.

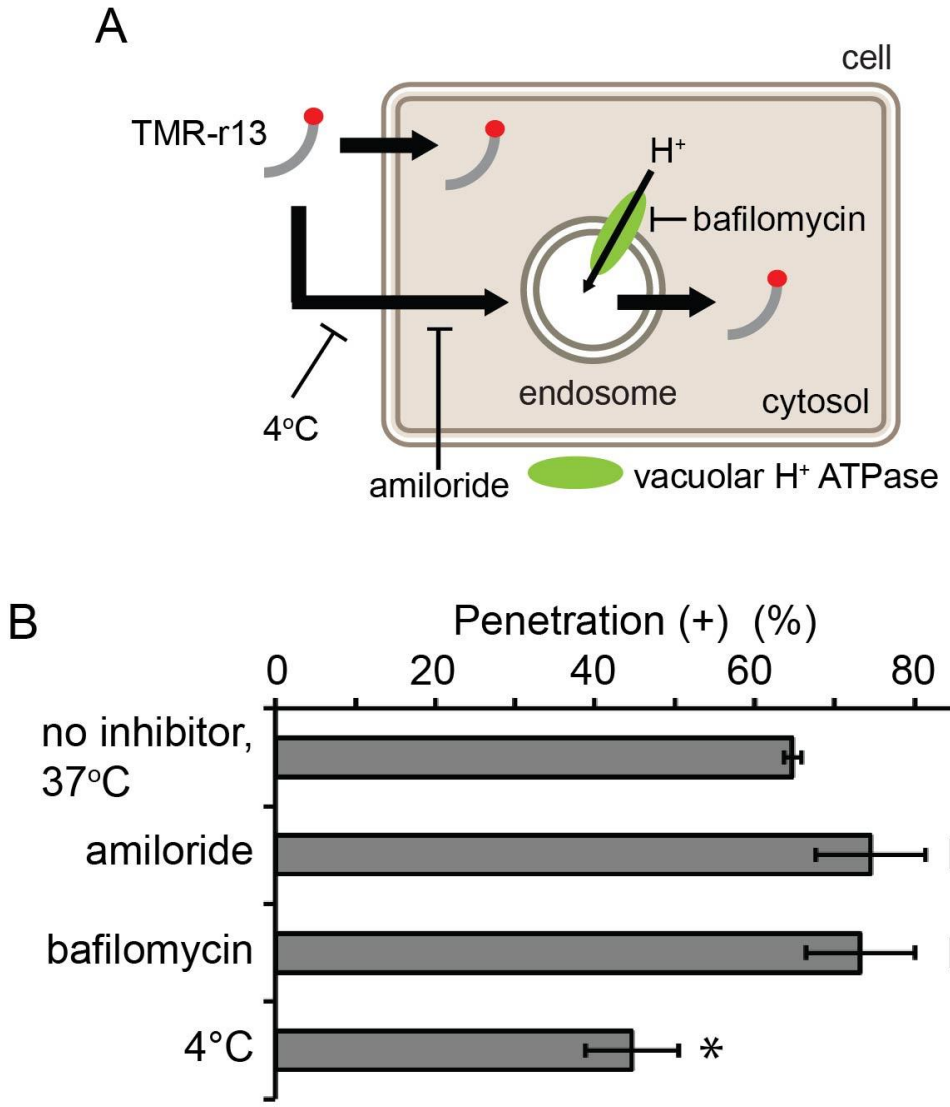

Figure 2-8. Inhibitors of endocytic processes do not prevent cytosolic penetration of TMR-r13 peptide. A, Scheme of inhibitory treatment on different endocytic processes. B, MCH58 cells were pretreated with 50 µM amiloride, 200 nM bafilomycin, or PBS supplemented with calcium and magnesium (no inhibitor, 37°C) for 20 min. Cells were then incubated with 1 µM TMR-r13 peptide in the presence of inhibitors for 1 hour. Alternatively, cells were maintained at 4°C during peptide incubation. NS (not significant) represents $P>0.05$ and * represents $P\leq0.05$ compared to cells with no inhibitor at 37°C.

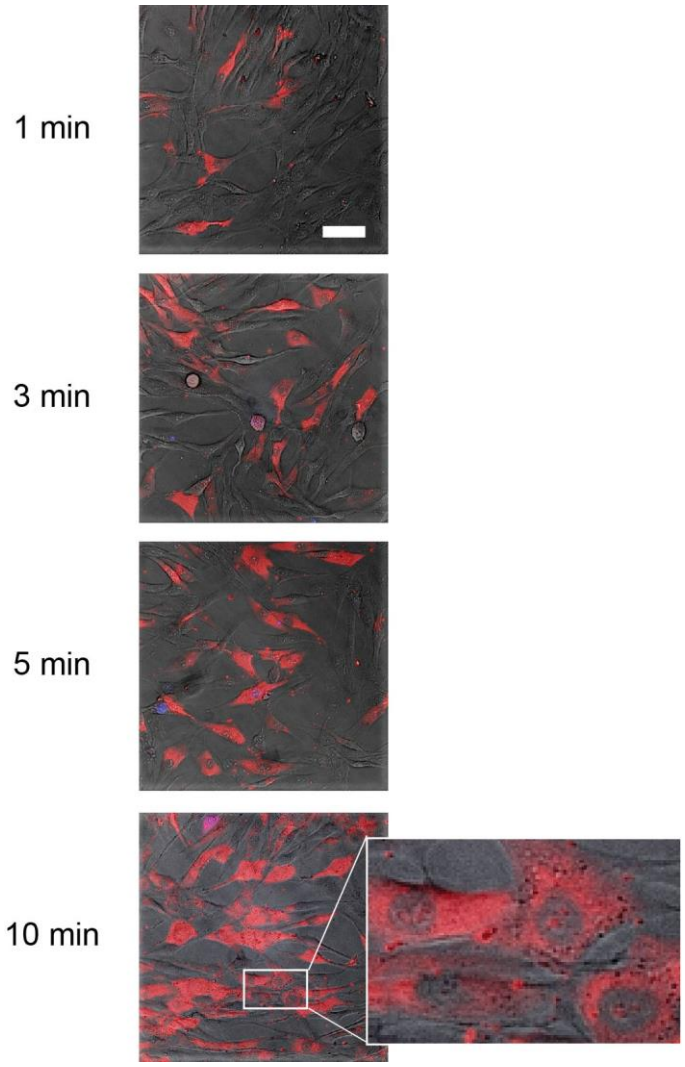

Figure 2-9. Fast cytosolic penetration of TMR-r13 peptide in MCH58 cells. MCH58 cells were treated with 5 µM TMR-r13 peptide for the indicated times. Images are the overlay of bright field, TMR-r13 peptide (pseudocolored red) and SYTOX Blue (pseudocolored blue). A zoomed-in image shows distinct nucleolar staining of delivered TMR-r13 peptide without SYTOX Blue staining. Scale bar, 50 µm.

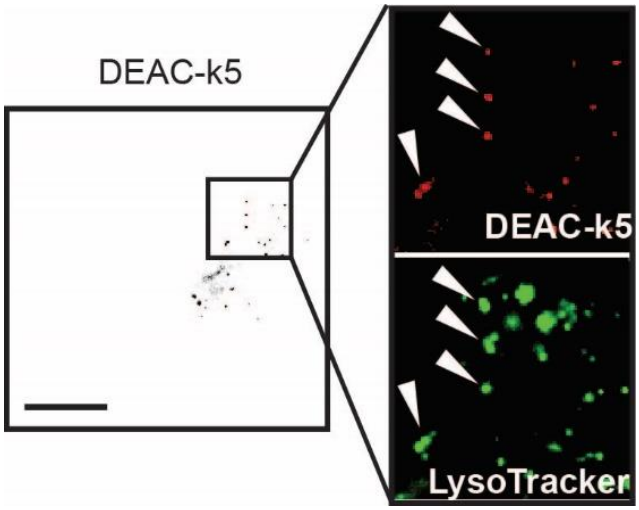

Figure 2-10. Entrapment of internalized DEAC-k5 peptide in the endocytic organelles of HDF cells. HDF cells were incubated with DEAC-k5 peptide (20 µM, 1 hour, k is the one-letter code for D-lysine). The image is the inverted monochrome of fluorescence emission of DEAC. Accumulation of DEAC-k5 peptide (pseudocolored red) within endocytic vesicles after 1-hour incubation is established by co-localization with LysoTracker (pseudocolored green) (co-localization is highlighted by arrows in the zoomed-in images). Scale bar, 20 µm.

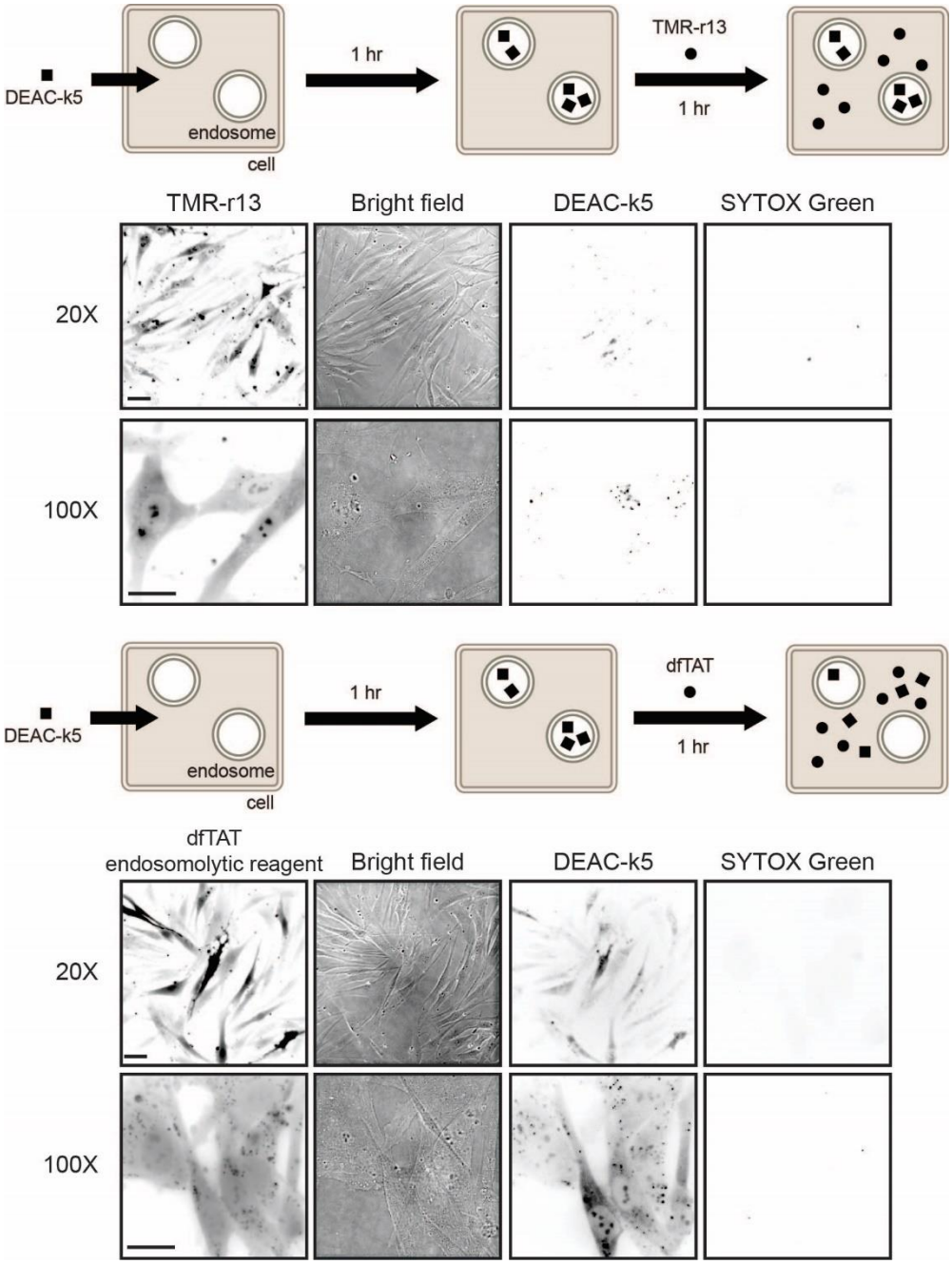

Figure 2-11. TMR-r13 peptide fails to release internalized DEAC-k5 peptide from endocytic pathway in HDF cells when the endosomolytic agent dfTAT peptide does. HDF cells were pre-incubated with 20 μM DEAC-k5 peptide for 1 hour. Cells were then treated with TMR-r13 or dfTAT peptide and imaged by fluorescence microscopy. The cells were not stained by SYTOX Green, indicating insignificant cytotoxicity after peptide delivery. The acquired images are inverted monochrome of fluorescence emission and monochrome of bright field imaging. Scale bar, 20 μm.

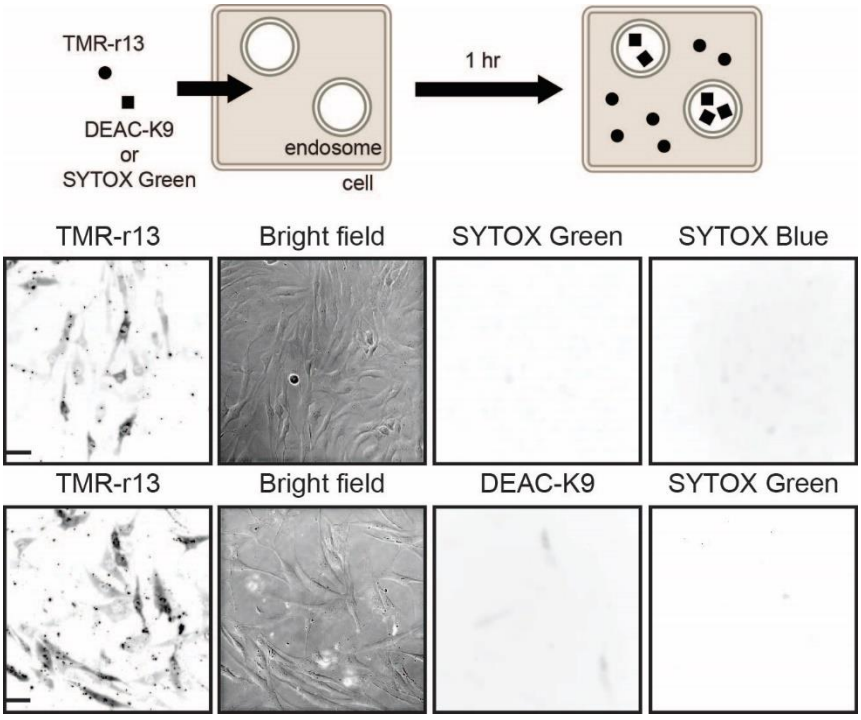

Figure 2-12. Membrane translocation by TMR-r13 peptide is not accompanied by penetration of the small molecule SYTOX Green or DEAC-K9 peptide. Cells were incubated for 1 hour at 37°C with both TMR-r13 peptide (1 µM) and SYTOX Green (5 µM), a green fluorescent cell-impermeable nuclear staining dye that can enter cells upon permeation of the plasma membrane. After peptide delivery, cells were washed and incubated with SYTOX Blue, a nuclear stain similar to SYTOX Green but with an extinct excitation wavelength. TMR-r13 peptide penetrated cells while excluding both SYTOX Green and SYTOX Blue. Similar results were obtained when SYTOX Green was substituted for DEAC-K9 (an oligolysine peptide labeled with the blue fluorophore DEAC). Fluorescence images are represented as inverted monochrome. Scale bars, 20 µm.

2.2.3. Reduced oxidative stress decreases cytosolic penetration of TMR-r13

The experiments described above were carried out with cells exposed to 20% oxygen during culture (ambient air supplemented with 5% carbon dioxide, standard protocol). If oxidation affects transport of the peptide across membranes as originally postulated, one would expect that reducing oxidative stress should decrease cytosolic penetration. In order to test this hypothesis, MCH58 cells were grown for a week at either 20% oxygen or in a sealed chamber flushed with 2% oxygen, 5% carbon dioxide, and 93% nitrogen. MCH58 cells were chosen for this assay because they appear to be more prone to cell penetration than HDF cells and therefore provide a cell line more adequate for inhibition studies (Figure 2-3). Cells were then exposed to TMR-r13 peptide (1 μM) for 1 hour and the number of cells positively displaying nucleolar staining was counted. Under these conditions, hypoxia did not appear to impact the percentage of cells positive for cell penetration (Figure 2-13). Yet, a more careful examination of the process showed significant differences when the incubation time with peptide was shorter (Figure 2-14). In addition, the overall amount of peptide entering cells, quantified by flow cytometry, was reduced when compared to 20% oxygen (Figure 2-14). This indicates that while cytosolic penetration is still possible at low oxygen levels, this process is partially inhibited, as less peptide is able to enter cells. Assuming that cytosolic penetration might still be permitted by oxidized species that remain present even at low oxygen tension, I next added an antioxidant cocktail to the growth media to further reduce oxidative stress experienced by cells. This cocktail includes pyruvate, α-tocopherol, Trolox, ascorbic acid, 2-phospho-L-ascorbic acid and sodium selenite. These species are either scavengers of

oxidants or cofactors of enzymes that deplete cells from oxidized species[205-208]. The antioxidant cocktail had a pronounced effect on reducing the percentage of cells positive for TMR-r13 peptide and, in combination with 2% oxygen, almost abolished cytosolic penetration (Figure 2-13).

Because TMR-r13 peptide is the most active compound tested in our polyarginine series, I next examined how hypoxia would impact a less potent peptide (Figure 2-3). For this assay, TMR-r9 peptide was tested since nona-arginine CPPs that are widely used as delivery agents[117, 124, 209]. When using MCH58 cells grown at 20% oxygen, the TMR-r9 peptide required an incubation concentration of 1 μM to achieve a penetration efficiency equivalent to that obtained with TMR-r13 peptide (approximately 65% penetration positive cells after 1 hour incubation). When these conditions were used with cells grown at 2% oxygen, the penetration of TMR-r9 peptide was abolished (Figure 2-15). Overall, this indicates that the impact of hypoxia is increasingly more pronounced as the potency of the CPP is reduced. Inversely, this also suggests that oxidative processes are required for the penetration of CPPs.

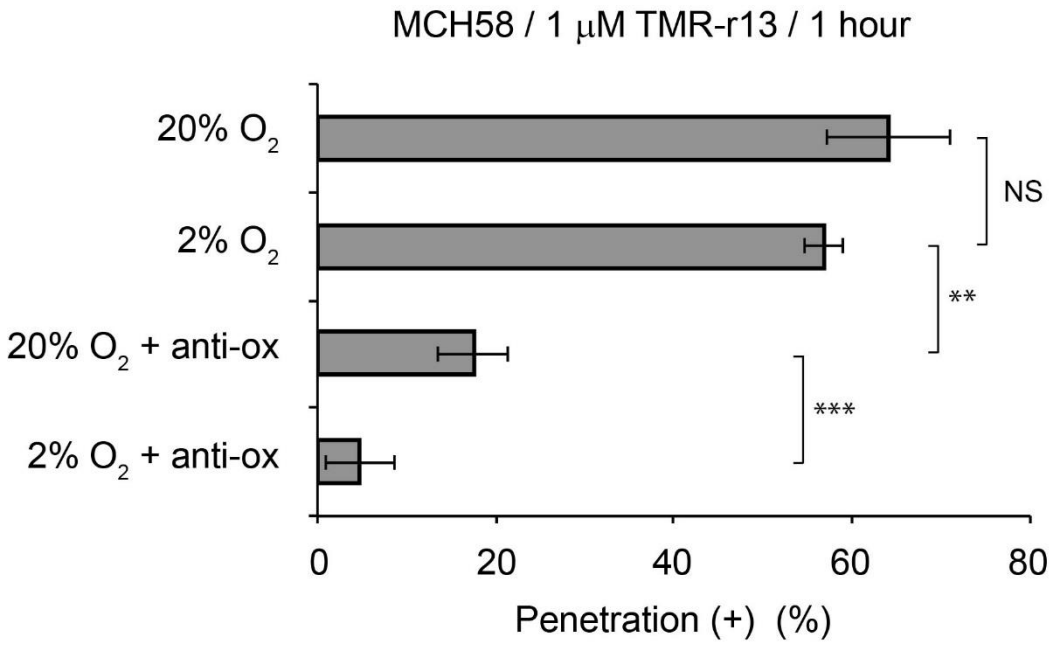

Figure 2-13. Conditions of reduced oxidative stress decrease cytosolic penetration of TMR-r13 peptide. MCH58 cells were grown under atmospheric (20% oxygen) or hypoxic (2% oxygen) conditions, in the presence or absence of a cocktail of antioxidants. Cells were then treated with 1 μM TMR-r13 peptide for 1 hour. Anti-ox corresponds to the antioxidant cocktail. NS represents $P>0.05$, ** represents $P\leq0.01$, and *** represents $P\leq0.001$.

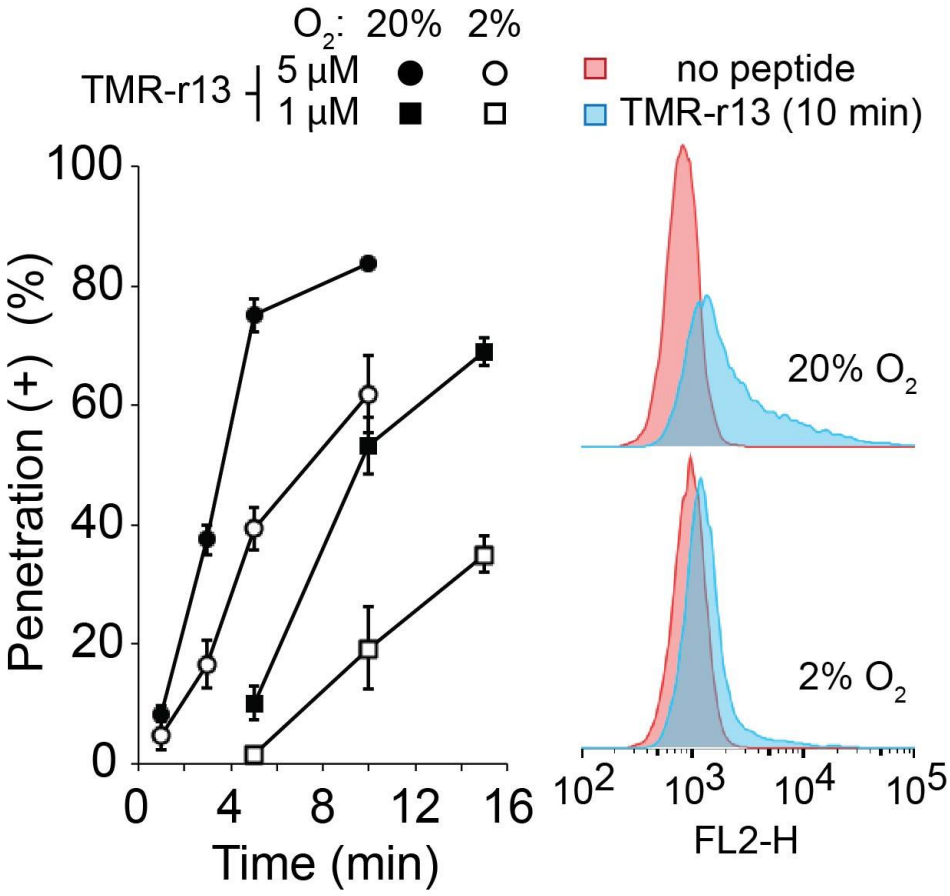

Figure 2-14. Cytosolic penetration of TMR-r13 peptide is slower in cells grown at 2% than 20% oxygen. MCH58 cells cultured under 20% O_2 were incubated with 5 µM TMR-r13 peptide for 1, 3, 5, and 10 min. The cytosolic delivery efficiency of TMR-r13 was determined by measuring the TMR signal using fluorescence microscope. In parallel, the experimental conditions were carried out with cells cultured under 2% O_2. Similarly, both cells cultured under 20% and 2% O_2 were incubated with 1 µM TMR-r13 peptide for 5, 10, and 15 min. Hypoxia also reduces the amount of peptide penetrating cells, as shown by flow cytometry analysis (on the left) of cells incubate with 1 µM TMR-r13 for 10 min. FL2-H is signal intensity of sample in the FL2 channel (Ex = 488 nm/Em = 585 ± 40 nm, used for detection of TMR-r13).

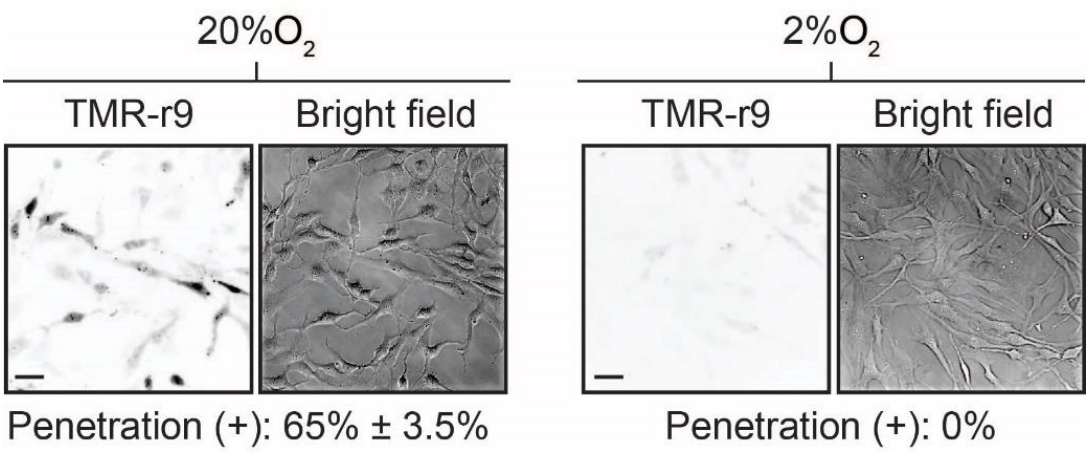

Figure 2-15. Cytosolic penetration of TMR-r9 peptide is abolished in MCH58 cells cultured at 2% oxygen. MCH58 cells cultured at 20% or 2% oxygen were incubated with 1 μM TMR-r9 peptide for 1 hour and imaged using fluorescence microscopy. Acquired images are inverted monochromes of TMR fluorescence emission (RFP filter) and monochromes of bright field imaging. Scale bars, 20 μm.

2.2.4. Increasing oxidation enhances cytosolic penetration of TMR-r13

If a reduction in oxygen tension decreases cell penetration, one would expect that increasing oxidative stress might conversely enhance cellular entry. To test this hypothesis, cells were partially oxidized with oxidants and the impact of these reagents on penetration was established. In these assays, I used HDF cells because of their lower propensity for polyarginine cytosolic penetration (Figure 2-3). Cells were treated with the lipophilic oxidant cumene hydroperoxide (cumene-OOH) or with hydrogen peroxide (H_2O_2). The concentration of oxidants was kept low in these experiments in order to not impact cell viability and proliferation (Figure 2-16). As tested using the MTT assay, the similarity between the proliferation rates of treated versus untreated cells is an indication that cells remain relatively healthy after mild oxidation. Treatment with both cumene-OOH and H_2O_2 increased the cytosolic penetration efficiency of TMR-r13 peptide (Figure 2-17). Cumene, a non-oxidant control compound, did not significantly impact TMR-r13 delivery, indicating that the lipid bilayer insertion of the cumene moiety of cumene-OOH is not significantly altering the permeability of the membrane. Moreover, treatment with cumene-OOH increased the cytosolic penetration efficiency of TMR-r13, TMR-r11, and TMR-r9 peptides at detectable levels (Figure 2-18). However, other polyarginine or polylysine CPPs such as TMR-R7 or DEAC-K9 peptide did not penetrate these oxidized cells, indicating that the cells are not simply more permeable to all peptides (data not shown).

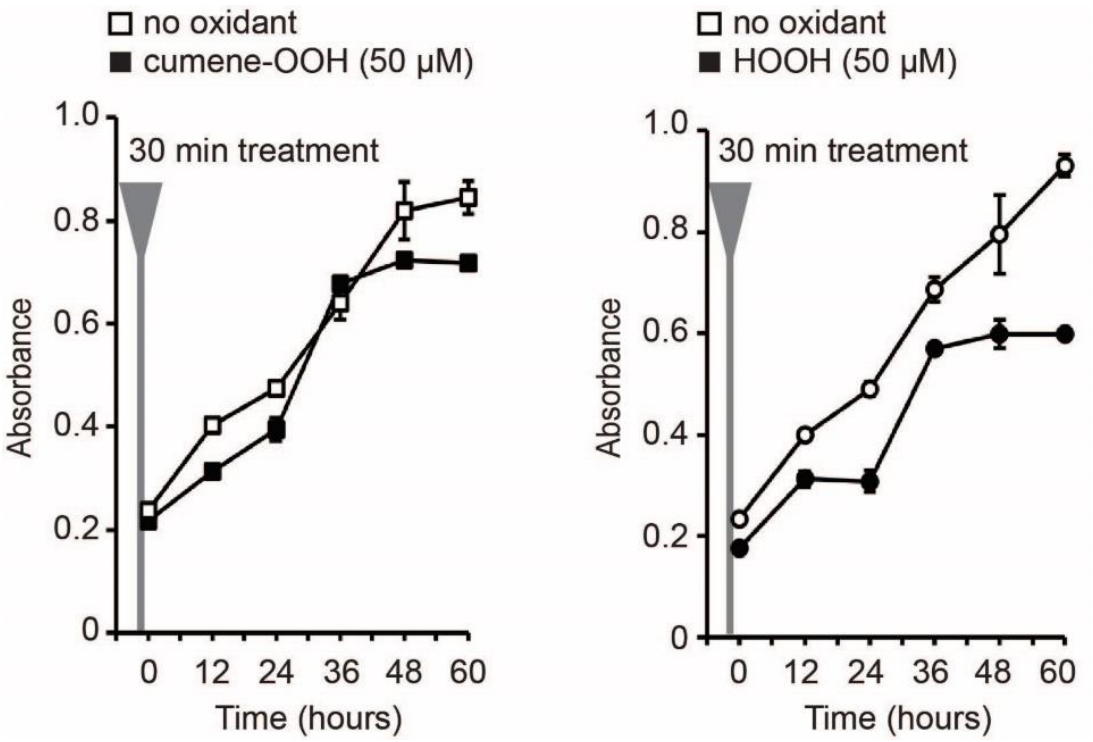

Figure 2-16. HDF cells treated with cumene-OOH display a proliferation rate similar to untreated cells. HDF cells were challenged with 50 μM cumene-OOH or H_2O_2 for 30 min and monitored the proliferation rate by using MTT assay.

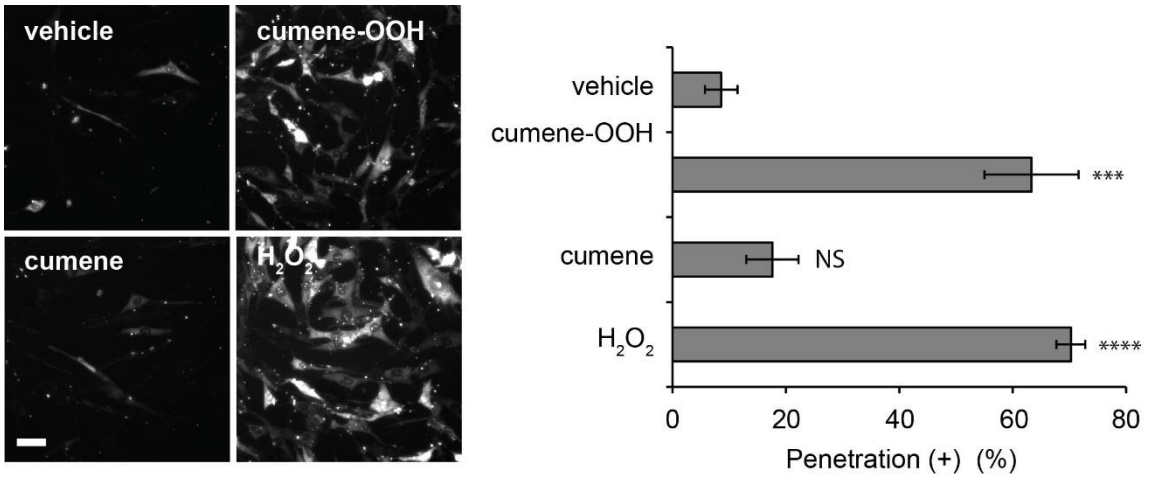

Figure 2-17. Cell penetration activity of TMR-r13 peptide in HDF cells increases significantly in the presence of oxidants. HDF cells were pretreated with lipophilic oxidant cumene hydroperoxide (cumene-OOH), cumene, or H_2O_2 for 30 min and incubated with 1 μM TMR-r13 peptide for 1 hour. *** represents $P \leq 0.001$, **** represents $P \leq 0.0001$, and NS represents $P > 0.05$ compared to vehicle (PBS supplemented with calcium and magnesium). Scale bars, 20 μm.

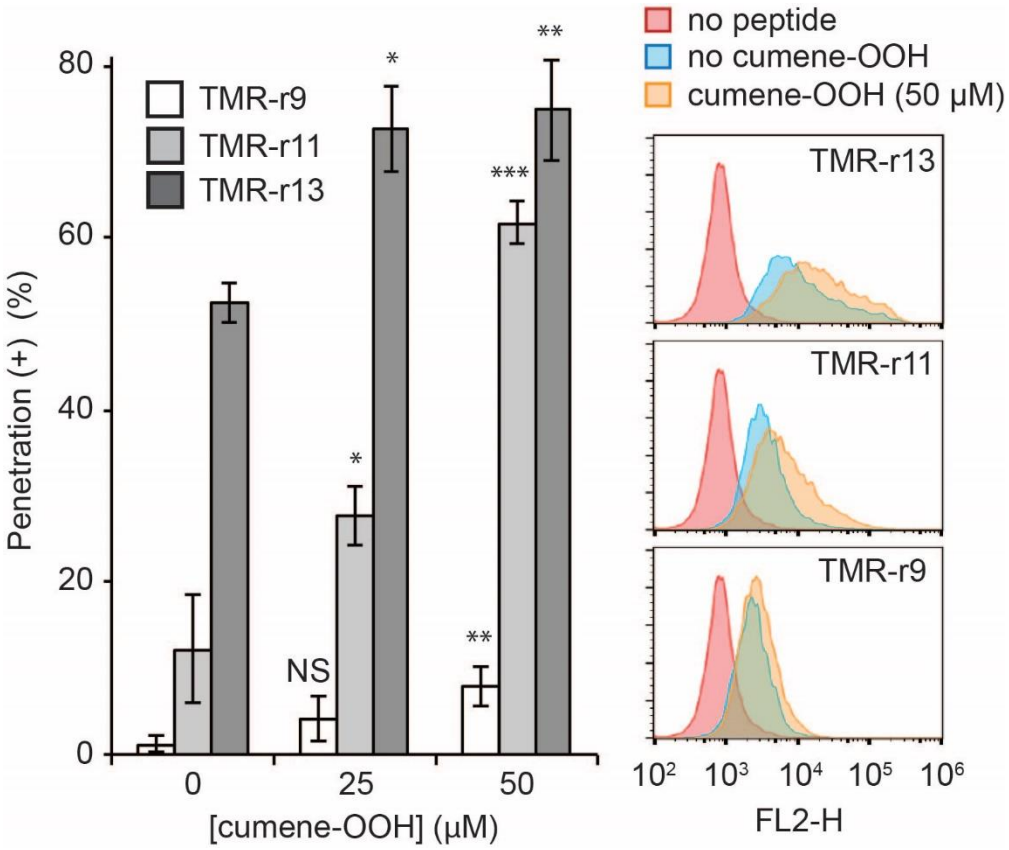

Figure 2-18. Cumene-OOH increases the activity of TMR-r13, TMR-r11, and TMR-r9 peptides in a dose-dependent manner in HDF cells. HDF cells were pretreated with cumene-OOH (0, 25, or 30 μM) for 30 min and then incubated with the peptides (3 μM) for 1 hour. The cytosolic penetration of peptides were quantified by fluorescence microscope (histogram) and flow cytometry. NS represents $P>0.05$, * represents $P\leq0.05$, ** represents $P\leq0.01$, and *** represents $P\leq0.001$ compared to cells not treated with cumene-OOH. FL2-H is the signal intensity of sample in the FL2 channel (Ex = 488 nm/Em = 585 ± 40 nm, used for detection of TMR).

2.2.5. Membrane oxidation correlates with cell penetration of TMR-r13 peptide

Oxidative stress can result in a broad spectrum of effects. Given that the TMR-r13 peptide appears to directly cross the plasma membrane of cells, I next chose to determine whether membrane oxidation correlates with the efficiency with which the peptide penetrates cells. First, I examined whether the conditions utilized in the previous oxidation experiments led to changes in membrane chemistry. The lipophilic reporter C11-BODIPY$^{581/591}$ was used to quantify the oxidation state of cellular cellular membranes. The fluorescence emission of C11-BODIPY$^{581/591}$ changes from red (595 nm) to green (520 nm) upon oxidation[210]. The susceptibility of C11-BODIPY$^{581/591}$ to oxidation is equivalent to that of endogenous polyunsaturated lipids present in cell membranes; a change in fluorescence of this reporter can be used to infer overall lipid oxidation. An increase in green fluorescence was observed by both microscopy and flow cytometry when cells grown at 20% oxygen were treated with an increasing amount of cumene-OOH (no increase was observed with the control compound cumene). This indicates that cellular membranes are oxidized by the lipophilic oxidant (Figure 2-19). Notably, the cytosolic penetration of TMR-r13 peptide correlated positively with the green fluorescence of C11-BODIPY$^{581/591}$ (Figure 2-19), supporting the notion that the oxidized membrane components might be involved in the membrane translocation of the peptide.

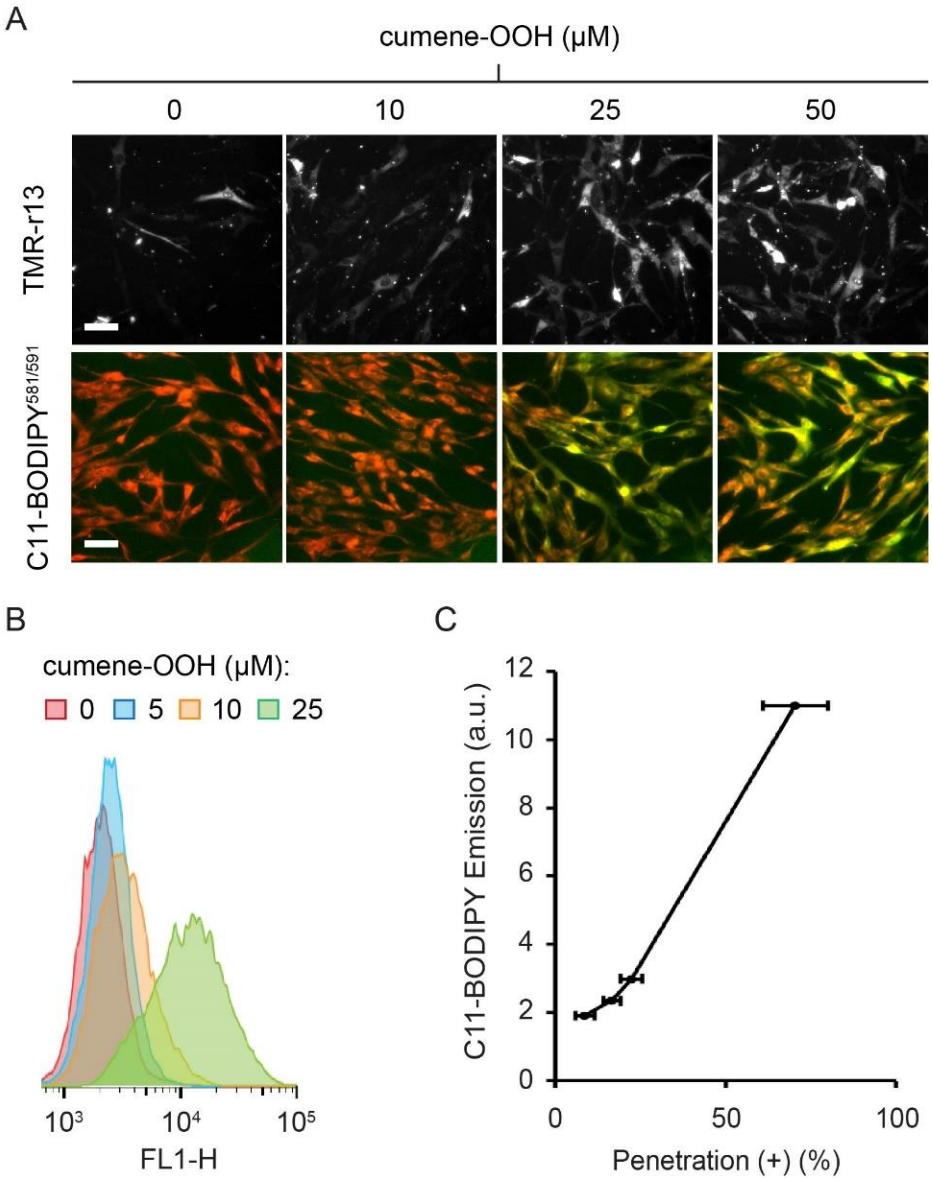

Figure 2-19. Membrane oxidation and cytosolic penetration of TMR-r13 peptide are positively correlated. A, HDF cells were treated with cumene-OOH at various concentrations (0, 10, 25 or 50 μM) for 30 min and the cytosolic penetration efficiency of delivered TMR-r13 peptide (1 μM, 1 hour) was detected. Images of TMR-r13 peptide delivery are monochromes of TMR fluorescence emission (RFP filter). In parallel, membrane oxidation level after cumene-OOH treatment was measured using the green fluorescence of the lipophilic oxidation reporter C11-BODIPY$^{581/591}$. Scale bar, 20 μm. B, Flow cytometry analysis of C11-BODIPY$^{581/591}$ green fluorescence signal upon oxidation of HDF cells. FL1-H corresponds to the signal intensity of sample in the FL1 channel (Ex = 488 nm/Ex = 533 ± 30 nm). C, The correlation between the geometric mean of the C11-BODIPY$^{581/591}$ emission and the cytosolic penetration efficiency is reported.

Since MCH58 cells are more prone to cell penetration than HDF cells (Figure 2-3), I next examined whether the variation in peptide activity between these two cell types could be accounted for by a difference in the overall level of membrane oxidation. The previous C11-BODIPY$^{581/591}$ assay was, however, not sufficiently sensitive to compare cells cultured under 20% oxygen, as shown in Figure 2-19 that only a weak C11-BODIPY$^{581/591}$ green fluorescence signal is obtained when cumene-OOH is absent. Therefore to circumvent this issue, an assay using diphenyl 1-pyrenylphosphine (DPPP) was performed instead. DPPP is a non-fluorescent lipophilic compound that reacts stoichiometrically with lipid hydroperoxides to yield a fluorescent DPPP oxide[211]. The MCH58 and HDF cells cultured at 2% or 20% oxygen were incubated with DPPP and the fluorescence of DPPP oxide obtained was quantified. The number of cells present in each sample was analyzed by flow cytometry. Given that MCH58 and HDF cells have similar morphologies and sizes, the DPPP oxide fluorescence was then normalized to the total number of cells for comparison. As shown in Figure 2-20, the fluorescence of DPPP oxide was significantly greater in cells grown at 20% oxygen than in cells grown at 2% oxygen. In addition, MCH58 cells were also consistently more fluorescent than HDF cells under similar growth conditions, suggesting higher levels of lipid peroxides in MCH58 cells than in HDF cells. Overall, these data indicate a positive correlation between membrane oxidation and cell penetration of the peptide.

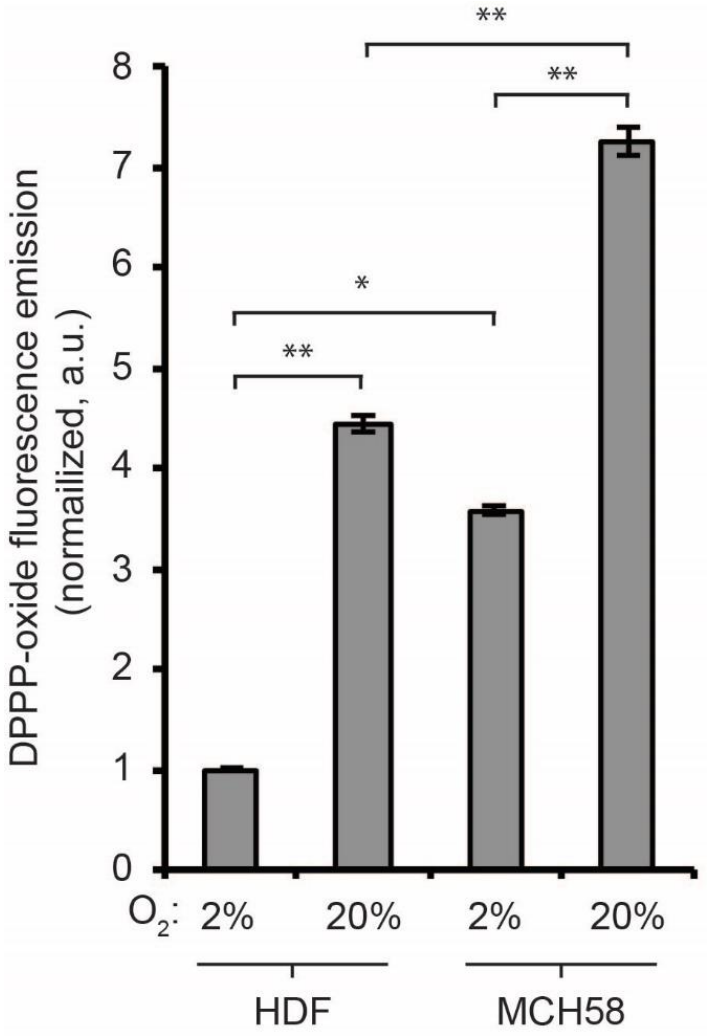

Figure 2-20. The level of lipid peroxides in the membrane of MCH58 cells is higher than of HDF cells. The membrane oxidation of cells were compared by using the lipophilic DPPP probe. The fluorescence of oxidized DPPP present in cellular membranes of cells grown at 2% or 20% oxygen is reported as normalized to the total number of cells per sample and to the least oxidized sample (2%, HDF cells). * represents $P \leq 0.05$ and ** represents $P \leq 0.01$.

2.3. Discussion

My results establish that the conditions utilized during cell growth markedly impact the permeability of cells for polyarginine CPPs. Under all conditions tested, the oxidation index positively correlates with the cell penetration efficiency of examined CPPs (Figure 2-21). Given that the translocation of the peptides appears to take place at the plasma membrane, it is reasonable to postulate that oxidation alters the properties of plasma membrane and that certain oxidized membrane components mediate or facilitate the translocation process. Differences in the level of oxidative damage or, conversely, how efficiently cells repair oxidative damage, could possibly explain the variability in CPP performance from cell to cell, from cell type to cell type, or among various experimental conditions (*e.g.* media with or without antioxidant supplements).

An important question is whether membrane oxidation is necessary for the cytosolic penetration of CPPs or merely facilitates the process. Anaerobic conditions are lethal to human cells and suppression of oxidative stress generation by the complete removal of oxygen is therefore not testable. In contrast, cells thrive in the environment of 2% oxygen[212, 213]. This growth condition was however not sufficient to completely abolish the cytosolic penetration of CPPs. In addition, the presence of lipid peroxides was able to be detected in the cellular membranes under these conditions, indicating that some level of membrane oxidation persists even at a low-oxygen environment. Notably, addition of antioxidants showed a more pronounced inhibitory effect on CPP delivery, which is presumably by further diminishing the number of oxidized species present at the plasma

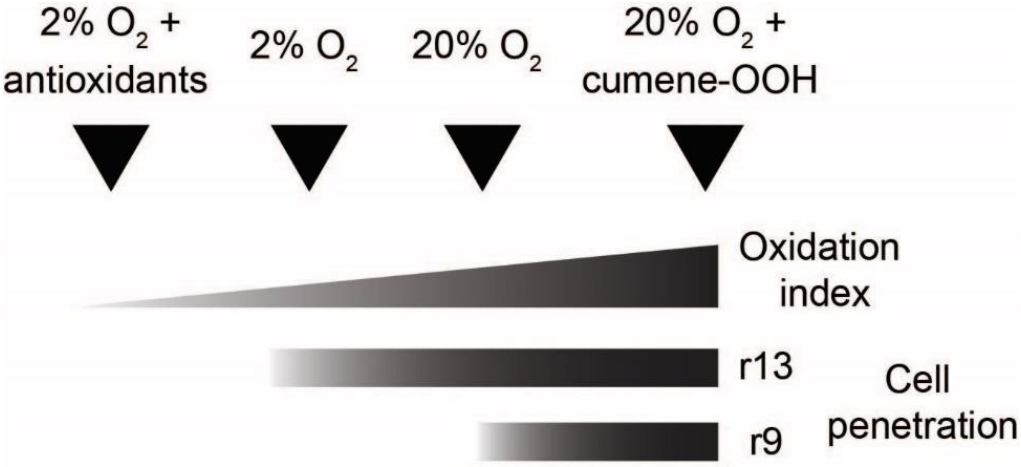

Figure 2-21. A scheme illustrates the relationship between the cellular penetration of CPPs and the membrane oxidation index.

membrane. This result would then support the notion that oxidized species are required to achieve membrane translocation. In addition, comparison between the TMR-r13 peptide and the shorter oligoarginine peptides suggests that the TMR-r13 peptide represents a highly active member within a large family of CPPs. If membrane oxidation is critical in mediating the translocation activity of the TMR-r13 peptide, it should be even more so for the less active peptide. My data support this notion as hypoxia completely inhibited the cytosolic penetration of TMR-r9 peptide. I therefore conclude that membrane oxidation is essential for the cytosolic penetration by linear oligoarginine CPPs at low micromolar concentrations.

How membrane oxidation mediates peptide penetration at the molecular level remains currently unclear. It is possible that membrane oxidation changes the general properties of the plasma membrane and that peptide translocation does not directly involve oxidized species. For instance, membrane oxidation can alter membrane fluidity and this alone could change the permeability of the cell[214, 215]. In addition, Melikov and co-workers have suggested that surface-exposed phosphatidylserine (PS) mediates the translocation of polyarginine peptides into cells[175]. Interestingly, lipid bilayer oxidation has been shown to promote the flip-flop of PS, a lipid that is otherwise typically present on the inner leaflet of the plasma membrane[216]. In this context, membrane oxidation might contribute to an increase in the amount of PS present on the cell surface and thereby promote peptide translocation. Alternatively, oxidized species, including oxidized lipids, could be directly involved in interacting with polyarginine peptides and mediate their transport. Oxidation chemistry is, however, extremely complex and gives rise to a wide variety of products.

For instance, simple exposure of a dry unsaturated phospholipid to air produces a wide spectrum of oxidized by-products (> 20 species)[189]. Non-enzymatic oxidation reactions also involve propagation steps that can dramatically amplify the effect of an initial oxidation event. This is the case for lipid peroxidation where the abstraction of a single hydrogen from a poly-unsaturated fatty acid by reactive oxygen species (ROS) initiates a cascade of oxidation reactions that can subsequently damage a large number of neighboring lipids within a membrane[217]. Each lipid peroxide formed in this process can then decompose into a multitude of products. The cell counteracts this damage using a wide variety of mechanisms, ranging from protection with antioxidants to enzymatic repair or degradation[192]. As a result of this complexity, the identity of oxidized lipids present in a membrane and their respective levels remains poorly characterized. This work, however, highlights that a thorough examination of how composition of cellular membranes changes with oxidation is now required in order to shed light on the mechanisms of membrane translocation.

2.4. Materials and methods

2.4.1. Peptide synthesis and purification

All peptides were synthesized by following a Fmoc chemistry-based solid-phase peptide synthesis (SPPS) standard protocol. The Rink Amide MBHA resin (Novabiochem) was swollen in dimethylformamide (DMF) (Thermo Fisher Scientific) for 1 hour in a SPPS glass vessel (Chemglass Life Sciences). The resin was activated by performing Fmoc deprotection using 20% (v/v) piperidine (Sigma-Aldrich) in DMF. A

thorough wash of the activated resin with DMF was applied before amino acid coupling. The amino acid Fmoc-Arg(Pbf)-OH (Novabiochem) was dissolved in DMF and activated by adding 2-(1H-Benzotriazole-1-yl)-1,1,3,3-tetramethyluronium (HBTU, Novabiochem) and *N*,*N*-Diisopropylethylamine (DIEA, Sigma-Aldrich) to a molar ratio of 4:3.9:10 (amino acid:HBTU:DIEA). The coupling reaction was carried out by mixing activated amino acid to the activated resin under a stream of dry nitrogen gas for at least 4 hours at room temperature. The amino acid was extended on the resin by repeating the procedures of Fmoc protection removal and amino acid coupling. Fmoc-Arg(Pbf)-OH, Fmoc-D-Arg(Pbf)-OH, Fmoc-Lys(Boc)-OH, and Fmoc-D-Lys(Boc)-OH (Novabiochem) were utilized for synthesizing L-polyarginine peptides (Rn, n = 5, 7, 9, 11, and 13), D-polyarginine peptides (rn, n = 9, 11, 13), L-polylysine peptide (K9), and D-oligolysine peptide (k5), respectively. To visualize the peptides in cell delivery experiments, the fluorophore 5(6)-carboxytetramethylrhodamine (TMR) (Novabiochem) or 7-diethylaminocoumarin-3-carboxylic acid (DEAC) (AnaSpec) was labeled at the N-terminal amino group of the peptide after Fmoc deprotection. The fluorophores were activated by mixing with HBTU and DIEA in DMF to a molar ratio of 2:1.9:5 (fluorophore:HBTU:DIEA) and were then added to the resin and allowed to react for 24 hours. To cleave the synthesized peptide off the resin, 4 ml of cleaving solution composed of trifluoroacetic acid (TFA) (Sigma-Aldrich), Triisopropylsilane (TIS) (Sigma-Aldrich), and deionized distilled water (H_2O) (TFA:TIS:H_2O = 95%:2.5%:2.5%) was used. The resin was transferred to a polypropylene column (Bio-Rad) and mixing vigorously with cleaving solution on a shaker for 3 hours. The cleaved peptide solution was then

precipitated in a cold anhydrous ethyl ether and collected by centrifugation at 4,000 rpm for 10 min at 4°C. To examine the purity of the synthesized peptide, the cleaved crude peptide was dissolved in Buffer A (99.9% H_2O and 0.1% TFA) and analyzed on reverse-phase HPLC Agilent 1200 Series system (Agilent) using Vydac C18 column (5-µm particle size, 4 mm x 150 mm) with a linear gradient of Buffer A (99.9% H_2O and 0.1% TFA) and Buffer B (90% acetonitrile, 9.9% H_2O, and 0.1% TFA) at a flow rate of 1 ml/min. The peptide was purified using a semi-prep column, Vydac C18 (10 mm x 150 mm) at a flow rate of 4 ml/min. The identity of peptide was confirmed by MALDI-TOF mass spectrometry analysis (Shimadzu) using α-cyano-4-hydroxycinnamic acid (CHCA) (Sigma-Aldrich) matrix. TMR-R13 peptide (TMR-RRRRRRRRRRRRG-NH_2) expected mass: 2515.50, observed mass: 2516.95; TMR-R11 peptide (TMR-RRRRRRRRRRG-NH_2) expected mass: 2203.30, observed mass: 22204.82; TMR-R9 peptide (TMR-RRRRRRRRG-NH_2) expected mass: 1891.10, observed mass: 1892.96; TMR-R7 peptide (TMR-RRRRRRG-NH_2) expected mass: 1578.90, observed mass: 1579.99; TMR-R5 peptide (TMR-RRRRG-NH_2) expected mass: 1266.70, observed mass: 1267.74; TMR-r13 peptide (TMR-rrrrrrrrrrrrr-NH_2) expected mass: 2460.94, observed mass: 2463.48; TMR-r11 peptide (TMR-rrrrrrrrrr-NH_2) expected mass: 2147.29, observed mass: 2148.92; TMR-r9 peptide (TMR-rrrrrrrr-NH_2) expected mass: 1835.09, observed mass: 1835.43; DEAC-K9 peptide (DEAC-KKKKKKKKK-NH_2) expected mass: 1412.97, observed mass: 1415.59; DEAC-k5 peptide (DEAC-kkkkk-NH_2) expected mass: 900.59, observed mass: 900.84. The dfTAT peptide were obtained by following published protocols[17].

2.4.2. Protein expression and purification

The pTXB1-EGFP plasmid encoding EGFP protein was transformed into *Escherichia coli* BL21(DE3) cells (Agilent Technologies). EGFP protein was expressed in the cytoplasm of *E. coli* as a fusion protein containing a C-terminal Intein protein and chitin binding domain (CBD) at 16^{o}C for 24 hours. The transformed *E. coli* cells were lysed by sonication with lysis buffer (50 mM HEPES, 200 mM NaCl, pH 7.5) supplemented with protease inhibitor cocktail (Sigma-Aldrich). The cell lysate was centrifuged at 14,000 rpm for 45 min to remove cell debris. To purify the protein, the supernatant was incubated with chitin resin (New England BioLabs) at 4^{o}C overnight. The bound proteins were purified by incubating with cleaving buffer (50 mM HEPES, 50 mM dithiothreitol, pH 7.5) for 24 hours at 4^{o}C. The cleaved EGFP proteins, which have no Intein-CBD tag, were combined and dialysed against 50 mM HEPES buffer using dialysis tubing (10 kDa MWCO, Spectrumlabs) to remove excess of salt. The EGFP proteins were further purified by anion-exchange chromatography (HiTrap SP HP 5ml, GE Healthcare) using AKTA fast protein liquid chromatography (FPLC) system (GE Healthcare) with a linear gradient of purification buffer (50 mM HEPES, 0-1000 mM NaCl, pH 7.5) to remove protein-bound bacterial nucleic acids and presumably lipopolysaccharides (LPS). The purified proteins were combined and concentrated using a centrifugal filter concentrator (membrane cut-off size: 10 kDa, Millipore) to the desired concentration. The purity of EGFP proteins was checked during the purification procedure by analyzing by

the 12% SDS-PAGE with standard Coomassie Brilliant Blue staining (Sigma-Aldrich) or fluorescence scanning by Typhoon scanner (GE Healthcare).

2.4.3. Live-cell delivery and imaging

Human dermal fibroblast (HDF) (ATCC PCS-201-010) and MCH58 cells (human skin fibroblast, obtained from E. Shoubridge, Montreal Neurological Institute and Hospital) were cultured in Dulbecco's Modified Eagle's Medium (DMEM) (HyClone) supplemented with 10% (v/v) fetal bovine serum (FBS) (HyClone) and 1x penicillin/streptomycin (P/S) (MP Biomedicals)[218]. For standard cultures (under 20% oxygen), cells were placed in an incubator (NuAire) with humidified ambient atmosphere containing 5% carbon dioxide at 37°C. Alternatively, for hypoxic cultures (under 2% oxygen), cells were grown in a closed camber (modular incubator chamber, Billups-Rothenberg), which was purged with humidified 2% oxygen, 5% carbon dioxide, and 93% nitrogen gas (Praxair) at 20 L/min for 4 min. The chamber was then sealed and placed in an incubator at 37°C (Figure 2-22). Cells were subcultured under normoxic (20% oxygen) or hypoxic environment (2% oxygen) for at least a week before performing live-cell delivery assays. Both normoxically and hypoxically cultured cells were maintained with the same passage number throughout all the experiments.

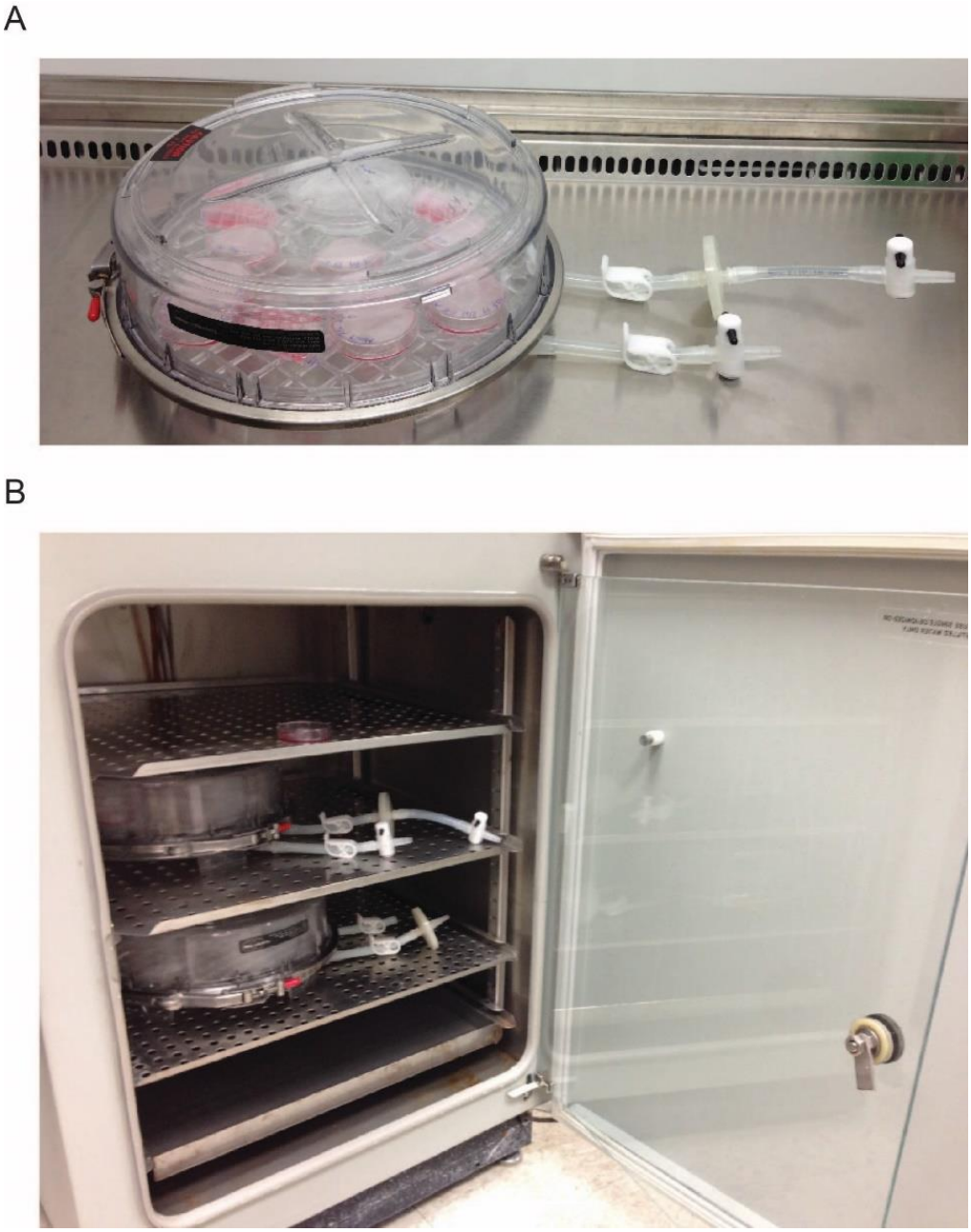

Figure 2-22. Hypoxic and normoxic setup for mammalian cell culture. A, Cells were placed in a closed chamber flushed with 2% oxygen, 5% carbon dioxide, and 93% nitrogen. B, The chamber was deposited in the regular cell culture incubator at 37ºC to perform hypoxic cell culture. For regular cell culture (normoxic), cells were placed directly in the incubator as shown (Top shelf).

To perform cell delivery experiments, HDF or MCH58 cells were seeded in 8-well chambered glass plate (Nunc) for 24 hours to reach 80-90% cell confluency. Each well of cells was washed three times with Dulbecco's Phosphate Buffered Saline (PBS) (HyClone), followed by washing three times with Leibovitz's L-15 medium (HyClone). Cells were then incubated with 1-10 μM peptide in L-15 medium (no supplementation with serum) for 1-60 min at 37ºC (the peptide concentration and incubation time were varied and were dependent on the condition tested in each experiment). To remove extracellular and plasma membrane-bound peptides, cells were washed three times with 1 mg/ml heparin (Sigma-Aldrich) in L-15 medium. Five μM SYTOX Blue (Molecular Probes) was added to the cells to monitor the viability after peptide delivery. All images were captured by an inverted epifluorescence microscope (Model IX81, Olympus) equipped with a Rolera-MGI Plus back-illuminated electron-multiplying charge-coupled device (EMCCD) camera (Qimagining). Images were acquired using phase contrast and three standard fluorescence filter sets: CFP (excitation (Ex) = 436 ± 10 nm/emission (Em) = 480 ± 20 nm), RFP (Ex = 560 ± 20 nm/Em = 630 ± 35 nm), and FITC (Ex = 488 ± 10 nm/Em = 520 ± 20 nm). The fluorescence intensities of cells were analyzed with SlideBook 4.2 software (Olympus).

2.4.4. Cell viability and proliferation assays

To monitor the permeability of the plasma membrane after peptide delivery or oxidant treatment, cells were incubated with the cell-impermeable nucleic acid-staining SYTOX Blue dye. The proliferation of treated cells was examined by MTT assay

(Molecular Probes) following manufacturer's instructions. Briefly, cells were cultured in a 6-well plate to 80-90% confluency and were treated with 1 µM TMR-r13 for 1 hour or 50 µM oxidant (cumene-OOH or H_2O_2) for 30 min at 37°C. Then cells were washed with PBS for three times and were detached by 0.5% trypsin solution (HyClone). Trypsinized cells were resuspended in DMEM medium supplemented with 10% FBS and 1x P/S and seeded in 96-well plates. The cell proliferation rate was measured every 12 hours. The measurement was performed by removing the old DMEM medium in the well followed by adding 100 µl fresh DMEM medium and 10 µl of 12 mM 3-(4,5-dimethylthiazol-2-yl)-2,5-diphenyltetrazolium bromide (MTT) solution (Molecular Probes). The 96-well plate was incubated at 37°C for 4 hours. The contents of each well were then mixed thoroughly with 100 µl of 10 mM SDS-HCl solution and incubated at 37°C for 12 hours. The formation of formazan from MTT compound catalyzed by cell mitochondrial reductase was measured by spectrometry at 560 nm. In parallel, cells incubated with vehicle (either PBS supplemented with calcium and magnesium or L-15 medium, depending on the reagent tested) served as controls.

2.4.5. Cell penetration mechanism assays

To inhibit cellular endocytic processes, cells were first washed with warm PBS three times and pre-treated with 50 µM amiloride (Sigma-Aldrich) or 200 nM bafilomycin A1 (Sigma-Aldrich) for 20 min. Alternatively, cells were washed with cold PBS and pre-incubated at 4°C for 30 min. Then cells were incubated with 1 µM TMR-r13 peptide with presence of the same concentration of inhibitor (50 µM amiloride or 200 nM bafilomycin

A1) for 1 hour at 37ºC, or at 4ºC with TMR-r13 peptide alone for 1 hour. Alternatively, cells were pre-loaded with peptide cargo in late endosomes/lysosomes by incubating with 20 µM DEAC-k5 peptide in L-15 medium for 1 hour at 37ºC. Extracellular DEAC-k5 peptide was removed by washing cells with PBS and heparin solution for three times. The DEAC-k5-loaded cells were then incubated with 5 µM TMR-r13 peptide for 1 hour at 37ºC. The cytosolic penetration efficiency of TMR-r13 and DEAC-k5 peptides was evaluated by the method described in section 2.4.2. As a control, the peptide cargo-loaded cells were treated with 5 µM dfTAT peptide in L-15 medium without cystine for 1 hour at 37ºC.

To illustrate the accumulation of incubated peptide in endocytic vesicles, cells were incubated with 3 µM TMR-r13 peptide or 20 µM DEAC-k5 peptide for 1 hour at 37ºC. Extracellular peptides were removed by washing the cells three times with heparin solution and L-15 medium. LysoTracker Green (500 nM, Molecular Probes) was then added to cells for 30 min at 37ºC. Cells were washed three times with L-15 medium and imaged using the method described in section 2.4.2.

2.4.6. Cell redox treatments

HDF cells were pre-oxidized with various concentrations of freshly prepared oxidants (cumene-OOH or H_2O_2) in PBS supplemented with 100 mg/L calcium and 100 mg/L magnesium (PBS+, HyClone) for 30 min at 37ºC. In contrast, to reduce cellular oxidative stress, cells were cultured in low glucose DMEM supplemented with various antioxidants, including 1 mM pyruvate (HyClone), 250 µM α-tocopherol (Sigma-

Aldrich), 250 µM Trolox (Sigma-Aldrich), 75 µM ascorbic acid (MP Biomedicals), 500 µM 2-phospho-L-ascorbic acid (Simga-Aldrich), and 100 nM sodium selenite (Mallinckrodt Pharmaceuticals) for 48 hours. Medium containing freshly prepared antioxidants was added every 24 hours.

2.4.7. Cell membrane oxidation detection

The C11-BODIPY$^{581/591}$ probe (Molecular Probes) purchased from the vendor was resuspended in pure ethanol to create a stock solution. The probe was diluted in L-15 medium to 15 µM and was then incubated with the cells for 30 min at 37^{o}C. The unincorporated probe was removed by washing the cells with PBS and L-15 medium for three times. The cellular oxidized C11-BODIPY$^{581/591}$ signal was measured by fluorescence microscopy using an FITC filter (Ex = 488 ± 10 nm/Em = 520 ± 20 nm), followed by quantitative analysis utilizing flow cytometry. The cells for flow cytometric analysis were prepared by detaching with 0.5% trypsin solution. The trypsinized cells were resuspended in the L-15 medium. The signal of oxidized probe was examined by a flow cytometer (BD Accuri C6 model) installed with standard detector FL1 (Ex = 488 nm/Em = 533 ± 30 nm) and FL2 (Ex = 488 nm/Em = 585 ± 40 nm). All data was acquired at the flow rate of 66 µl/min with a minimum of 20,000 events. The obtained signal was statistically analyzed by Flowjo v10 software. Alternatively, the stock solution of DPPP (Molecular Probes) was prepared by dissolving DPPP in dimethyl sulfoxide (DMSO) (Sigma-Aldrich) under a nitrogen atmosphere and was stored at -20^{o}C. HDF or MCH58 cells grown in 60-mm culture dish (Corning) were detached with 0.5% trypsin solution

and resuspended in L-15 medium. The resuspended cell solution was incubated with 100 μM DPPP for 5 min and was transferred to 96-well plates. The fluorescence intensity of the oxidized DPPP probe was measured by GloMax-Multi Microplate Multimode Reader (Promega) equipped with the UV Optical Kit (Ex = 365 nm/Em = 435 ± 25 nm). The oxidized DPPP signal was normalized by cell numbers counted using the flow cytometer (BD Accuri C6 model). The samples without adding DPPP or cells serve as negative controls.

2.4.8. Statistical analysis

All statistical analyses were performed using Paired Two Sample for Means t-Test by Microsoft Excel 2013.

3. PRESENCE OF ANIONIC OXIDIZED LIPIDS IS SUFFICIENT TO MODULATE MEMBRANE TRANSLOCATION OF POLYARGININE PEPTIDE[2]

3.1. Introduction

Previously, I established the correlation between the cell penetration activity of polyarginine CPPs and cell membrane oxidation level. The tested oxidants, cumene-OOH and H_2O_2, presumably generate a broad array of lipidic or proteinaceous membrane products. Similarly, the transition between 2% and 20% oxygen potentially leads to a variety of changes in cellular membrane composition. Identifying which membrane components impact translocation, directly or indirectly, will be the focus of this section. It has been shown that cationic polyarginine CPPs displayed strong affinity towards anionic lipophilic molecules, which mediate the permeation of the peptide into the milieu of hydrophobic environment. Therefore, I propose that the generated anionic oxidized phospholipids upon membrane oxidation are involved in the membrane translocation of polyarginine CPPs.

3.2. Results

3.2.1. Membrane oxidation promotes peptide binding to the lipid bilayer

In principle, the TMR-r13 peptide must interact with a cellular membrane prior to

[2] Reprinted with permission from "Membrane oxidation enables the cytosolic entry of polyarginine cell-penetrating peptides" by Wang, T.-Y., Sun, Y., Muthukrishnan, N., Erazo-Oliverase, A., Najjar, K., and Pellois, J.-P., 2016. *The Journal of Biological Chemistry*, 291(15): 7902-7914. Copyright 2016 by the American Society for Biochemistry and Molecular Biology.

crossing it. Consequently, I examined whether oxidation could change the overall affinity of polyarginine peptide to the membrane. Testing surface binding of a peptide is challenging with live epithelial cells because of the competition of cellular endocytic uptake. I therefore chose to test how TMR-r13 peptide interacts with human erythrocytes, also known as red blood cells (RBCs), as the mature RBCs are not typically competent for endocytosis while the cells have similar lipid composition, lipid asymmetry, and membrane structures as other mammalian cells[219, 220]. The RBCs were oxidized with H_2O_2 at a low concentration to avoid hemolysis. The oxidized cells were then directly incubated with the peptide or were further trypsinized in order to evaluate the importance of extracellular protein domains. When incubated with 1 μM TMR-r13 peptide at a peptide concentration that is low to prevent hemolysis, the non-oxidized RBCs displayed only a faint surface staining of the peptide (Figure 3-1). In contrast, upon oxidation treatment, the fluorescence signal of the peptide at RBC membrane increased approximately 5-fold (Figure 3-1). The oxidation of RBCs alone did not result in the membrane autofluorescence (data not shown). Notably, these results were obtained regardless of trypsin treatment, indicating that the extracellular proteins were not required for this phenomenon. Together, these data suggested that the interaction of TMR-r13 peptide with the lipid bilayer increases upon oxidation, presumably by the formation of oxidized lipid species.

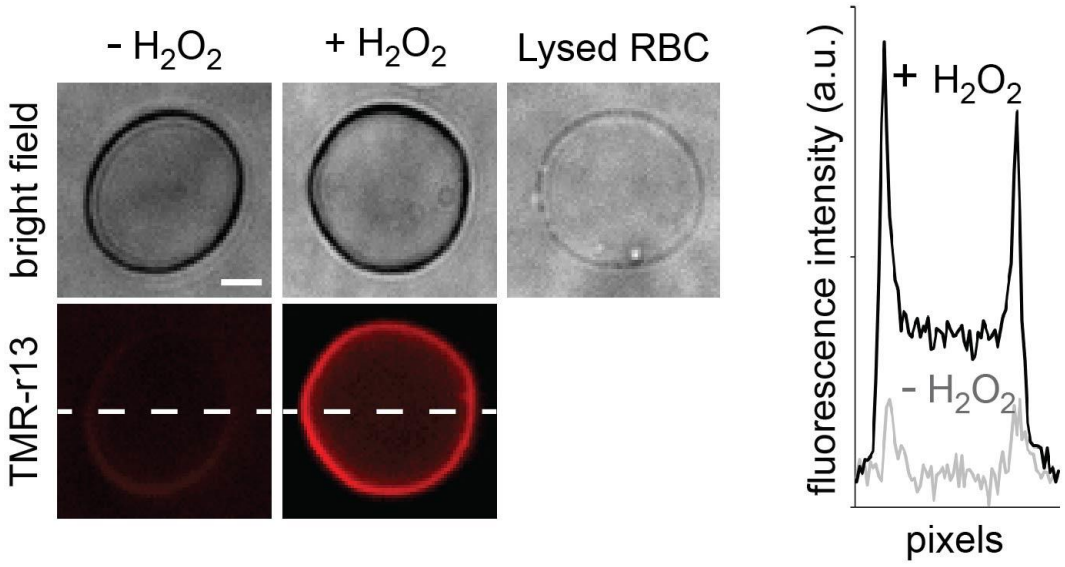

Figure 3-1. Membrane oxidation increases the binding of TMR-r13 peptide to cell surface components. The human RBCs were oxidized by treatment with 50 µM H_2O_2. The cells were then trypsinized, incubated with 1 µM TMR-r13, and imaged with fluorescence microscopy. The bright field images of cells with a dark contrast indicates that the cells were not lysed, compared to the image of a lysed RBC. The fluorescence intensity distribution along the dashed lines is displayed. Scale bar, 2 µm.

3.2.2. Cytosolic penetration of TMR-r13 peptide is blocked by an antibody against oxidized lipids

Based on the notion that oxidized lipids might bind to the TMR-r13 peptide and participate in its translocation across a lipid layer, I next examined whether biomoleucles that interfere with oxidized lipids on the cell surface might inhibit the cytosolic penetration. To test this hypothesis, an E06 monoclonal antibody (E06 mAb) was used. The E06 mAb binds to several byproducts of the oxidation of phosphatidylcholine, often referred to as Ox-PC[221]. Considering that phosphatidylcholine (PC) is a major component of the outer leaflet of the plasma membrane, it seemed to be reasonable that this antibody would be sufficient to display an effect[222]. MCH58 cells were pretreated with 50 µg/ml E06 mAb or a control IgM monoclonal antibody that does not target oxidized lipids (its epitope is advanced glycation end products)[223]. The phosphorylcholine salt (PC salt) was also premixed with E06 mAb, as this molecule inhibits the binding of E06 mAb to the polar head of Ox-PC[224]. The IgM and the combination of E06 mAb/PC salt did not impact the cytosolic penetration activity of TMR-r13 peptide (Figure 3-2). In contrast, E06 mAb caused a significant reduction in cytosolic penetration, suggesting that the Ox-PC might be directly or indirectly mediating the activity of TMR-r13 peptide.

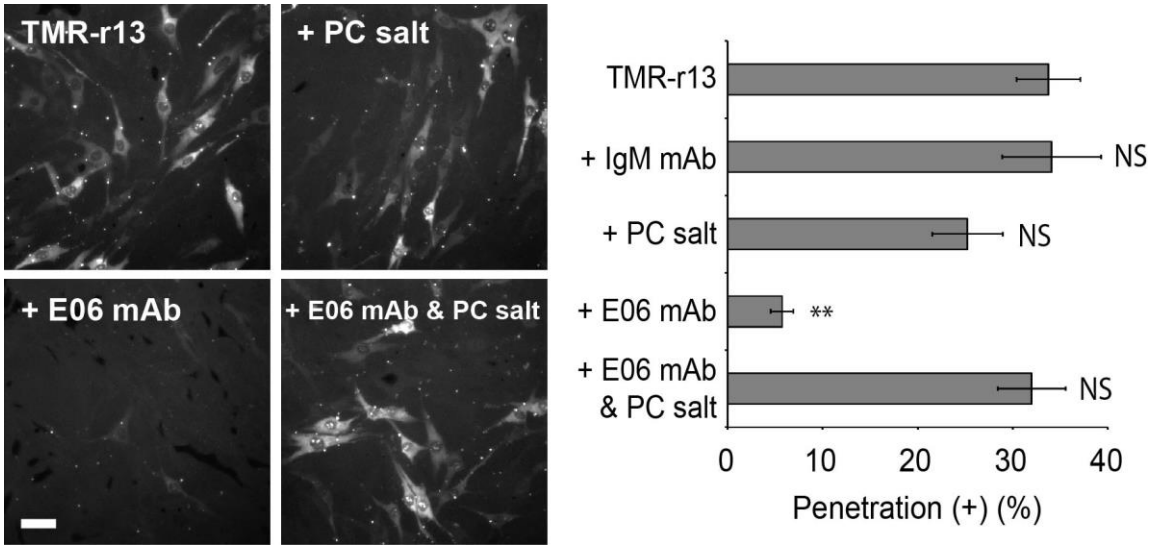

Figure 3-2. Anti-oxidized lipids antibody E06 inhibits cytosolic penetration of TMR-r13 peptide. MCH58 cells were pre-incubated with IgM (50 μg/ml), phosphorylcholine salt (PC salt, 20 μg/ml), E06 mAb (50 μg/ml), or E06 mAb plus PC salt. Cells were then delivered with 1 μM TMR-r13 peptide for 10 min. The cytosolic penetration efficiency of the peptide was measured by fluorescence microscopy and quantified. The acquired images are monochromes of TMR fluorescence emission (RFP filter). Scale bar, 20 μm. NS represents $P>0.05$ and ** represents $P\leq0.01$ compared to cells treated with TMR-r13 peptide alone.

3.2.3. Anionic oxidized lipids mediate the lipid bilayer translocation of polyarginine peptides

Arginine-rich peptides are known to interact promiscuously with negatively charged molecules[52]. I therefore considered whether membrane oxidation might lead to the presence of such a species on the surface of cells. This can, for instance, take place by oxidation-induced flip-flop of phosphatidylserine (PS) from the inner to the outer leaflet of a bilayer[216], by the reaction of the lipid head of phosphatidylethanolamine (PE) with aldehydes generated upon fatty acid peroxidation[225], or by the degradation of lipid peroxides and the introduction of carboxylates within lipid fatty acid chains[189]. These mechanisms are not mutually exclusive and each could be directly or indirectly impacted by E06 mAb. I therefore chose to examine the behavior of TMR-r13 peptide in the presence of 1,2-dioleoyl-*sn*-glycero-3-phospho-L-serine (DOPS), of the naturally occurring negatively charged adduct formed between 1,2-dioleoyl-*sn*-glycero-3-phosphoethanolamine (DOPE) and the oxidation by-product malondialdehyde (MDA) (DOPE-MDA), or of 1-palmitoyl-2-glutaryl-*sn*-glycero-3-phosphocholine (PGPC) and 1-palmitoyl-2-azelaoyl-*sn*-glycero-3-phosphocholine (PazePC), two lipids obtained upon oxidation of PC containing C-5 or C-9 unsaturated fatty acids, respectively[189]. To test whether such species can interact with the TMR-r13 peptide and mediate its transport across a lipid bilayer, I tested how these lipids impact the partitioning of the peptide between PBS and hexanes. In this assay, hexanes are used to mimic the environment of low dielectric constant of the lipid bilayer. As shown in Figure 3-3, TMR-r13 is present in the aqueous phase when incubated by itself or in the presence of the zwitterionic lipids

1,2-dioleoyl-*sn*-glycero-3-phosphocholine (DOPC) and DOPE. In contrast, the peptide partitions into hexanes in the presence of DOPS or DOPE-MDA (Figure 3-3). This result is indicative of inverted micelle formation where the amphiphilic anion is capable of shielding the charges of the peptide and mediating its transfer into the hydrophobic milieu[52]. The results obtained with either PGPC or PazePC were more complex. Both PGPC and PazePC were insoluble in the hexanes and therefore no partitioning of the peptide can be observed. However, the partitioning into hexanes was achieved when PGPC or PazePC were mixed with an excess of DOPC, suggesting that the anionic oxidized lipids mediate the binding to the cationic peptide while the zwitterionic lipid contributed to the formation of inverted micelles (Figure 3-3). This model is supported by the result that no translocation of the peptide was observed, when replacing anionic oxidized lipids with their zwitterionic analogs, 1-palmitoyl-2-(5'-oxo-valeroyl)-*sn*-glycero-3-phosphocholine (POVPC) and 1-palmitoyl-2-(9'-oxo-valeroyl)-*sn*-glycero-3-phosphocholine (PoxnoPC) (Figure 3-3). Finally, the propensity of the peptide to partition into hexanes in the presence of anionic oxidized lipids was inversely proportional to the number of arginine residues present, consistent with their cytosolic penetration activities (Figure 3-4).

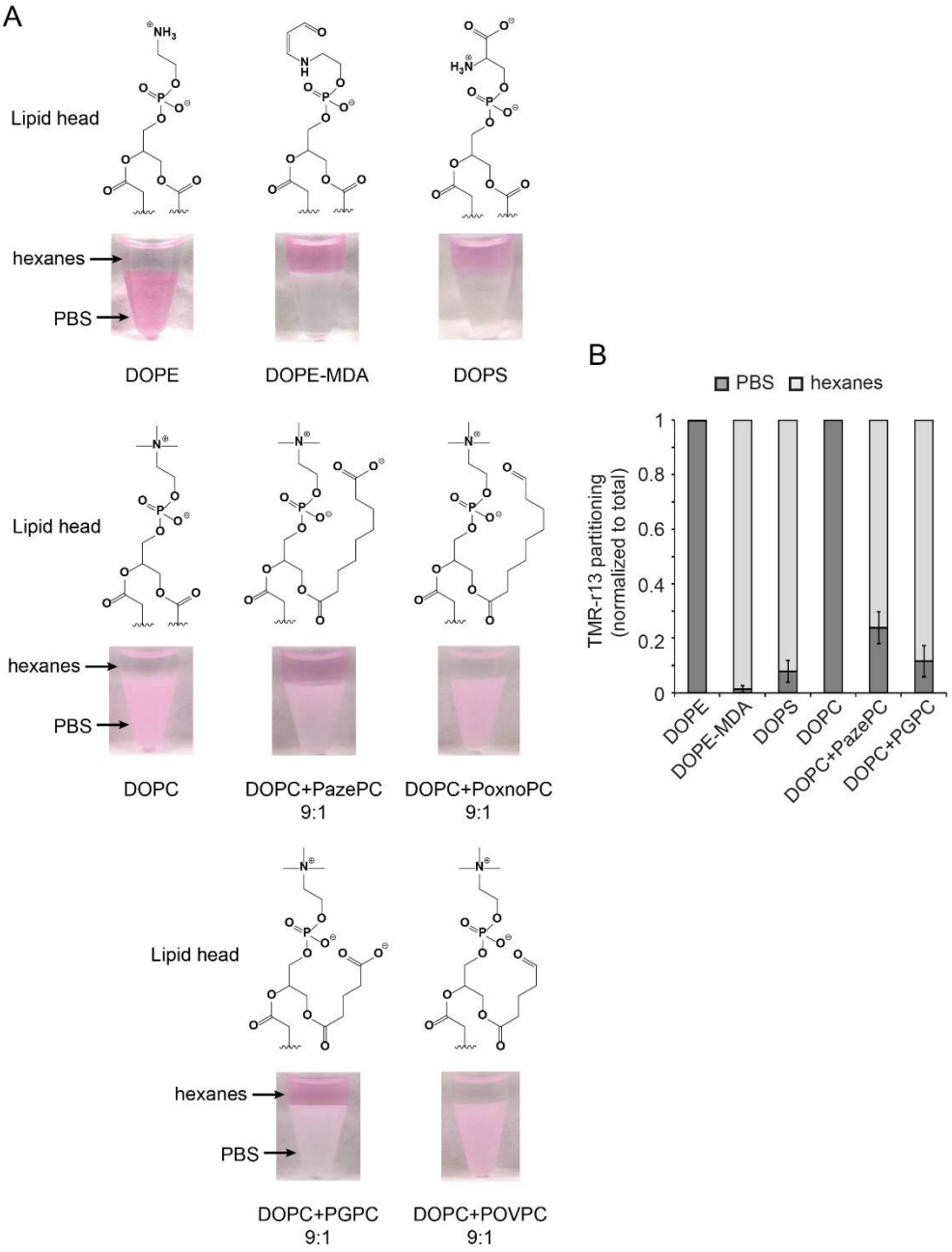

Figure 3-3. Anionic lipids mediate the transfer of TMR-r13 peptide from an aqueous phase to a milieu of low dielectric constant. A, The TMR-r13 peptide (5 µM) was diluted in PBS (pH 7) and an equal volume of hexanes containing 3 mM lipids was added and mixed. The shown structures are the lipid head of phospholipids tested in the assay. The amount of peptide equilibrating between each phase after mixing was quantified by fluorescence spectrometry. B, The graph represents the relative fraction of peptides present in the aqueous and organic phase. DOPC was pre-mixed with PGPC or PazePC at a molar ration of 9:1.

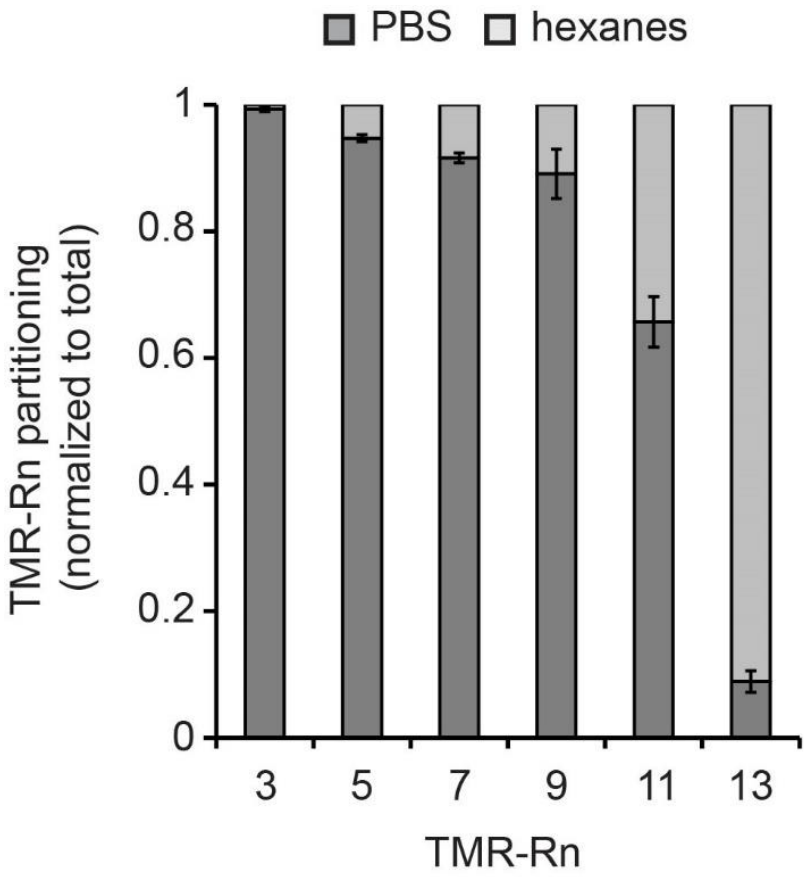

Figure 3-4. Anionic oxidized lipid-mediated partitioning of linear polyarginine peptide is arginine content dependent. Partitioning of 5 μM TMR-Rn (n = 3-13) peptide in PBS/hexanes was supplemented with DOPC:PGPC (9:1, 3 mM total lipid concentration).

To test the plausibility of oxidized membrane components mediating cytosolic entry of the peptide, I chose to establish whether the oxidized lipids identified above could facilitate membrane translocation. For this assay, DOPS and DOPE-MDA could not be incubated with cells without causing cytotoxicity. In contrast, PGPC and PazePC are water-soluble and can be tolerated by cells at low concentrations and with a short incubation time[226]. I therefore tested how these anionic phospholipids would alter the activity of TMR-r13 peptide upon addition to the growth media. PGPC and PazePC (37.5 μM) were first pre-incubated with HDF cells for 15 min. Cells were then washed to remove extracellular unincorporated lipids and the penetration activity of TMR-r13 peptide was subsequently tested. I incubated with cells at 1 μM for 10 min, the peptide displayed poor penetration in cells treated with vehicle alone (PBS+ only, no oxidized lipids added) (Figure 3-5). In contrast, cells treated with PGPC and PazePC showed a significant increase in peptide penetration activity without impacting the cell viability (Figure 3-5). Overall, these results establish that these oxidized species can enhance the cytosolic penetration activity of TMR-r13 peptide and that, given the partitioning results obtained, the lipids mediate this effect by directly interacting with the peptide.

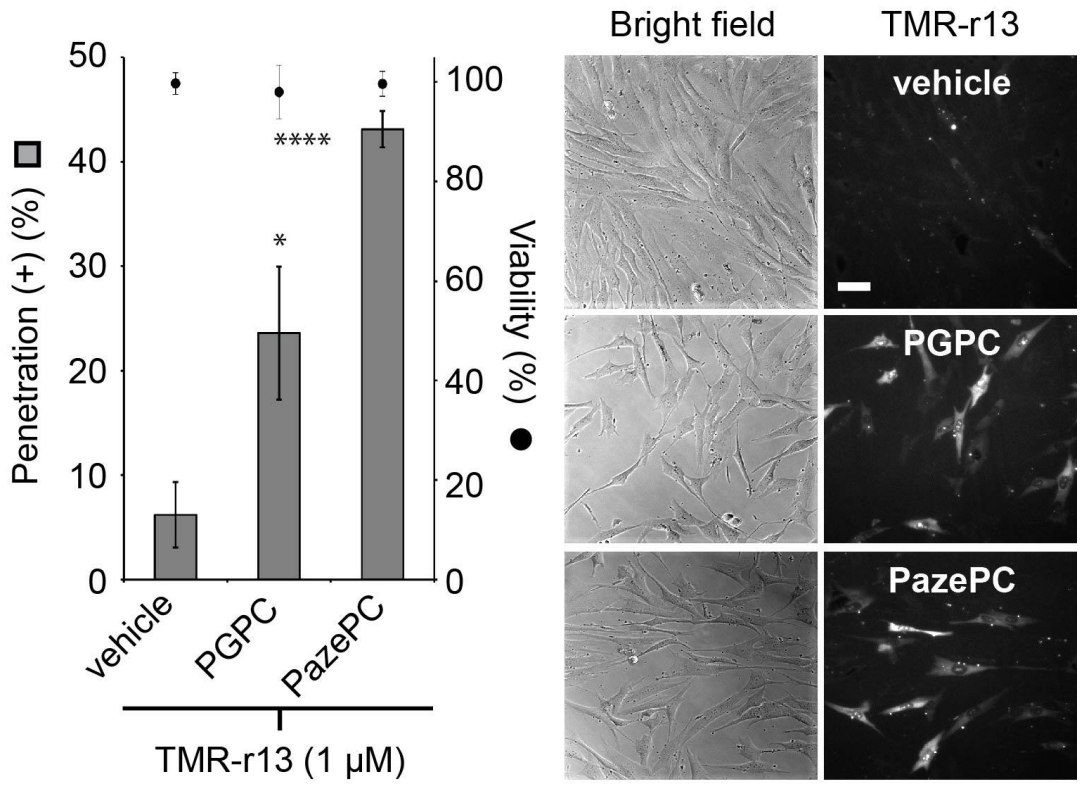

Figure 3-5. The oxidized lipids PGPC and PazePC promote the cytosolic penetration of TMR-r13 peptide. HDF cells were pretreated with the lipids, followed by washing, and then incubated with 1 μM TMR-r13 for 10 min. The vehicle was PBS+. * represents $P \leq 0.05$ and **** represents $P \leq 0.0001$ compared to vehicle. Representative bright field images and monochrome images of TMR fluorescence emission (RFP filter) are shown. Scale bar, 20 μm.

3.3. Discussion

In order to gain mechanistic insights into oxidation-dependent cell penetration of TMR-r13, I decided to test whether pure, physiologically relevant oxidized lipids could modulate the activity of TMR-r13 peptide. Several reports have already highlighted that anionic amphiphiles can enhance the translocation of polyarginine peptides by acting as lipophilic counterions. Pyrenebutyrate can, for instance, be used as an extracellular additive that improves the cell penetration of nona-arginine peptide (R9)[100]. Other anionic amphiphiles have displayed similar behavior[14, 52, 56, 80]. A proposed mechanism of action involves the formation of anionic oxidized lipids. To test this idea, two lipids formed as a result of oxidative processes were tested: PGPC and PazePC. These two lipids were chosen because they are physiologically relevant and produced under oxidative stress *in vivo*. Both lipids contain a carboxylate with which arginine residues can potentially interact electrostatically[52]. Finally, they are relatively water-soluble and can equilibrate between the aqueous phase and cell membranes when added to growth media. When tested with live cells, both PGPC and PazePC enabled the translocation of TMR-r13. In principle, addition of these lipids could have numerous effects and, as noted above, influence cell penetration directly or indirectly. Yet, these lipids also mediated the partitioning of TMR-r13 into hexane, a solvent of low dielectric constant that mimics the hydrophobic environment of a lipid bilayer. Together, these data show that TMR-r13 binds to PGPC and PazePC and that lipid and peptide form structures that can exist in a hydrophobic environment (e.g. inverted micelles). In principle, these oxidized lipid species are therefore capable of transporting polyarginine peptides across membranes by direct

interactions. Overall I propose that oxidized lipids with similar properties to PGPC and PazePC might act as direct mediators of membrane translocation. Based on the aforementioned chemical complexity intrinsic to the process of membrane oxidation, this could include a broad variety of species that work in concert to facilitate peptide transport.

Taken together, my results support a novel model for cytosolic penetration where arginine-rich peptides translocate across the plasma membrane of cells by interacting with anionic phospholipids present on the cell surface as a result of oxidative stress (Figure 3-6, the whisker model is used to represent the oxidized lipids containing truncated anionic fatty acyl chains exposed on the surface of the bilayer)[227]. Oxidative conditions, including high oxygen concentration, presence of oxidants, or lack of antioxidants, can increase the number of anionic species present on the cell surface by a number of mechanisms[189]. This then leads to an increase in membrane association by the peptide such as TMR-r13, followed by the transfer of peptide into the lipid layer. The transport of peptide across the membrane is presumably driven in part by the concentration gradient existing between the outside and the inside of the cell. The formation of inverted micelles between peptide and anionic phospholipids, including oxidized lipids, are the plausible structures that can mediate the peptide translocation without generating membrane leakage. Notably, short polyarginine peptides that poorly penetrate the cells do not form inverted micelles with anionic phospholipids in my partitioning assays while longer peptides that enter cells do (Figure 2-2 and 3-4). The agreement between *in cellulo* and *in vitro* assays therefore further supports the model presented in Figure 3-6. This model is consistent with other proposed membrane translocation models that involves anionic molecules, such as fatty

acids and pyrenebutyrate[14, 228]. An important distinction however is that membrane oxidation can explain how anionic lipids are naturally presented on the cell surface. It is possible that CPPs also exploit the hydrophobic or hydrophilic defects existing in the bilayer (e.g. changes in membrane fluidity and lipid packing) known to increase the permeabilization of oxidized membranes[194, 201]. Such effects could in principle synergize with inverted micelle formation and further facilitate translocation.

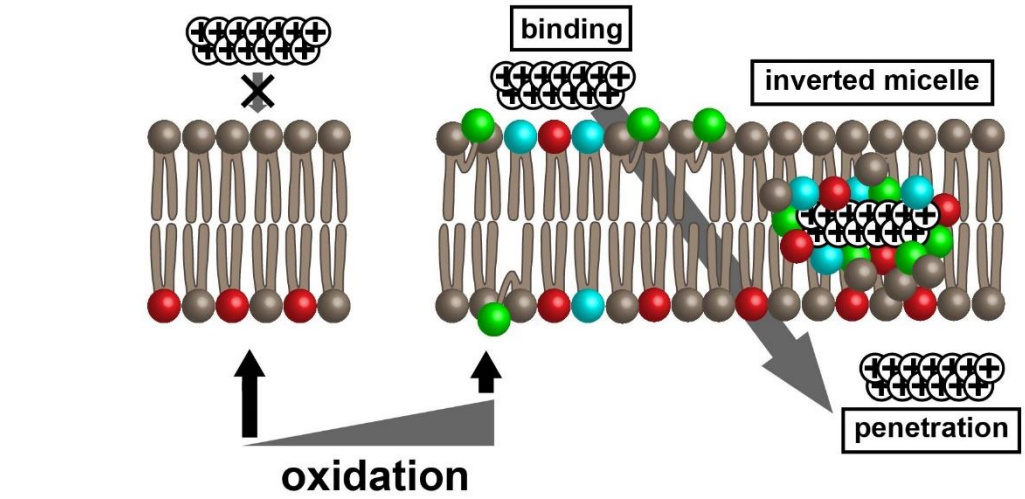

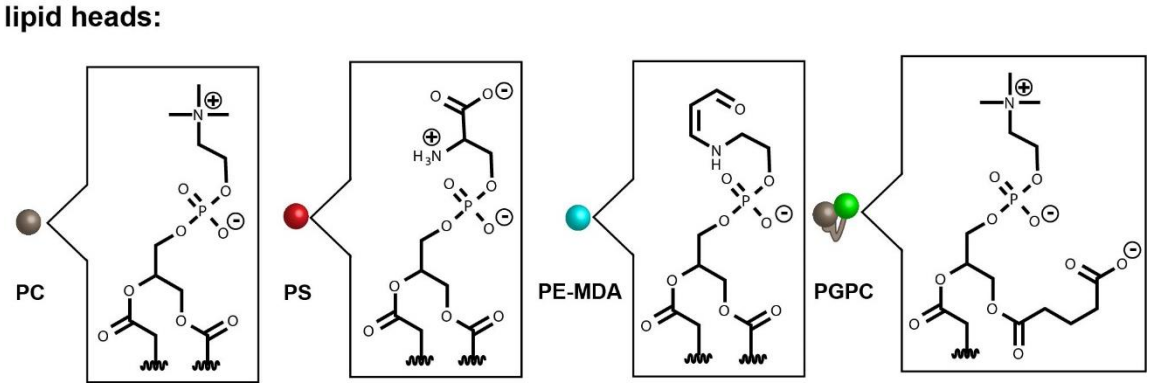

Figure 3-6. Proposed model for the oxidation-dependent cytosolic penetration of polyarginine peptide. A simplified lipid bilayer is represented with only the lipids of PC, PS, PE-MDA, and PGPC. The polyarginine peptide is expressed as a string of positive charges. Under low oxidative stress, the surface of the lipid bilayer is neutral, resulting in no binding and no cytosolic penetration from the peptide. At high oxidative stress, anionic lipids are present that promote the binding, inverted micelle formation and membrane translocation of the peptide.

3.4. Materials and methods

3.4.1. Membrane binding assay

Whole human blood purchased from Gulf Coast Regional Blood Center (Houston, Texas) was centrifuged at 1500 *g* for 5 min to separate the erythrocytes from the buffy coat and the plasma. The obtained erythrocyte pellet was resuspended in cold PBS; this procedure was repeated three times. The erythrocytes were treated with 0.1% trypsin (HyClone) in PBS at 37^{o}C for 30 min in order to remove the extracellular domains of proteins at the plasma membrane. The trypsinized red blood cells (tRBCs) were then washed with PBS for five times. The 0.05% tRBCs diluted in the PBS were incubated with 50 μM H_2O_2 for 10 min at room temperature. The oxidized tRBCs were then mixed with 1 μM TMR-r13 in a 384-well plate (μ-Plate 384 well, ibidi) on a heating stage at 37^{o}C for 15 min. The images were acquired by the microscope (Model IX81, Olympus) using an 100X objective. The fluorescence intensity of erythrocytes was analyzed using SlideBook 4.2 software. The bright field was utilized to distinguish the intact RBCs (dark contrast) from lysed RBC ghosts (transparent). All experiments were performed under conditions of minimal hemolysis as membrane rupture during lysis leads to exposure of PS, which would result in the peptide binding irrespective to membrane oxidation[229].

3.4.2. Anti-Ox-PC antibody treatment

The anti-oxidized PC E06 monoclonal antibody (E06 mAb, Avanti Polar Lipids) was diluted in L-15 medium to a final concentration of 50 μg/ml and then was incubated with MCH58 cells for 2 hours at 37^{o}C. After washing the antibody-treated cells with PBS

and L-15 medium three times, the cells were incubated with 1 μM TMR-r13 in L-15 medium for 10 min at 37°C. Heparin (1 mg/ml, Sigma-Aldrich) in L-15 medium wash was applied three times to remove excess and membrane-bound peptides. The cell images were recorded as described in the previous section. The anti-AGEs mouse IgM κ (ab18400, abcam), the same isotype with E06 mAb, serves as a negative control[223]. To inactivate E06 mAb, the antibody was pre-mixed with 20 μg/ml phosphorylcholine salt (PC salt, Thermo Fisher Scientific) in L-15 medium before incubating with the cells.

3.4.3. Partitioning assay

Anhydrous DOPC (Avanti Polar Lipids) lipid film was prepared and resuspended in hexanes by sonication for 10 min. Alternatively, PGPC or PazePC (Avanti Polar Lipids) was dissolved in 1-octanol (Sigma-Aldrich) and was mixed with DOPC solution to a molar ratio of 9:1 (DOPC:PGPC or DOPC:PazePC). The partitioning was performed by adding 3 mM lipid solution to an equal volume of 5 μM peptide in PBS (pH 7) in a microcentrifuge tube and mixing vigorously. The fluorescence signal of the peptides in either organic or aqueous phase was quantified by GloMax-Multi Microplate Multimode Reader (Promega) with Green Optical Kit (Ex = 525 nm/Em = 610 ± 30 nm).

3.4.4. Cell redox treatment

To feed cells with oxidized phospholipids, a lipid suspension was first prepared. PGPC or PazePC stock solution in chloroform was dried under a nitrogen stream to obtain a lipid film. The film was placed in a desiccator under vacuum overnight to eliminate any

trace of solvent. The dry lipid film was resuspended in PBS+ by sonication for 10 min. The 37.5 µM PGPC or PazePC solution was incubated with HDF cells and incubated for 15 min at 37^{o}C. Cells were washed three times with PBS+ and L-15 medium, followed by incubation with 1 µM TMR-r13 for 10 min at 37^{o}C. The delivery efficiency of peptides was measured by fluorescence microscopy as described in the previous section.

3.4.5. Statistical analysis

All statistical analyses were performed using Paired Two Sample for Means t-Test by Microsoft Excel 2013.

4. CONCLUSION[3]

4.1. Summary of results

I examined the interplay between cellular oxidation and cytosolic penetration of peptides using polyarginine CPPs as model compounds. I showed that the cytosolic penetration of nona- or trideca-arginine CPPs (r9 and r13 where r is D-Arg, an unnatural arginine residue used to confer protease-resistance to the peptide) was abolished or significantly reduced, respectively, when cells were cultured at 2% oxygen as opposed to 20% oxygen. Cell penetration was also reduced when the cellular growth media was supplemented with antioxidants. Together, these results indicated that reducing oxidative cellular stress diminishes the transport of polyarginine CPPs into cells. Conversely, an increase in the oxidation state of the plasma membrane of cells led to an increase in polyarginine CPP cytosolic penetration. For instance, r13 efficiently entered cells pretreated with lipophilic oxidants (oxidation conditions were mild and did not affect cell viability and proliferation rates). Overall, the penetration activity of polyarginine CPP positively correlates with the oxidation status of the membrane of cells.

Given that lipids are possible targets of both oxidative damage and potential cellular factors interacting with polyarginine CPPs, I next tested whether oxidized lipids might be involved in the oxidation-dependent translocation of the peptides. I observed that

[3] Reprinted with permission from "Peptide translocation through the plasma membrane of human cells: can oxidative stress be exploited to gain better intracellular access?" by Wang, T.-Y. and Pellois, J.-P., 2016. *Communicative & Integrative Biology*. Copyright 2016 by Taylor & Francis Group.

E06, a monoclonal antibody that binds oxidized phosphatidylcholine (oxPC) lipids, blocked the intracellular delivery of polyarginine CPP after a simple pre-incubation with cells. Furthermore, extracellular addition of the anionic oxPC lipids, PGPC or PazePC, enhanced the cytosolic penetration of polyarginine CPPs. Notably, an *in vitro* partitioning assay established that both PGPC and PazePC can transport polyarginine CPPs into a milieu of low dielectric constant. This, in turn, is consistent with the notion that polyarginine CPPs and anionic oxPC species have the ability to form structures, most likely inverted micelles, that allow transfer of the hydrophilic peptide across a hydrophobic lipid bilayer.

4.2. Proposed model based on current data

My results support a novel model for cytosolic penetration where arginine-rich peptides translocate across the plasma membrane of cells by interacting with anionic lipids exposed on the cell surface as a result of oxidative membrane damage. In particular, oxidized lipids might act as direct mediator of peptide transport. In agreement with the lipid whisker model, lipid oxidation leads to the formation of anionic truncated fatty acid moieties that become exposed on the cell surface (Figure 4-1)[227]. PACPPs interact with these moieties and inverted micelles form between cationic peptide and anionic lipids. The concentration gradient generated during incubation (e.g. micromolar concentration of peptide outside cells and no CPP inside cells at initial incubation conditions) as well as the membrane potential may then drive the accumulation of PACPPs inside cells.

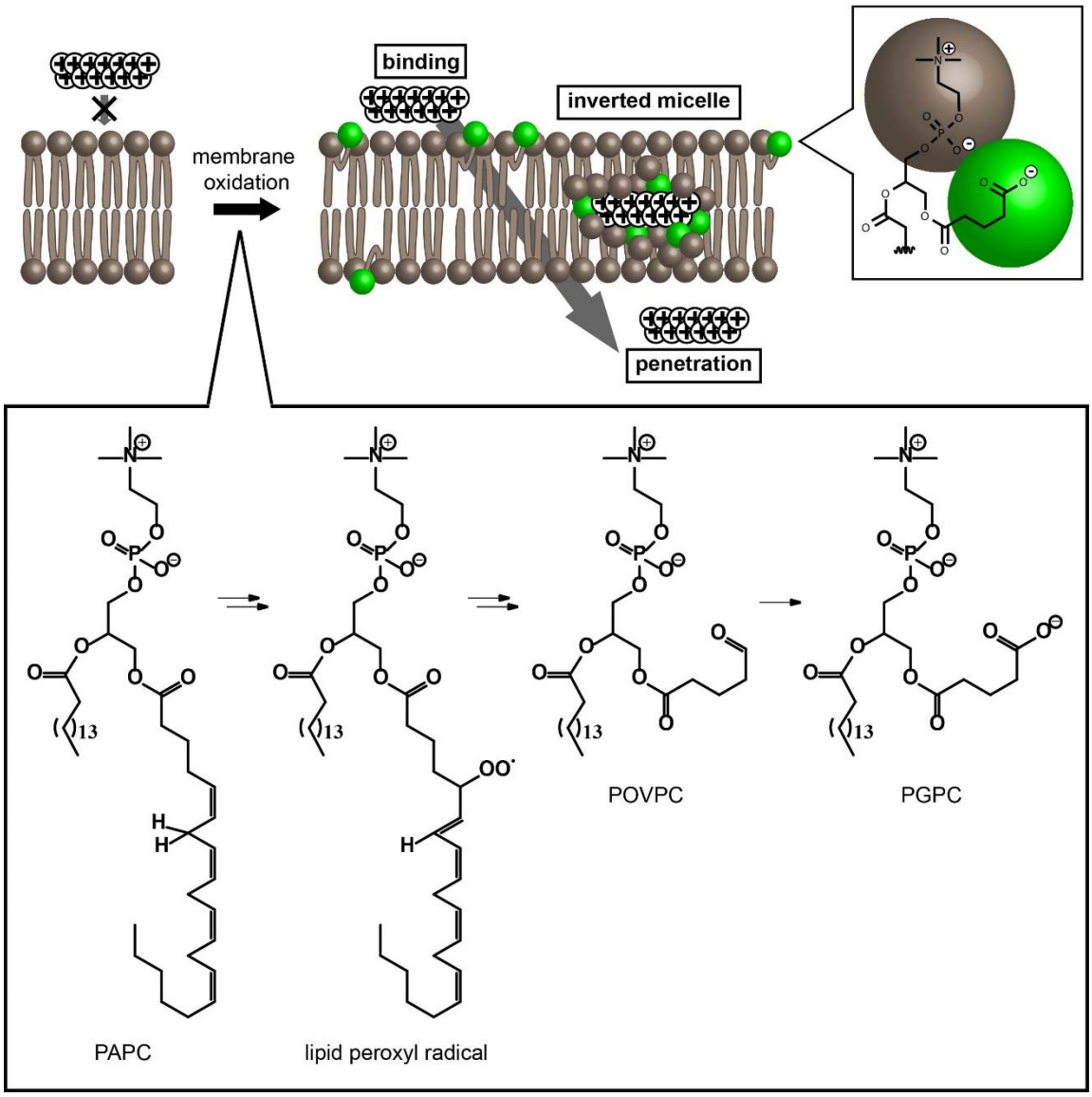

Figure 4-1. Membrane oxidation can lead to the exposure of anionic phospholipid on the cell surface. In this illustration, the oxidation of arachidonic fatty acid of PAPC yields POVPC. Further oxidation of POVPC forms PGPC. The carboxylate formed is negatively charged and exposed on the surface of the bilayer. The chemical structure of the lipid head and newly formed anionic fatty acyl chain of PGPC is shown and labeled with dark brown and green spheres accordingly.

4.3. Other possible models connecting lipid oxidation and cell penetration

The involvement of oxidized phosphatidylcholine (oxPC) lipids such as PGPC and PazePC provide a plausible explanation for peptide translocation. Yet, due to the complexities of cell membrane composition and oxidation chemistry, it is likely that other oxidized lipids or that other oxidation-dependent processes might also play a role. Below, I present alternative and non-mutually exclusive scenari that might also provide a molecular basis for the oxidation-dependent behavior of polyarginine CPPs. Melikov and co-workers have proposed that phosphatidylserine (PS), an anionic phospholipid normally present in human cell membrane may mediate the translocation of polyarginine CPPs[175]. This lipid typically resides in the inner leaflet of mammalian plasma membrane and whether polyarginine CPPs can interact with PS on the cell surface remains therefore unclear. Yet, it has been established that membrane oxidation can disrupt the lipid asymmetry of biological lipid bilayers and that the level of PS exposed extracellularly can increase during membrane oxidation[216]. It is therefore possible that upon membrane oxidation, PS partially and transiently relocalizes to the outer leaflet of the plasma membrane. It might then bind polyarginine CPPs electrostatically and assist their membrane translocation in a micelle-dependent manner similar to that described for oxPCs (Figure 4-2). In this scenario, oxidation does not lead to the formation of new species, but simply influences the level at which an anionic lipid is exposed on the cell surface.

Another possible scenario relates to the fact that oxidation of polyunsaturated fatty acids generates a wild array of oxidized species, including aldehydes such as

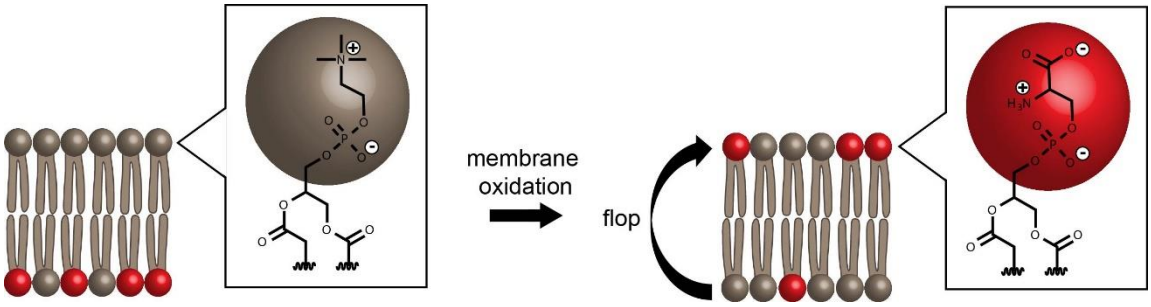

Figure 4-2. Externalization of PS upon membrane oxidation. A simplified lipid bilayer is represented with only the phospholipid phosphatidylcholine (PC) and phosphatidylserine (PS). The PS asymmetry of the lipid bilayer, maintained by flippases in the plasma membrane of human cells, is potentially disrupted upon membrane oxidation. The chemical structure of the lipid head of PC and PS are shown in the box and labeled with dark brown and red spheres, respectively.

malondialdehyde (MDA)[189]. The formation of MDA is in fact often used as a quantitative measure of cellular oxidative stress. In addition, MDA reacts with the amino groups of biomolecules to form Schiff-base[230]. In particular, MDA can react with phosphatidylethanolamine (PE), a phospholipid containing a positively charged amine in its polar head[225]. Notably, while PE is zwitterionic, a PE-MDA adduct is anionic (reaction with the amino group removes the positive charge of this functional group, leaving a single negative charge on the phosphate). Thus, the by-products of lipid oxidation can lead to the formation of an anionic lipid on the cell surface. This anionic lipid represents therefore another target for possible polyarginine CPP binding and translocation (Figure 4-3).

It is also possible that polyarginine CPPs, in addition to binding anionic lipids, exploit oxidation-induced hydrophobic or hydrophilic defects present in the bilayer. Membrane defects can, for example, be formed upon generation of lipids containing truncated fatty acyl chain (anionic or non-anionic). Such species are formed as a consequence of lipid peroxidation and of repair by detoxifying enzymes (eg: phospholipase A2)[231]. These oxidized lipids have an inverted cone shape and detergent-like properties. These species form membrane microdomain and change membrane dynamics (e.g. membrane fluidity and lipid packing). These changes are thought to increase the permeability of membranes (Figure 4-4)[232, 233]. Overall I propose that these effects could in principle synergize with inverted micelle formation and further facilitate translocation of polyarginine CPPs (Figure 3-6).

Overall, the models described herein are speculative and have not been tested to date. Yet, preliminary results, presented in Figure 3-3, suggest that PGPC, PazePC, PS,

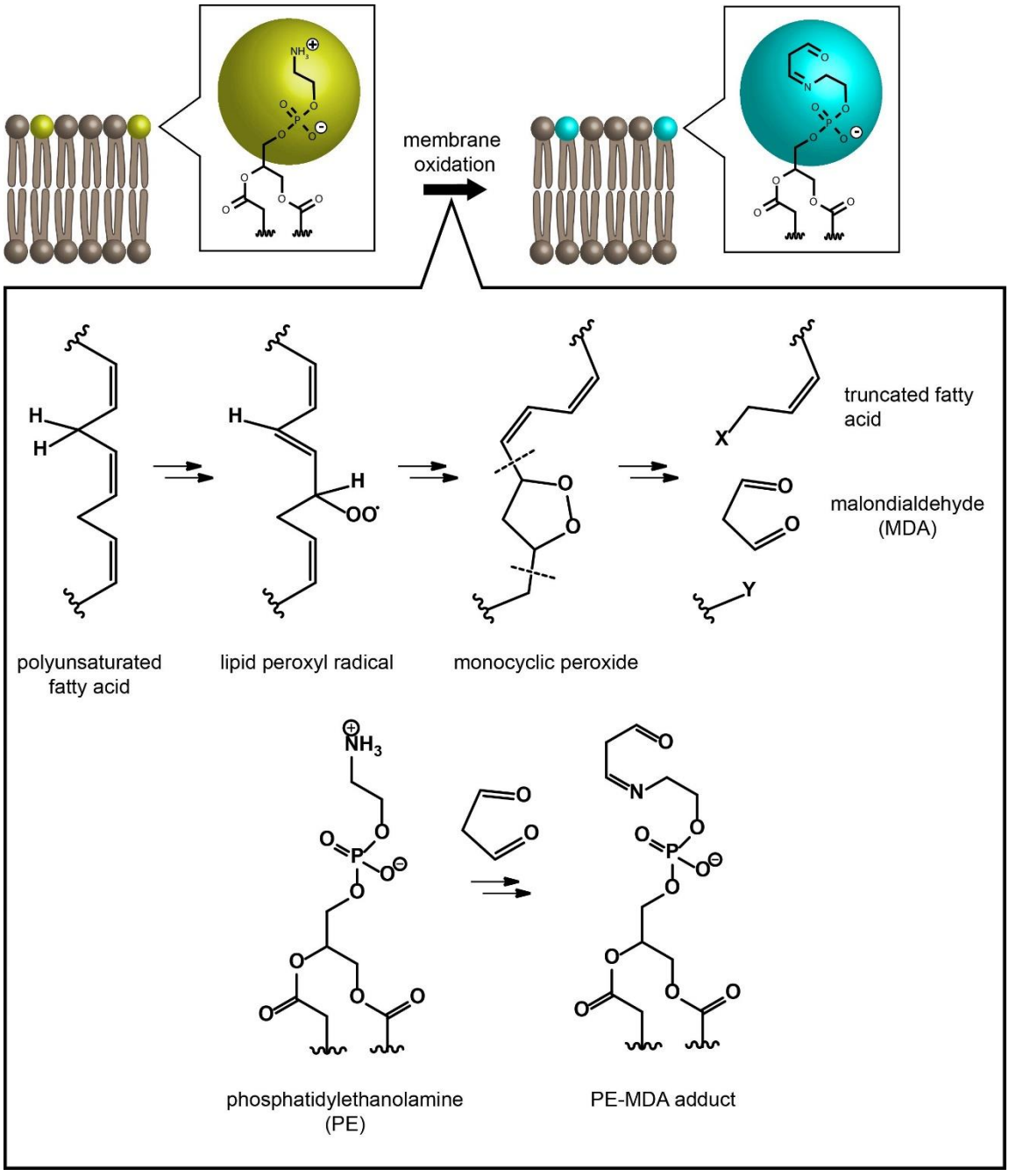

Figure 4-3. Oxidation-dependent modification of the polar heads of lipids. PE-MDA production is used as an example. MDA is created upon oxidation of polyunsaturated fatty acids. The generated MDA reacts with the amino group of the zwitterionc lipid phosphatidylethanolamine (PE) to form PE-MDA adduct, an anionic species. The chemical structure of the lipid head of PE and PE-MDA is shown and labeled with yellow green and cyan spheres, respectively.

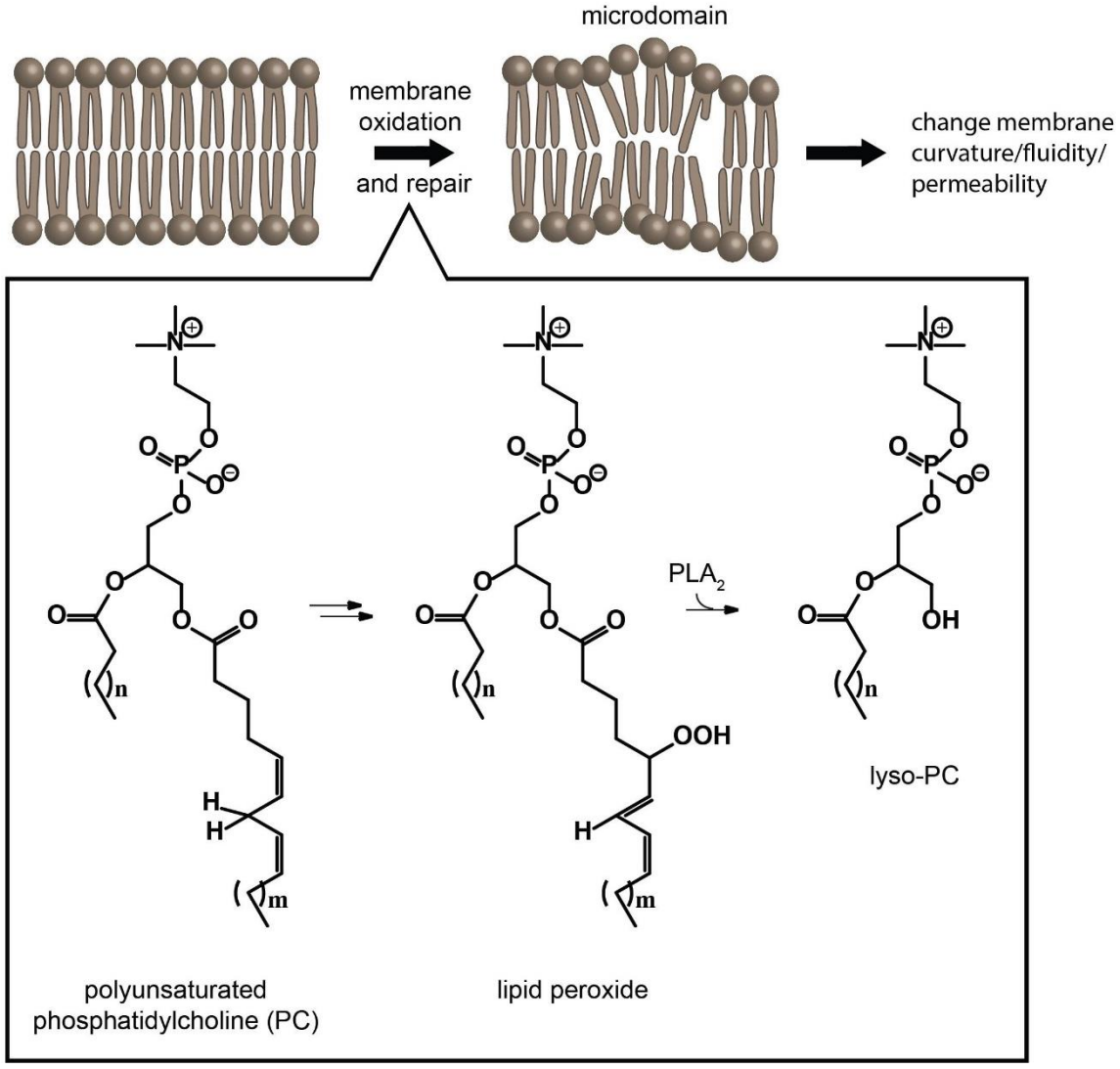

Figure 4-4. Generation of lysophospholipids and membrane defects upon oxidation. Oxidation of PC is given as an example. The unsaturated fatty acid of PC is oxidized to form lipid peroxide. Phospholipase A2 (PLA_2) cleaves the oxidized fatty acid. The generated lyso-phosphatidylcholine (lyso-PC) induces the formation of microdomain, leading to alterations in membrane packing, membrane curvature, fluidity, and permeability.

and PE-MDA all share a similar behavior *in vitro*. In particular, a simple partitioning assay between water and hexane, show that PGPC, PazePC, PS, and PE-MDA can mediate the transfer of r13 into a milieu of low dielectric constant while the neutral oxidized lipids POVPC and PoxonPC can not. In principle, all these anionic lipids are capable of interacting with polyarginine CPPs and bringing them in an environment resembling the lipid bilayer. It is therefore possible that several anionic lipid species, while concomitantly generated during oxidative stress, might act in concert to interact with polyarginine CPPs during cell penetration.

4.4. Implications for cell culture experiments

The oxidation-dependent activity of polyarginine CPPs can explain the variations often observed in polyarginine CPP performance in live cell delivery experiments. As described herein, differences in delivery efficiency can arise from distinct oxidation levels of the cell membrane that are generated by exogenous and endogenous factors. Cell culture conditions and media composition can impact cell metabolism and oxidative stress levels. For instance, the antioxidant ascorbic acid (i.e. vitamin C) is present in certain cell culture media but not in others (for example, ascorbic acid is present in CMRL-1066 medium but not in the commonly used media DMEM)[199]. In addition, selenium is a cofactor that is essential to the activity of glutathione peroxidase, an enzyme that protect cells from oxidative damage and educes lipid hydroperoxides. Selenium is typically introduced in cell cultures by addition of serum. Yet, the amount of selenium in serum varies from batch to batch and from brand to brand[234]. These variations have been shown to significantly

impact the activities of enzymes involving in antioxidant defense pathways[234]. It is therefore conceivable that variations in growth conditions lead to variations in plasma membrane oxidation and in peptide translocation.

The oxidation-dependent activity of polyarginine CPPs can explain the variations often observed in polyarginine CPP performance in live cell delivery experiments. As described herein, differences in delivery efficiency can arise from distinct oxidation levels of the cell membrane that are generated by exogenous and endogenous factors. Cell culture conditions and media composition can impact cell metabolism and oxidative stress levels. For instance, the antioxidant ascorbic acid (i.e. vitamin C) is present in certain cell culture media but not in others (for example, ascorbic acid is present in CMRL-1066 medium but not in the commonly used media DMEM)[199]. In addition, selenium is a cofactor that is essential to the activity of glutathione peroxidase, an enzyme that protect cells from oxidative damage and educes lipid hydroperoxides. Selenium is typically introduced in cell cultures by addition of serum. Yet, the amount of selenium in serum varies from batch to batch and from brand to brand[234]. These variations have been shown to significantly impact the activities of enzymes involving in antioxidant defense pathways[234]. It is therefore conceivable that variations in growth conditions lead to variations in plasma membrane oxidation and in peptide translocation.

Similar oxidation-related principles might explain why certain cell types are more resistant to peptide penetration than others. For instance, it is interesting to note that endogenous level of antioxidants and activities of antioxidation enzymes differ in various cell types[235]. Whether these differences lead to changes in plasma membrane compositions

and structures has not been explored. Yet, one can envision how cells displaying low oxidative damage at the plasma membrane because of a highly active antioxidative defense system would be less susceptible to polyarginine CPP penetration than cells more prone to oxidation[236]. Finally, the level of lipid peroxides present in cells increases with the number of passages used in a particular cell culture[237]. It is therefore possible that cells with high passage numbers ("old" cells) differ significantly from freshly cultured cells ("young" cells) in their responses to polyarginine CPP treatment.

Many parameters can impact the oxidative status of the cell and this, in turn, will influence peptide translocation outcomes. When comparing the activity of different polyarginine CPPs, controlling membrane oxidation is therefore important as different experimental settings might lead to highly variable results. Moreover, favoring mild oxidative cell culture conditions might lead to improvements in polyarginine CPP-based delivery applications. However, excessive oxidative damage at the plasma membrane can severely alter cell physiology. Overall, cell culture conditions optimal for both polyarginine CPP delivery and cell biology remain to be established.

4.5. Implications for *in vivo* applications

It is also not clear how the insights I have gained with *in vitro* experiments might apply to how polyarginine CPPs behave *in vivo*. This is in part because it is hard to measure or predict what the *in vivo* oxidation status of cells is. One can, however, envision how a polyarginine CPP that penetrates cells efficiently *in vitro* might not do so *in vivo* simply because *in vivo* tissues are better protected from oxidative damage (e.g. cells grown

at 20% oxygen vs. tissue exposed to 2% oxygen *in vivo*). This would then suggest that cytosolic penetration studies should not be performed with cells grown under oxidative stress (*i.e.* ambient air) when a goal is to develop cell-permeable peptides for therapeutic applications. In particular, assays performed with cells protected from oxidation (e.g. culture at 2% rather than 20% oxygen) might offer better predictions for how such peptides might perform *in vivo*. Yet, this issue is complicated by the fact that certain tissues are more prone to oxidation than others. For instance, airways are exposed to 20% oxygen. Inflamed tissues and tumors are also sites of elevated oxidative stress[189, 190]. How CPPs behave in these tissues based on *in vitro* data is again hard to predict. Yet, it is possible that CPPs have the ability to more readily permeate cells in these environments.

4.6. Future prospects

More molecular details are still needed to fully elucidate how polyarginine CPPs enter cells. It is plausible that polyarginine CPPs enter cells by multiple routes while associating with a wide variety of cellular species. Herein, I describe how several oxidized lipid species might play equal roles in this process. The anionic lipids presented are, however, not exclusive candidates and other oxidized species might be involved in the process of peptide translocation. Further testing of the hypotheses described herein will require a thorough examination of the composition of the plasma membrane of cells under various conditions of oxidative stress, something that is currently lacking. Useful protocols for the analysis of oxidized lipids by mass spectrometry have been developed[238]. Sample preparation remain however a challenge. It is for instance important to protect

samples from oxidation during analysis so as to not generate artifacts. In addition, selectively purifying the components of the plasma membrane from other cellular membranes is not trivial (one can for instance envision that the membrane of mitochondria contains oxidized lipids that are not present in the plasma membrane and vice versa). Techniques that involve the formation and purification of plasma membrane vesicles might be useful in this respect[239]. However, given that oxidized lipids display a wide range of biophysical properties, it is not clear whether a single purification scheme can capture all the species present in the plasma membrane. For instance, while many oxidized lipids are lipophilic, others are water-soluble. It is therefore possible that these oxidized lipids equilibrate in solution during purification and that they do not partition in the organic solvents typically used to separate lipids from other cell components. To circumvent some of these problems, I am currently developing pull-down protocols, using TMR-r13 as a bait for lipid enrichment. While this approach will not identify all the oxidized lipids present in the plasma membrane, it might help establish which species interact with the peptide during translocation.

While much remains to be done to reveal how a highly hydrophilic and charged peptide such as TMR-r13 crosses a hydrophobic membrane, the interplay between cytosolic penetration and oxidation presented herein should have immediate implications. For instance, inducing oxidative damage to cellular membranes might offer a novel strategy to improve the cell permeability of therapeutic peptides. As indicated by experiments involving co-incubation with PGPC or PazePC, formulations that include CPPs and oxidized lipids might represent one such strategy.

REFERENCES

1. Sternson, L.A. Obstacles to polypeptide delivery. *Ann N Y Acad Sci* **507**, 19-21 (1987).

2. Kim, T.K. & Eberwine, J.H. Mammalian cell transfection: the present and the future. *Analytical and bioanalytical chemistry* **397**, 3173-3178 (2010).

3. Bechara, C. & Sagan, S. Cell-penetrating peptides: 20 years later, where do we stand? *FEBS letters* **587**, 1693-1702 (2013).

4. Ryser, H.J. & Hancock, R. Histones and basic polyamino acids stimulate the uptake of albumin by tumor cells in culture. *Science* **150**, 501-503 (1965).

5. Shen, W.C. & Ryser, H.J. Conjugation of poly-L-lysine to albumin and horseradish peroxidase: a novel method of enhancing the cellular uptake of proteins. *Proceedings of the National Academy of Sciences of the United States of America* **75**, 1872-1876 (1978).

6. Green, M. & Loewenstein, P.M. Autonomous functional domains of chemically synthesized human immunodeficiency virus tat trans-activator protein. *Cell* **55**, 1179-1188 (1988).

7. Frankel, A.D. & Pabo, C.O. Cellular uptake of the tat protein from human immunodeficiency virus. *Cell* **55**, 1189-1193 (1988).

8. Vives, E., Brodin, P. & Lebleu, B. A truncated HIV-1 Tat protein basic domain rapidly translocates through the plasma membrane and accumulates in the cell nucleus. *The Journal of biological chemistry* **272**, 16010-16017 (1997).

9. Kim, D.T. et al. Introduction of soluble proteins into the MHC class I pathway by conjugation to an HIV tat peptide. *The Journal of Immunology* **159**, 1666-1668 (1997).

10. Wender, P.A. et al. The design, synthesis, and evaluation of molecules that enable or enhance cellular uptake: peptoid molecular transporters. *Proceedings of the National Academy of Sciences of the United States of America* **97**, 13003-13008 (2000).

11. Joliot, A., Pernelle, C., Deagostini-Bazin, H. & Prochiantz, A. Antennapedia homeobox peptide regulates neural morphogenesis. *Proceedings of the National Academy of Sciences of the United States of America* **88**, 1864-1868 (1991).

12. Derossi, D., Joliot, A.H., Chassaing, G. & Prochiantz, A. The third helix of the Antennapedia homeodomain translocates through biological membranes. *The Journal of biological chemistry* **269**, 10444-10450 (1994).

13. Gautam, A. et al. CPPsite: a curated database of cell penetrating peptides. *Database (Oxford)* **2012**, bas015 (2012).

14. Herce, H.D., Garcia, A.E. & Cardoso, M.C. Fundamental molecular mechanism for the cellular uptake of guanidinium-rich molecules. *Journal of the American Chemical Society* **136**, 17459-17467 (2014).

15. Eudes, F. & Chugh, A. Cell-penetrating peptides: From mammalian to plant cells. *Plant Signal Behav* **3**, 549-550 (2008).

16. Chen, Y.J. et al. A gene delivery system for insect cells mediated by arginine-rich cell-penetrating peptides. *Gene* **493**, 201-210 (2012).

17. Erazo-Oliveras, A. et al. Protein delivery into live cells by incubation with an endosomolytic agent. *Nature methods* **11**, 861-867 (2014).

18. Lim, S., Koo, J.-H. & Choi, J.-M. Use of Cell-Penetrating Peptides in Dendritic Cell-Based Vaccination. *Immune Netw* **16**, 33-43 (2016).

19. Kaitsuka, T. & Tomizawa, K. Cell-Penetrating Peptide as a Means of Directing the Differentiation of Induced-Pluripotent Stem Cells. *International Journal of Molecular Sciences* **16**, 25986 (2015).

20. Milletti, F. Cell-penetrating peptides: classes, origin, and current landscape. *Drug discovery today* **17**, 850-860 (2012).

21. Lindgren, M. & Langel, U. Classes and prediction of cell-penetrating peptides. *Methods in molecular biology* **683**, 3-19 (2011).

22. Lee, Y.-J., Erazo-Oliveras, A. & Pellois, J.-P. Delivery of Macromolecules into Live Cells by Simple Co-incubation with a Peptide. *ChemBioChem* **11**, 325-330 (2010).

23. Wadia, J.S., Stan, R.V. & Dowdy, S.F. Transducible TAT-HA fusogenic peptide enhances escape of TAT-fusion proteins after lipid raft macropinocytosis. *Nature medicine* **10**, 310-315 (2004).

24. Pooga, M., Hällbrink, M., Zorko, M., Langel, U. & lo Cell penetration by transportan. *The FASEB Journal* **12**, 67-77 (1998).

25. Li, W., Nicol, F. & Szoka, F.C., Jr. GALA: a designed synthetic pH-responsive amphipathic peptide with applications in drug and gene delivery. *Adv Drug Deliv Rev* **56**, 967-985 (2004).

26. Chen, S. et al. Gelatinase activity imaged by activatable cell-penetrating peptides in cell-based and in vivo models of stroke. *J Cereb Blood Flow Metab* (2015).

27. Eiriksdottir, E., Konate, K., Langel, U., Divita, G. & Deshayes, S. Secondary structure of cell-penetrating peptides controls membrane interaction and insertion. *Biochimica et biophysica acta* **1798**, 1119-1128 (2010).

28. Martin, I., Teixido, M. & Giralt, E. Design, synthesis and characterization of a new anionic cell-penetrating peptide: SAP(E). *Chembiochem* **12**, 896-903 (2011).

29. Yamada, T., Das Gupta, T.K. & Beattie, C.W. p28, an anionic cell-penetrating peptide, increases the activity of wild type and mutated p53 without altering its conformation. *Molecular pharmaceutics* **10**, 3375-3383 (2013).

30. Cascales, L. et al. Identification and characterization of a new family of cell-penetrating peptides: cyclic cell-penetrating peptides. *The Journal of biological chemistry* **286**, 36932-36943 (2011).

31. Huang, Y.H., Chaousis, S., Cheneval, O., Craik, D.J. & Henriques, S.T. Optimization of the cyclotide framework to improve cell penetration properties. *Frontiers in pharmacology* **6**, 17 (2015).

32. White, C.J. & Yudin, A.K. Contemporary strategies for peptide macrocyclization. *Nature chemistry* **3**, 509-524 (2011).

33. Verdine, G.L. & Hilinski, G.J. Stapled peptides for intracellular drug targets. *Methods in enzymology* **503**, 3-33 (2012).

34. Bernal, F., Tyler, A.F., Korsmeyer, S.J., Walensky, L.D. & Verdine, G.L. Reactivation of the p53 tumor suppressor pathway by a stapled p53 peptide. *Journal of the American Chemical Society* **129**, 2456-2457 (2007).

35. Chu, Q. et al. Towards understanding cell penetration by stapled peptides. *Medchemcomm* **6**, 111-119 (2015).

36. Lattig-Tunnemann, G. et al. Backbone rigidity and static presentation of guanidinium groups increases cellular uptake of arginine-rich cell-penetrating peptides. *Nature communications* **2**, 453 (2011).

37. Nischan, N. et al. Covalent attachment of cyclic TAT peptides to GFP results in protein delivery into live cells with immediate bioavailability. *Angewandte Chemie* **54**, 1950-1953 (2015).

38. Mitchell, D.J., Kim, D.T., Steinman, L., Fathman, C.G. & Rothbard, J.B. Polyarginine enters cells more efficiently than other polycationic homopolymers. *The journal of peptide research : official journal of the American Peptide Society* **56**, 318-325 (2000).

39. Futaki, S. et al. Arginine-rich peptides. An abundant source of membrane-permeable peptides having potential as carriers for intracellular protein delivery. *The Journal of biological chemistry* **276**, 5836-5840 (2001).

40. Richard, J.P. et al. Cell-penetrating peptides. A reevaluation of the mechanism of cellular uptake. *The Journal of biological chemistry* **278**, 585-590 (2003).

41. Lundberg, M., Wikstrom, S. & Johansson, M. Cell surface adherence and endocytosis of protein transduction domains. *Molecular therapy : the journal of the American Society of Gene Therapy* **8**, 143-150 (2003).

42. Thoren, P.E. et al. Uptake of analogs of penetratin, Tat(48-60) and oligoarginine in live cells. *Biochem Biophys Res Commun* **307**, 100-107 (2003).

43. Luedtke, N.W., Carmichael, P. & Tor, Y. Cellular uptake of aminoglycosides, guanidinoglycosides, and poly-arginine. *Journal of the American Chemical Society* **125**, 12374-12375 (2003).

44. Khafagy el, S. et al. Efficiency of cell-penetrating peptides on the nasal and intestinal absorption of therapeutic peptides and proteins. *International journal of pharmaceutics* **381**, 49-55 (2009).

45. Fretz, M.M. et al. Temperature-, concentration- and cholesterol-dependent translocation of L- and D-octa-arginine across the plasma and nuclear membrane of CD34+ leukaemia cells. *The Biochemical journal* **403**, 335-342 (2007).

46. Kamei, N. et al. Molecular imaging analysis of intestinal insulin absorption boosted by cell-penetrating peptides by using positron emission tomography. *Journal of controlled release : official journal of the Controlled Release Society* **146**, 16-22 (2010).

47. Tunnemann, G. et al. Live-cell analysis of cell penetration ability and toxicity of oligo-arginines. *Journal of peptide science : an official publication of the European Peptide Society* **14**, 469-476 (2008).

48. Rothbard, J.B. et al. Arginine-rich molecular transporters for drug delivery: role of backbone spacing in cellular uptake. *J Med Chem* **45**, 3612-3618 (2002).

49. Nakase, I. et al. Cellular uptake of arginine-rich peptides: roles for macropinocytosis and actin rearrangement. *Molecular therapy : the journal of the American Society of Gene Therapy* **10**, 1011-1022 (2004).

50. Naik, R.J., Chandra, P., Mann, A. & Ganguli, M. Exogenous and cell surface glycosaminoglycans alter DNA delivery efficiency of arginine and lysine homopeptides in distinctly different ways. *The Journal of biological chemistry* **286**, 18982-18993 (2011).

51. Takechi-Haraya, Y. et al. Enthalpy-driven interactions with sulfated glycosaminoglycans promote cell membrane penetration of arginine peptides. *Biochimica et biophysica acta* **1858**, 1339-1349 (2016).

52. Sakai, N. & Matile, S. Anion-mediated transfer of polyarginine across liquid and bilayer membranes. *Journal of the American Chemical Society* **125**, 14348-14356 (2003).

53. Nakase, I., Takeuchi, T., Tanaka, G. & Futaki, S. Methodological and cellular aspects that govern the internalization mechanisms of arginine-rich cell-penetrating peptides. *Advanced Drug Delivery Reviews* **60**, 598-607 (2008).

54. Schmidt, N.W. et al. Molecular basis for nanoscopic membrane curvature generation from quantum mechanical models and synthetic transporter sequences. *Journal of the American Chemical Society* **134**, 19207-19216 (2012).

55. Meerovich, I., Muthukrishnan, N., Johnson, G.A., Erazo-Oliveras, A. & Pellois, J.-P. Photodamage of lipid bilayers by irradiation of a fluorescently labeled cell-penetrating peptide. *Biochimica et Biophysica Acta (BBA) - General Subjects* **1840**, 507-515 (2014).

56. Rothbard, J.B., Jessop, T.C., Lewis, R.S., Murray, B.A. & Wender, P.A. Role of Membrane Potential and Hydrogen Bonding in the Mechanism of Translocation of Guanidinium-Rich Peptides into Cells. *Journal of the American Chemical Society* **126**, 9506-9507 (2004).

57. Wender, P.A., Rothbard, J.B., Jessop, T.C., Kreider, E.L. & Wylie, B.L. Oligocarbamate molecular transporters: design, synthesis, and biological evaluation of a new class of transporters for drug delivery. *Journal of the American Chemical Society* **124**, 13382-13383 (2002).

58. Rueping, M., Mahajan, Y., Sauer, M. & Seebach, D. Cellular uptake studies with beta-peptides. *Chembiochem* **3**, 257-259 (2002).

59. Tezgel, A.O. et al. Novel protein transduction domain mimics as nonviral delivery vectors for siRNA targeting NOTCH1 in primary human T cells. *Molecular therapy : the journal of the American Society of Gene Therapy* **21**, 201-209 (2013).

60. Tezgel, A.O., Telfer, J.C. & Tew, G.N. De novo designed protein transduction domain mimics from simple synthetic polymers. *Biomacromolecules* **12**, 3078-3083 (2011).

61. Kim, T.I., Ou, M., Lee, M. & Kim, S.W. Arginine-grafted bioreducible poly(disulfide amine) for gene delivery systems. *Biomaterials* **30**, 658-664 (2009).

62. Erazo-Oliveras, A., Muthukrishnan, N., Baker, R., Wang, T.-Y. & Pellois, J.-P. Improving the Endosomal Escape of Cell-Penetrating Peptides and Their Cargos: Strategies and Challenges. *Pharmaceuticals* **5**, 1177-1209 (2012).

63. Fuchs, S.M. & Raines, R.T. Pathway for Polyarginine Entry into Mammalian Cells†. *Biochemistry* **43**, 2438-2444 (2004).

64. Heitz, F., Morris, M.C. & Divita, G. Twenty years of cell-penetrating peptides: from molecular mechanisms to therapeutics. *British journal of pharmacology* **157**, 195-206 (2009).

65. Madani, F., Lindberg, S., Langel, U., Futaki, S. & Graslund, A. Mechanisms of cellular uptake of cell-penetrating peptides. *Journal of biophysics* **2011**, 414729 (2011).

66. Jones, A.T. & Sayers, E.J. Cell entry of cell penetrating peptides: tales of tails wagging dogs. *Journal of controlled release : official journal of the Controlled Release Society* **161**, 582-591 (2012).

67. Varkouhi, A.K., Scholte, M., Storm, G. & Haisma, H.J. Endosomal escape pathways for delivery of biologicals. *Journal of controlled release : official journal of the Controlled Release Society* **151**, 220-228 (2011).

68. Brock, R. The uptake of arginine-rich cell-penetrating peptides: putting the puzzle together. *Bioconjugate chemistry* **25**, 863-868 (2014).

69. Palm-Apergi, C., Lonn, P. & Dowdy, S.F. Do cell-penetrating peptides actually "penetrate" cellular membranes? *Molecular therapy : the journal of the American Society of Gene Therapy* **20**, 695-697 (2012).

70. Hirose, H. et al. Transient focal membrane deformation induced by arginine-rich peptides leads to their direct penetration into cells. *Molecular therapy : the journal of the American Society of Gene Therapy* **20**, 984-993 (2012).

71. Belting, M. Heparan sulfate proteoglycan as a plasma membrane carrier. *Trends Biochem Sci* **28**, 145-151 (2003).

72. Bishop, J.R., Schuksz, M. & Esko, J.D. Heparan sulphate proteoglycans fine-tune mammalian physiology. *Nature* **446**, 1030-1037 (2007).

73. Bechara, C. et al. Massive glycosaminoglycan-dependent entry of Trp-containing cell-penetrating peptides induced by exogenous sphingomyelinase or cholesterol depletion. *Cellular and molecular life sciences : CMLS* **72**, 809-820 (2015).

74. Letoha, T. et al. Cell-penetrating peptide exploited syndecans. *Biochimica et biophysica acta* **1798**, 2258-2265 (2010).

75. Fromm, J.R., Hileman, R.E., Caldwell, E.E., Weiler, J.M. & Linhardt, R.J. Pattern and spacing of basic amino acids in heparin binding sites. *Archives of biochemistry and biophysics* **343**, 92-100 (1997).

76. Goncalves, E., Kitas, E. & Seelig, J. Binding of oligoarginine to membrane lipids and heparan sulfate: structural and thermodynamic characterization of a cell-penetrating peptide. *Biochemistry* **44**, 2692-2702 (2005).

77. Ziegler, A. Thermodynamic studies and binding mechanisms of cell-penetrating peptides with lipids and glycosaminoglycans. *Adv Drug Deliv Rev* **60**, 580-597 (2008).

78. Ziegler, A. & Seelig, J. Contributions of glycosaminoglycan binding and clustering to the biological uptake of the nonamphipathic cell-penetrating peptide WR9. *Biochemistry* **50**, 4650-4664 (2011).

79. Thoren, P.E. et al. Membrane binding and translocation of cell-penetrating peptides. *Biochemistry* **43**, 3471-3489 (2004).

80. Sakai, N., Takeuchi, T., Futaki, S. & Matile, S. Direct observation of anion-mediated translocation of fluorescent oligoarginine carriers into and across bulk liquid and anionic bilayer membranes. *Chembiochem* **6**, 114-122 (2005).

81. Pankov, R., Markovska, T., Antonov, P., Ivanova, L. & Momchilova, A. The plasma membrane lipid composition affects fusion between cells and model membranes. *Chem Biol Interact* **164**, 167-173 (2006).

82. Blixt, Y., Valeur, A. & Everitt, E. Cultivation of HeLa cells with fetal bovine serum or Ultroser G: effects on the plasma membrane constitution. *In Vitro Cell Dev Biol* **26**, 691-700 (1990).

83. Guttler, F. & Clausen, J. Changes in lipid pattern of HeLa cells exposed to immunoglobulin G and complement. *The Biochemical journal* **115**, 959-968 (1969).

84. Fadeel, B. & Xue, D. The ins and outs of phospholipid asymmetry in the plasma membrane: roles in health and disease. *Critical reviews in biochemistry and molecular biology* **44**, 264-277 (2009).

85. Daleke, D.L. Regulation of transbilayer plasma membrane phospholipid asymmetry. *Journal of lipid research* **44**, 233-242 (2003).

86. Gavino, V.C., Miller, J.S., Dillman, J.M., Milo, G.E. & Cornwell, D.G. Polyunsaturated fatty acid accumulation in the lipids of cultured fibroblasts and smooth muscle cells. *Journal of lipid research* **22**, 57-62 (1981).

87. Lee, P.H., Trowbridge, J.M., Taylor, K.R., Morhenn, V.B. & Gallo, R.L. Dermatan sulfate proteoglycan and glycosaminoglycan synthesis is induced in fibroblasts by transfer to a three-dimensional extracellular environment. *The Journal of biological chemistry* **279**, 48640-48646 (2004).

88. Tanaka, G. et al. CXCR4 stimulates macropinocytosis: implications for cellular uptake of arginine-rich cell-penetrating peptides and HIV. *Chem Biol* **19**, 1437-1446 (2012).

89. Tsumuraya, T. & Matsushita, M. COPA and SLC4A4 are required for cellular entry of arginine-rich peptides. *PloS one* **9**, e86639 (2014).

90. West, M.A., Bretscher, M.S. & Watts, C. Distinct endocytotic pathways in epidermal growth factor-stimulated human carcinoma A431 cells. *The Journal of cell biology* **109**, 2731-2739 (1989).

91. Swanson, J.A. & Watts, C. Macropinocytosis. *Trends in cell biology* **5**, 424-428 (1995).

92. Meier, O. et al. Adenovirus triggers macropinocytosis and endosomal leakage together with its clathrin-mediated uptake. *The Journal of cell biology* **158**, 1119-1131 (2002).

93. Al-Taei, S. et al. Intracellular traffic and fate of protein transduction domains HIV-1 TAT peptide and octaarginine. Implications for their utilization as drug delivery vectors. *Bioconjugate chemistry* **17**, 90-100 (2006).

94. Duchardt, F., Fotin-Mleczek, M., Schwarz, H., Fischer, R. & Brock, R. A comprehensive model for the cellular uptake of cationic cell-penetrating peptides. *Traffic* **8**, 848-866 (2007).

95. Al Soraj, M. et al. siRNA and pharmacological inhibition of endocytic pathways to characterize the differential role of macropinocytosis and the actin cytoskeleton on cellular uptake of dextran and cationic cell penetrating peptides octaarginine (R8) and HIV-Tat. *Journal of controlled release : official journal of the Controlled Release Society* **161**, 132-141 (2012).

96. Appelbaum, J.S. et al. Arginine topology controls escape of minimally cationic proteins from early endosomes to the cytoplasm. *Chem Biol* **19**, 819-830 (2012).

97. He, J. et al. Direct cytosolic delivery of polar cargo to cells by spontaneous membrane-translocating peptides. *The Journal of biological chemistry* **288**, 29974-29986 (2013).

98. Walrant, A. et al. Different membrane behaviour and cellular uptake of three basic arginine-rich peptides. *Biochimica et biophysica acta* **1808**, 382-393 (2011).

99. Takayama, K. et al. Enhanced intracellular delivery using arginine-rich peptides by the addition of penetration accelerating sequences (Pas). *Journal of controlled release : official journal of the Controlled Release Society* **138**, 128-133 (2009).

100. Takeuchi, T. et al. Direct and Rapid Cytosolic Delivery Using Cell-Penetrating Peptides Mediated by Pyrenebutyrate. *ACS Chemical Biology* **1**, 299-303 (2006).

101. Michiue, H. et al. The NH2 terminus of influenza virus hemagglutinin-2 subunit peptides enhances the antitumor potency of polyarginine-mediated p53 protein transduction. *The Journal of biological chemistry* **280**, 8285-8289 (2005).

102. Yamazaki, C.M. et al. Collagen-like cell-penetrating peptides. *Angewandte Chemie* **52**, 5497-5500 (2013).

103. Takayama, K. et al. Effect of the attachment of a penetration accelerating sequence and the influence of hydrophobicity on octaarginine-mediated intracellular delivery. *Molecular pharmaceutics* **9**, 1222-1230 (2012).

104. Puckett, C.A. & Barton, J.K. Fluorescein redirects a ruthenium-octaarginine conjugate to the nucleus. *Journal of the American Chemical Society* **131**, 8738-8739 (2009).

105. Watkins, C.L., Schmaljohann, D., Futaki, S. & Jones, A.T. Low concentration thresholds of plasma membranes for rapid energy-independent translocation of a cell-penetrating peptide. *The Biochemical journal* **420**, 179-189 (2009).

106. Jiao, C.Y. et al. Translocation and endocytosis for cell-penetrating peptide internalization. *The Journal of biological chemistry* **284**, 33957-33965 (2009).

107. Kosuge, M., Takeuchi, T., Nakase, I., Jones, A.T. & Futaki, S. Cellular internalization and distribution of arginine-rich peptides as a function of extracellular peptide concentration, serum, and plasma membrane associated proteoglycans. *Bioconjugate chemistry* **19**, 656-664 (2008).

108. Zaro, J.L., Rajapaksa, T.E., Okamoto, C.T. & Shen, W.C. Membrane transduction of oligoarginine in HeLa cells is not mediated by macropinocytosis. *Molecular pharmaceutics* **3**, 181-186 (2006).

109. Vercauteren, D. et al. The use of inhibitors to study endocytic pathways of gene carriers: optimization and pitfalls. *Molecular therapy : the journal of the American Society of Gene Therapy* **18**, 561-569 (2010).

110. Ivanov, A.I. Pharmacological inhibition of endocytic pathways: is it specific enough to be useful? *Methods in molecular biology* **440**, 15-33 (2008).

111. Verdurmen, W.P., Thanos, M., Ruttekolk, I.R., Gulbins, E. & Brock, R. Cationic cell-penetrating peptides induce ceramide formation via acid sphingomyelinase: implications for uptake. *Journal of controlled release : official journal of the Controlled Release Society* **147**, 171-179 (2010).

112. Pae, J. et al. Translocation of cell-penetrating peptides across the plasma membrane is controlled by cholesterol and microenvironment created by membranous proteins. *Journal of controlled release : official journal of the Controlled Release Society* **192**, 103-113 (2014).

113. Saalik, P. et al. Penetration without cells: membrane translocation of cell-penetrating peptides in the model giant plasma membrane vesicles. *Journal of*

controlled release : official journal of the Controlled Release Society **153**, 117-125 (2011).

114. Zhang, T. et al. Inhibiting bladder tumor growth with a cell penetrating R11 peptide derived from the p53 C-terminus. *Oncotarget* **6**, 37782-37791 (2015).

115. Boland, K. et al. Targeting the 19S proteasomal subunit, Rpt4, for the treatment of colon cancer. *Eur J Pharmacol* (2016).

116. Oba, M., Demizu, Y., Yamashita, H., Kurihara, M. & Tanaka, M. Plasmid DNA delivery using fluorescein-labeled arginine-rich peptides. *Bioorganic & medicinal chemistry* **23**, 4911-4918 (2015).

117. Liu, J., Gaj, T., Patterson, J.T., Sirk, S.J. & Barbas, C.F., 3rd Cell-penetrating peptide-mediated delivery of TALEN proteins via bioconjugation for genome engineering. *PloS one* **9**, e85755 (2014).

118. Alhakamy, N.A. & Berkland, C.J. Polyarginine molecular weight determines transfection efficiency of calcium condensed complexes. *Molecular pharmaceutics* **10**, 1940-1948 (2013).

119. Wender, P.A. et al. Taxol-oligoarginine conjugates overcome drug resistance in-vitro in human ovarian carcinoma. *Gynecologic oncology* **126**, 118-123 (2012).

120. Yukawa, H. et al. Transduction of cell-penetrating peptides into induced pluripotent stem cells. *Cell transplantation* **19**, 901-909 (2010).

121. Banoczi, Z. et al. Synthesis and in vitro antitumor effect of vinblastine derivative-oligoarginine conjugates. *Bioconjugate chemistry* **21**, 1948-1955 (2010).

122. Zhou, H. et al. Generation of induced pluripotent stem cells using recombinant proteins. *Cell Stem Cell* **4**, 381-384 (2009).

123. Patel, L.N. et al. Conjugation with cationic cell-penetrating peptide increases pulmonary absorption of insulin. *Molecular pharmaceutics* **6**, 492-503 (2009).

124. Kim, D. et al. Generation of human induced pluripotent stem cells by direct delivery of reprogramming proteins. *Cell Stem Cell* **4**, 472-476 (2009).

125. Miklan, Z. et al. New ferrocene containing peptide conjugates: synthesis and effect on human leukemia (HL-60) cells. *Biopolymers* **88**, 108-114 (2007).

126. Dubikovskaya, E.A., Thorne, S.H., Pillow, T.H., Contag, C.H. & Wender, P.A. Overcoming multidrug resistance of small-molecule therapeutics through conjugation with releasable octaarginine transporters. *Proceedings of the National Academy of Sciences of the United States of America* **105**, 12128-12133 (2008).

127. Mitsui, H., Inozume, T., Kitamura, R., Shibagaki, N. & Shimada, S. Polyarginine-mediated protein delivery to dendritic cells presents antigen more efficiently onto MHC class I and class II and elicits superior antitumor immunity. *J Invest Dermatol* **126**, 1804-1812 (2006).

128. Kumar, S. et al. Peptides as skin penetration enhancers: mechanisms of action. *Journal of controlled release : official journal of the Controlled Release Society* **199**, 168-178 (2015).

129. Mai, J.C., Shen, H., Watkins, S.C., Cheng, T. & Robbins, P.D. Efficiency of protein transduction is cell type-dependent and is enhanced by dextran sulfate. *The Journal of biological chemistry* **277**, 30208-30218 (2002).

130. Rothbard, J.B. et al. Conjugation of arginine oligomers to cyclosporin A facilitates topical delivery and inhibition of inflammation. *Nature medicine* **6**, 1253-1257 (2000).

131. Wender, P.A., Galliher, W.C., Goun, E.A., Jones, L.R. & Pillow, T.H. The design of guanidinium-rich transporters and their internalization mechanisms. *Advanced Drug Delivery Reviews* **60**, 452-472 (2008).

132. Lamaziere, A. et al. Non-metabolic membrane tubulation and permeability induced by bioactive peptides. *PloS one* **2**, e201 (2007).

133. Herce, H.D. et al. Arginine-rich peptides destabilize the plasma membrane, consistent with a pore formation translocation mechanism of cell-penetrating peptides. *Biophys J* **97**, 1917-1925 (2009).

134. Maiolo, J.R., Ferrer, M. & Ottinger, E.A. Effects of cargo molecules on the cellular uptake of arginine-rich cell-penetrating peptides. *Biochimica et biophysica acta* **1712**, 161-172 (2005).

135. Matsushita, M. et al. A high-efficiency protein transduction system demonstrating the role of PKA in long-lasting long-term potentiation. *J Neurosci* **21**, 6000-6007 (2001).

136. Futaki, S. et al. Stearylated arginine-rich peptides: a new class of transfection systems. *Bioconjugate chemistry* **12**, 1005-1011 (2001).

137. Futaki, S., Nakase, I., Suzuki, T., Youjun, Z. & Sugiura, Y. Translocation of branched-chain arginine peptides through cell membranes: flexibility in the spatial disposition of positive charges in membrane-permeable peptides. *Biochemistry* **41**, 7925-7930 (2002).

138. Robbins, P.B. et al. Peptide delivery to tissues via reversibly linked protein transduction sequences. *BioTechniques* **33**, 190-192, 194 (2002).

139. Suzuki, T. et al. Possible existence of common internalization mechanisms among arginine-rich peptides. *The Journal of biological chemistry* **277**, 2437-2443 (2002).

140. Takenobu, T. et al. Development of p53 protein transduction therapy using membrane-permeable peptides and the application to oral cancer cells. *Mol Cancer Ther* **1**, 1043-1049 (2002).

141. Siprashvili, Z. et al. Gene transfer via reversible plasmid condensation with cysteine-flanked, internally spaced arginine-rich peptides. *Hum Gene Ther* **14**, 1225-1233 (2003).

142. Fischer, R., Kohler, K., Fotin-Mleczek, M. & Brock, R. A stepwise dissection of the intracellular fate of cationic cell-penetrating peptides. *The Journal of biological chemistry* **279**, 12625-12635 (2004).

143. Khalil, I.A. et al. Mechanism of improved gene transfer by the N-terminal stearylation of octaarginine: enhanced cellular association by hydrophobic core formation. *Gene Ther* **11**, 636-644 (2004).

144. Burlina, F., Sagan, S., Bolbach, G. & Chassaing, G. Quantification of the cellular uptake of cell-penetrating peptides by MALDI-TOF mass spectrometry. *Angewandte Chemie* **44**, 4244-4247 (2005).

145. Jones, S.W. et al. Characterisation of cell-penetrating peptide-mediated peptide delivery. *British journal of pharmacology* **145**, 1093-1102 (2005).

146. Shiraishi, T., Pankratova, S. & Nielsen, P.E. Calcium ions effectively enhance the effect of antisense peptide nucleic acids conjugated to cationic tat and oligoarginine peptides. *Chem Biol* **12**, 923-929 (2005).

147. Choi, Y., McCarthy, J.R., Weissleder, R. & Tung, C.H. Conjugation of a photosensitizer to an oligoarginine-based cell-penetrating peptide increases the efficacy of photodynamic therapy. *ChemMedChem* **1**, 458-463 (2006).

148. Shiraishi, T. & Nielsen, P.E. Photochemically enhanced cellular delivery of cell penetrating peptide-PNA conjugates. *FEBS letters* **580**, 1451-1456 (2006).

149. Gerbal-Chaloin, S. et al. First step of the cell-penetrating peptide mechanism involves Rac1 GTPase-dependent actin-network remodelling. *Biology of the cell / under the auspices of the European Cell Biology Organization* **99**, 223-238 (2007).

150. Nakase, I. et al. Interaction of arginine-rich peptides with membrane-associated proteoglycans is crucial for induction of actin organization and macropinocytosis. *Biochemistry* **46**, 492-501 (2007).

151. Cooley, C.B. et al. Oligocarbonate molecular transporters: oligomerization-based syntheses and cell-penetrating studies. *Journal of the American Chemical Society* **131**, 16401-16403 (2009).

152. Duchardt, F. et al. A cell-penetrating peptide derived from human lactoferrin with conformation-dependent uptake efficiency. *The Journal of biological chemistry* **284**, 36099-36108 (2009).

153. Guterstam, P. et al. Elucidating cell-penetrating peptide mechanisms of action for membrane interaction, cellular uptake, and translocation utilizing the hydrophobic counter-anion pyrenebutyrate. *Biochimica et biophysica acta* **1788**, 2509-2517 (2009).

154. Hu, J.W., Liu, B.R., Wu, C.Y., Lu, S.W. & Lee, H.J. Protein transport in human cells mediated by covalently and noncovalently conjugated arginine-rich intracellular delivery peptides. *Peptides* **30**, 1669-1678 (2009).

155. Won, Y.W., Kim, H.A., Lee, M. & Kim, Y.H. Reducible poly(oligo-D-arginine) for enhanced gene expression in mouse lung by intratracheal injection. *Molecular therapy : the journal of the American Society of Gene Therapy* **18**, 734-742 (2010).

156. Baoum, A.A. & Berkland, C. Calcium condensation of DNA complexed with cell-penetrating peptides offers efficient, noncytotoxic gene delivery. *Journal of pharmaceutical sciences* **100**, 1637-1642 (2011).

157. Jha, D. et al. CyLoP-1: a novel cysteine-rich cell-penetrating peptide for cytosolic delivery of cargoes. *Bioconjugate chemistry* **22**, 319-328 (2011).

158. Ma, D.X., Shi, N.Q. & Qi, X.R. Distinct transduction modes of arginine-rich cell-penetrating peptides for cargo delivery into tumor cells. *International journal of pharmaceutics* **419**, 200-208 (2011).

159. Marks, J.R., Placone, J., Hristova, K. & Wimley, W.C. Spontaneous membrane-translocating peptides by orthogonal high-throughput screening. *Journal of the American Chemical Society* **133**, 8995-9004 (2011).

160. Srinivasan, D. et al. Conjugation to the cell-penetrating peptide TAT potentiates the photodynamic effect of carboxytetramethylrhodamine. *PloS one* **6**, e17732 (2011).

161. Verdurmen, W.P. et al. Preferential uptake of L- versus D-amino acid cell-penetrating peptides in a cell type-dependent manner. *Chem Biol* **18**, 1000-1010 (2011).

162. Hitsuda, T. et al. A protein transduction method using oligo-arginine (3R) for the delivery of transcription factors into cell nuclei. *Biomaterials* **33**, 4665-4672 (2012).

163. Kondo, E. et al. Tumour lineage-homing cell-penetrating peptides as anticancer molecular delivery systems. *Nature communications* **3**, 951 (2012).

164. Lee, J.H., Song, H.S., Park, T.H., Lee, S.G. & Kim, B.G. Screening of cell-penetrating peptides using mRNA display. *Biotechnol J* **7**, 387-396 (2012).

165. Ma, Y. et al. Direct cytosolic delivery of cargoes in vivo by a chimera consisting of D- and L-arginine residues. *Journal of controlled release : official journal of the Controlled Release Society* **162**, 286-294 (2012).

166. Mo, R.H., Zaro, J.L. & Shen, W.C. Comparison of cationic and amphipathic cell penetrating peptides for siRNA delivery and efficacy. *Molecular pharmaceutics* **9**, 299-309 (2012).

167. Liu, B.R. et al. Endocytic Trafficking of Nanoparticles Delivered by Cell-penetrating Peptides Comprised of Nona-arginine and a Penetration Accelerating Sequence. *PloS one* **8**, e67100 (2013).

168. Chakrabarti, A. et al. Multivalent presentation of the cell-penetrating peptide nona-arginine on a linear scaffold strongly increases its membrane-perturbing capacity. *Biochimica et biophysica acta* **1838**, 3097-3106 (2014).

169. Nakase, I., Osaki, K., Tanaka, G., Utani, A. & Futaki, S. Molecular interplays involved in the cellular uptake of octaarginine on cell surfaces and the importance of syndecan-4 cytoplasmic V domain for the activation of protein kinase Calpha. *Biochem Biophys Res Commun* **446**, 857-862 (2014).

170. Bertucci, A. et al. Combined Delivery of Temozolomide and Anti-miR221 PNA Using Mesoporous Silica Nanoparticles Induces Apoptosis in Resistant Glioma Cells. *Small* **11**, 5687-5695 (2015).

171. Chu, D. et al. Rational modification of oligoarginine for highly efficient siRNA delivery: structure-activity relationship and mechanism of intracellular trafficking of siRNA. *Nanomedicine* **11**, 435-446 (2015).

172. Gross, A. et al. Vesicular disruption of lysosomal targeting organometallic polyarginine bioconjugates. *Metallomics* **7**, 371-384 (2015).

173. LaRochelle, J.R., Cobb, G.B., Steinauer, A., Rhoades, E. & Schepartz, A. Fluorescence correlation spectroscopy reveals highly efficient cytosolic delivery of certain penta-arg proteins and stapled peptides. *Journal of the American Chemical Society* **137**, 2536-2541 (2015).

174. Lyu, S.K. & Kwon, H. Preparation of cell-permeable Cre recombinase by expressed protein ligation. *BMC biotechnology* **15**, 7 (2015).

175. Melikov, K. et al. Efficient entry of cell-penetrating peptide nona-arginine into adherent cells involves a transient increase in intracellular calcium. *The Biochemical journal* **471**, 221-230 (2015).

176. deRonde, B.M., Torres, J.A., Minter, L.M. & Tew, G.N. Development of Guanidinium-Rich Protein Mimics for Efficient siRNA Delivery into Human T Cells. *Biomacromolecules* **16**, 3172-3179 (2015).

177. Traboulsi, H. et al. Macrocyclic cell penetrating peptides: a study of structure-penetration properties. *Bioconjugate chemistry* **26**, 405-411 (2015).

178. Alhakamy, N.A., Dhar, P. & Berkland, C.J. Charge Type, Charge Spacing, and Hydrophobicity of Arginine-Rich Cell-Penetrating Peptides Dictate Gene Transfection. *Molecular pharmaceutics* (2016).

179. Backlund, C.M., Takeuchi, T., Futaki, S. & Tew, G.N. Relating structure and internalization for ROMP-based protein mimics. *Biochimica et biophysica acta* (2016).

180. Kamei, N. et al. Applicability and Limitations of Cell-Penetrating Peptides in Noncovalent Mucosal Drug or Carrier Delivery Systems. *Journal of pharmaceutical sciences* **105**, 747-753 (2016).

181. Kawaguchi, Y. et al. Syndecan-4 Is a Receptor for Clathrin-Mediated Endocytosis of Arginine-Rich Cell-Penetrating Peptides. *Bioconjugate chemistry* **27**, 1119-1130 (2016).

182. Oba, M., Kato, T., Furukawa, K. & Tanaka, M. A Cell-Penetrating Peptide with a Guanidinylethyl Amine Structure Directed to Gene Delivery. *Scientific reports* **6**, 19913 (2016).

183. Swiecicki, J.M. et al. How to unveil self-quenched fluorophores and subsequently map the subcellular distribution of exogenous peptides. *Scientific reports* **6**, 20237 (2016).

184. Szabo, I., Orban, E., Schlosser, G., Hudecz, F. & Banoczi, Z. Cell-penetrating conjugates of pentaglutamylated methotrexate as potential anticancer drugs against resistant tumor cells. *European journal of medicinal chemistry* **115**, 361-368 (2016).

185. Maiolo, J.R., 3rd, Ottinger, E.A. & Ferrer, M. Specific redistribution of cell-penetrating peptides from endosomes to the cytoplasm and nucleus upon laser illumination. *Journal of the American Chemical Society* **126**, 15376-15377 (2004).

186. Matsushita, M. et al. Photo-acceleration of protein release from endosome in the protein transduction system. *FEBS letters* **572**, 221-226 (2004).

187. Muthukrishnan, N., Johnson, G.A., Erazo-Oliveras, A. & Pellois, J.-P. Synergy Between Cell-Penetrating Peptides and Singlet Oxygen Generators Leads to Efficient Photolysis of Membranes. *Photochemistry and Photobiology* **89**, 625-630 (2013).

188. Philippova, M., Resink, T., Erne, P. & Bochkov, V. Oxidised phospholipids as biomarkers in human disease. *Swiss Med Wkly* **144**, w14037 (2014).

189. Bochkov, V.N. et al. Generation and biological activities of oxidized phospholipids. *Antioxidants & redox signaling* **12**, 1009-1059 (2010).

190. Barrera, G. Oxidative stress and lipid peroxidation products in cancer progression and therapy. *ISRN oncology* **2012**, 137289 (2012).

191. Niki, E., Yoshida, Y., Saito, Y. & Noguchi, N. Lipid peroxidation: Mechanisms, inhibition, and biological effects. *Biochemical and Biophysical Research Communications* **338**, 668-676 (2005).

192. Davies, K.J. Oxidative stress, antioxidant defenses, and damage removal, repair, and replacement systems. *IUBMB life* **50**, 279-289 (2000).

193. Gabriel, B. & Teissie, J. Generation of reactive-oxygen species induced by electropermeabilization of Chinese hamster ovary cells and their consequence on cell viability. *Eur J Biochem* **223**, 25-33 (1994).

194. Vernier, P.T. et al. Electroporating fields target oxidatively damaged areas in the cell membrane. *PloS one* **4**, e7966 (2009).

195. Smith, H.L. et al. Early stages of oxidative stress-induced membrane permeabilization: a neutron reflectometry study. *Journal of the American Chemical Society* **131**, 3631-3638 (2009).

196. Makky, A. & Tanaka, M. Impact of lipid oxidization on biophysical properties of model cell membranes. *The journal of physical chemistry. B* **119**, 5857-5863 (2015).

197. Wong-Ekkabut, J. et al. Effect of lipid peroxidation on the properties of lipid bilayers: a molecular dynamics study. *Biophys J* **93**, 4225-4236 (2007).

198. Halliwell, B. Oxidative stress in cell culture: an under-appreciated problem? *FEBS letters* **540**, 3-6 (2003).

199. Halliwell, B. Cell culture, oxidative stress, and antioxidants: avoiding pitfalls. *Biomedical journal* **37**, 99-105 (2014).

200. Israel, N. & Gougerot-Pocidalo, M.A. Oxidative stress in human immunodeficiency virus infection. *Cellular and molecular life sciences : CMLS* **53**, 864-870 (1997).

201. Kotova, E.A., Kuzevanov, A.V., Pashkovskaya, A.A. & Antonenko, Y.N. Selective permeabilization of lipid membranes by photodynamic action via formation of hydrophobic defects or pre-pores. *Biochimica et biophysica acta* **1808**, 2252-2257 (2011).

202. Martin, R.M. et al. Principles of protein targeting to the nucleolus. *Nucleus* **6**, 314-325 (2015).

203. Martin, R.M., Tunnemann, G., Leonhardt, H. & Cardoso, M.C. Nucleolar marker for living cells. *Histochem Cell Biol* **127**, 243-251 (2007).

204. Huotari, J. & Helenius, A. Endosome maturation. *The EMBO journal* **30**, 3481-3500 (2011).

205. Howard, A.C., McNeil, A.K. & McNeil, P.L. Promotion of plasma membrane repair by vitamin E. *Nature communications* **2**, 597 (2011).

206. Frikke-Schmidt, H. & Lykkesfeldt, J. Keeping the intracellular vitamin C at a physiologically relevant level in endothelial cell culture. *Analytical Biochemistry* **397**, 135-137 (2010).

207. Saito, Y., Yoshida, Y., Akazawa, T., Takahashi, K. & Niki, E. Cell death caused by selenium deficiency and protective effect of antioxidants. *The Journal of biological chemistry* **278**, 39428-39434 (2003).

208. Long, L.H. & Halliwell, B. Artefacts in cell culture: Pyruvate as a scavenger of hydrogen peroxide generated by ascorbate or epigallocatechin gallate in cell culture media. *Biochemical and Biophysical Research Communications* **388**, 700-704 (2009).

209. Ramakrishna, S. et al. Gene disruption by cell-penetrating peptide-mediated delivery of Cas9 protein and guide RNA. *Genome Res* **24**, 1020-1027 (2014).

210. Drummen, G.P., van Liebergen, L.C., Op den Kamp, J.A. & Post, J.A. C11-BODIPY(581/591), an oxidation-sensitive fluorescent lipid peroxidation probe: (micro)spectroscopic characterization and validation of methodology. *Free radical biology & medicine* **33**, 473-490 (2002).

211. Takahashi, M., Shibata, M. & Niki, E. Estimation of lipid peroxidation of live cells using a fluorescent probe, diphenyl-1-pyrenylphosphine. *Free radical biology & medicine* **31**, 164-174 (2001).

212. Falanga, V. & Kirsner, R.S. Low oxygen stimulates proliferation of fibroblasts seeded as single cells. *Journal of cellular physiology* **154**, 506-510 (1993).

213. Packer, L. & Fuehr, K. Low oxygen concentration extends the lifespan of cultured human diploid cells. *Nature* **267**, 423-425 (1977).

214. de la Haba, C., Palacio, J.R., Martinez, P. & Morros, A. Effect of oxidative stress on plasma membrane fluidity of THP-1 induced macrophages. *Biochimica et biophysica acta* **1828**, 357-364 (2013).

215. Benderitter, M., Vincent-Genod, L., Pouget, J.P. & Voisin, P. The Cell Membrane as a Biosensor of Oxidative Stress Induced by Radiation Exposure: A Multiparameter Investigation. *Radiation Research* **159**, 471-483 (2003).

216. Volinsky, R. et al. Oxidized phosphatidylcholines facilitate phospholipid flip-flop in liposomes. *Biophys J* **101**, 1376-1384 (2011).

217. Porter, N.A., Caldwell, S.E. & Mills, K.A. Mechanisms of free radical oxidation of unsaturated lipids. *Lipids* **30**, 277-290 (1995).

218. Jiang, N., Benard, C.Y., Kebir, H., Shoubridge, E.A. & Hekimi, S. Human CLK2 links cell cycle progression, apoptosis, and telomere length regulation. *The Journal of biological chemistry* **278**, 21678-21684 (2003).

219. Op den Kamp, J.A. Lipid asymmetry in membranes. *Annual review of biochemistry* **48**, 47-71 (1979).

220. Schrier, S.L., Hardy, B. & Bensch, K.G. Endocytosis in erythrocytes and their ghosts. *Progress in clinical and biological research* **30**, 437-449 (1979).

221. Friedman, P., Horkko, S., Steinberg, D., Witztum, J.L. & Dennis, E.A. Correlation of antiphospholipid antibody recognition with the structure of synthetic oxidized phospholipids. Importance of Schiff base formation and aldol condensation. *The Journal of biological chemistry* **277**, 7010-7020 (2002).

222. Ingolfsson, H.I. et al. Lipid organization of the plasma membrane. *Journal of the American Chemical Society* **136**, 14554-14559 (2014).

223. Chikazawa, M. et al. Multispecificity of immunoglobulin M antibodies raised against advanced glycation end products: involvement of electronegative potential of antigens. *The Journal of biological chemistry* **288**, 13204-13214 (2013).

224. Shaw, P.X. et al. Natural antibodies with the T15 idiotype may act in atherosclerosis, apoptotic clearance, and protective immunity. *The Journal of Clinical Investigation* **105**, 1731-1740 (2000).

225. Balasubramanian, K., Bevers, E.M., Willems, G.M. & Schroit, A.J. Binding of annexin V to membrane products of lipid peroxidation. *Biochemistry* **40**, 8672-8676 (2001).

226. Fruhwirth, G.O., Moumtzi, A., Loidl, A., Ingolic, E. & Hermetter, A. The oxidized phospholipids POVPC and PGPC inhibit growth and induce apoptosis in vascular smooth muscle cells. *Biochimica et biophysica acta* **1761**, 1060-1069 (2006).

227. Greenberg, M.E. et al. The lipid whisker model of the structure of oxidized cell membranes. *The Journal of biological chemistry* **283**, 2385-2396 (2008).

228. Katayama, S. et al. Effects of pyrenebutyrate on the translocation of arginine-rich cell-penetrating peptides through artificial membranes: recruiting peptides to the

membranes, dissipating liquid-ordered phases, and inducing curvature. *Biochimica et biophysica acta* **1828**, 2134-2142 (2013).

229. Lee, Y.J., Johnson, G. & Pellois, J.P. Modeling of the endosomolytic activity of HA2-TAT peptides with red blood cells and ghosts. *Biochemistry* **49**, 7854-7866 (2010).

230. Ayala, A., Munoz, M.F. & Arguelles, S. Lipid peroxidation: production, metabolism, and signaling mechanisms of malondialdehyde and 4-hydroxy-2-nonenal. *Oxidative medicine and cellular longevity* **2014**, 360438 (2014).

231. Hermann, P.M., Watson, S.N. & Wildering, W.C. Phospholipase A2 - nexus of aging, oxidative stress, neuronal excitability, and functional decline of the aging nervous system? Insights from a snail model system of neuronal aging and age-associated memory impairment. *Front Genet* **5**, 419 (2014).

232. Runas, K.A., Acharya, S.J., Schmidt, J.J. & Malmstadt, N. Addition of Cleaved Tail Fragments during Lipid Oxidation Stabilizes Membrane Permeability Behavior. *Langmuir : the ACS journal of surfaces and colloids* **32**, 779-786 (2016).

233. Catala, A. Lipid peroxidation of membrane phospholipids generates hydroxy-alkenals and oxidized phospholipids active in physiological and/or pathological conditions. *Chemistry and physics of lipids* **157**, 1-11 (2009).

234. Karlenius, T.C. et al. The selenium content of cell culture serum influences redox-regulated gene expression. *BioTechniques* **50**, 295-301 (2011).

235. Tiedge, M., Lortz, S., Drinkgern, J. & Lenzen, S. Relation Between Antioxidant Enzyme Gene Expression and Antioxidative Defense Status of Insulin-Producing Cells. *Diabetes* **46**, 1733-1742 (1997).

236. Wang, T.Y. et al. Membrane Oxidation Enables the Cytosolic Entry of Polyarginine Cell-penetrating Peptides. *The Journal of biological chemistry* **291**, 7902-7914 (2016).

237. Sitte, N., Merker, K., Von Zglinicki, T., Grune, T. & Davies, K.J. Protein oxidation and degradation during cellular senescence of human BJ fibroblasts: part I--effects of proliferative senescence. *FASEB journal : official publication of the Federation of American Societies for Experimental Biology* **14**, 2495-2502 (2000).

238. Spickett, C.M. & Pitt, A.R. Oxidative lipidomics coming of age: advances in analysis of oxidized phospholipids in physiology and pathology. *Antioxidants & redox signaling* **22**, 1646-1666 (2015).

239. Sezgin, E. et al. Elucidating membrane structure and protein behavior using giant plasma membrane vesicles. *Nature protocols* **7**, 1042-1051 (2012).